

Sandia National Laboratories
Waste Isolation Pilot Plant

Analysis Package for BRAGFLO: Compliance
Recertification Application

ERMS # 530163

Author: Joshua Stein (6821) Joshua S. Stein 10/23/03
Print Signature Date

Author: William Zelinski (6821) William Zelinski 10/23/03
Print Signature Date

Technical
Review: Teklu Hadgu (6852) Maria Chavez 10/23/03
Print Signature Date

Management
Review: David Kessel (6821) David Kessel 10/23/03
Print Signature Date

QA
Review: Mario Chavez (6820) Mario Chavez 10/23/03
Print Signature Date

WIPP:1.4.1.1:PA:QA-L:530162

Information Only

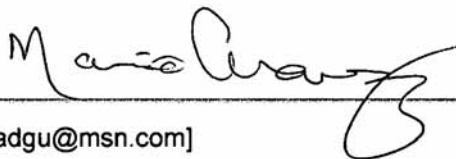
Orig 10/27/03
137
1 of 138

TABLE OF CONTENTS

ACRONYMS	III
1.0 INTRODUCTION	1
2.0 BACKGROUND	1
2.1 Compliance Certification Application	1
2.2 Technical Baseline Migration (TBM).....	2
2.3 Analysis Plan 106 (AP106).....	2
2.4 Compliance Recertification Application (CRA).....	2
3.0 CONCEPTUAL APPROACH FOR SALADO FLOW ANALYSIS.....	2
3.1 Model Geometry	3
3.1.1 Stratigraphic Modeling Units.....	4
3.1.2 Excavated Modeling Units.....	7
3.1.3 Borehole Modeling Units.....	8
3.1.4 Changes to the BRAGFLO Modeling Grid for CRA	8
3.2 Initial Conditions	12
3.3 Boundary conditions	13
4.0 SALADO FLOW MODELING METHODOLOGY.....	14
4.1 SALADO FLOW Modeling Process	14
4.1.1 Data Input and Pre-BRAGFLO Processing	15
4.1.2 BRAGFLO Calculations	22
4.1.3 Post-BRAGFLO Processing	22
4.1.4 Methods of Analysis	24
4.1.5 Execution and Run control.....	25
4.2 Data For the Salado Flow Analysis	25
4.2.1 WIPP Parameter Database	25
4.2.2 Input Control Files	26
4.2.3 Porosity Surface From SANTOS.....	26
4.2.4 Transfer of Information Between Software Modules	26
4.3 Uncertainty In Salado Flow Analysis	26
4.3.1 Uncertainty of Future Events - Scenarios	27
4.3.2 Variability and Uncertainty of Input Parameters	27
4.3.3 Statistical Uncertainty - Replicates	28
5.0 MODELING RESULTS	28
5.1 Exception Vectors.....	29
5.1.1 Replicate 1	30
5.1.2 Replicate 2	30
5.1.3 Replicate 3	31
5.2 Overview of the Salado Flow Analysis	31
5.2.1 Organization.....	31
5.2.2 Halite Creep	32
5.2.3 Summary of Gas Generation Factors	32
5.2.4 Coupling of Gas Generation and Brine/Gas Flow	33
5.3 Modeling Results for Undisturbed Performance (R1S1).....	34
5.3.1 Sequence of Events	34
5.3.2 Porosity and Halite Creep	34
5.3.3 Brine Inflow	37

Information Only

Chavez, Mario Joseph



From: TEKLU HADGU [dthadgu@msn.com]
Sent: Thursday, October 23, 2003 2:32 PM
To: mjchave@sandia.gov
Subject: Signature authority

Hi Mario,

I have completed review of the CRA BRAGFLO Calculations document and accepted all changes. Please sign the front page on my behalf.

Thanks,
Teklu

Information Only

10/23/2003

Information Only

5.3.4	Brine Saturation	42
5.3.5	Gas Generation.....	47
5.3.6	Pressure	52
5.3.7	Rock Fracturing	57
5.3.8	Brine Outflow	61
5.4	Drilling Disturbance Scenarios (2, 3, 4, 5 & 6)	66
5.4.1	Sequence of Events	66
5.4.2	Halite Creep	67
5.4.3	Brine Inflow	72
5.4.4	Brine Saturation	77
5.4.5	Gas Generation.....	83
5.4.6	Pressure	87
5.4.7	Rock Fracturing	95
5.4.8	Brine Flow Away From the Repository.....	99
5.5	Comparison of replicates	107
5.6	Summary and Conclusions	115
6.0	REFERENCES	116
	APPENDIX A: OUTPUT VARIABLES.....	120
	APPENDIX B: CREEP CLOSURE, MINIMUM POROSITIES.....	128
	APPENDIX C: ANALYSIS FILES ON CD'S.....	132

Information Only

ACRONYMS

CCA	Compliance Certification Application
CMS	Code Management System
CRA	Compliance Recertification Application
DOE	U.S. Department of Energy
DRZ	Disturbed Rock Zone
EPA	U.S. Environmental Protection Agency
MB	Marker Bed
PA	Performance Assessment
PAVT	Performance Assessment Verification Test
PCS	Panel Closure System
SNL	Sandia National Laboratories
TBM	Technical Baseline Migration
TRU	Transuranic Waste
WIPP	Waste Isolation Pilot Plant

Information Only

1.0 INTRODUCTION

The Waste Isolation Pilot Plant (WIPP) is located in southeastern New Mexico and has been developed by the U.S. Department of Energy (DOE) for the geologic (deep underground) disposal of transuranic (TRU) waste (U.S. DOE 1980, 1990, 1993). In 1992, Congress designated the U.S. Environmental Protection Agency (EPA) as WIPP's official certifier, and mandated that once DOE demonstrated to EPA's satisfaction that WIPP complied with Title 40 of the Code of Federal Regulations, Part 191 (U.S. DOE, 1996, U.S. EPA 1996), EPA would certify the repository. The regulation required the creation of computational models to predict whether the repository would continue to comply with the regulatory requirements for 10,000 years into the future. Called Performance Assessment (PA), this activity required examination of failure scenarios, quantification of their likelihoods, estimates of potential releases to the surface or the site boundary, and evaluation of potential consequences.

Salado Flow Analysis, which was conducted in accordance with Analysis Plan 099 (Stein, 2003), is the first computational activity in the WIPP PA analysis to support the first Compliance Recertification Application (CRA). This is an integrated process, which involves a sequence of software codes, to model expected and possible flow and transport performance in the vicinity of the WIPP repository. The BRAGFLO software generates brine and gas flow fields that define the hydrological environment for downstream modeling activities.

2.0 BACKGROUND

2.1 COMPLIANCE CERTIFICATION APPLICATION

In October 1996, DOE submitted the Compliance Certification Application (CCA) to the EPA, which incorporated the results of extensive PA analyses and modeling. In May 1997, EPA rendered its judgment that WIPP was safe for permanent disposal of transuranic waste, and the first shipment of radioactive waste from the nation's nuclear weapons complex arrived at the site in March 1999. The results of CCA PA analyses were subsequently summarized in a Sandia National Laboratories report (Helton, et al, 1998).

During the review of the CCA, EPA mandated an additional Performance Assessment Verification Test (PAVT) using revised input information. The PAVT, which consisted of three replicates, involved the full range of WIPP PA analyses beginning with the Salado Flow Analysis and culminating with the generation of complimentary cumulative distribution functions (CCDFs) for total normalized radionuclide releases to the accessible environment. PAVT results confirmed the conclusions of the CCA using the revised input parameters.

Information Only

2.2 TECHNICAL BASELINE MIGRATION (TBM)

The Technical Baseline Migration (TBM) was an effort to merge CCA (U.S. DOE, 1996) and PAVT (PAVT, 1997) baselines while at the same time implementing conceptual model changes being reviewed by the Salado Flow Peer Review, May 2002 (Caporuscio, 2002). The TBM grid, which is described by Hansen and others (2002), was the successor to the CCA/PAVT grid. The most important changes with respect to the TBM BRAGFLO grid were the removal of the shaft seal system and implementation of the Option D panel closures. Additional grid refinements were implemented to increase numerical accuracy and computational efficiency and to reduce numerical dispersion.

In May, 2002, the Salado Flow Peer Review panel met in Carlsbad to evaluate the proposed changes to conceptual models for the TBM. A set of PA calculations (TBM) was run to demonstrate the effects of these changes on BRAGFLO results. The peer review panel judged the changes to be "generally sound in their structure, reasonableness, and relationship to the original models". However the panel required that a total systems PA be run and complementary cumulative distribution functions (CCDFs) be generated before they would agree to the changes (Caporuscio et al., 2002).

2.3 ANALYSIS PLAN 106 (AP106)

After the first meeting of the Salado Flow Peer Review, the conceptual models were revised to address new concerns of the EPA and to incorporate new technical information from laboratory and field investigations (Stein and Zelinski, 2003). The Salado Flow Peer Review Panel held a second and final meeting in Carlsbad in February 2003 to consider the results of the total systems PA using the new revised grid and modeling assumptions. The panel approved the proposed conceptual model changes (Caporuscio et al., 2003) permitting the start of PA analyses for the Compliance Recertification Application (CRA) beginning with the Salado Flow Analysis of gas and brine flow in the vicinity of the repository.

2.4 COMPLIANCE RECERTIFICATION APPLICATION (CRA)

The Congressional act authorizing the EPA to certify the WIPP repository also requires re-certification at five-year intervals. The first CRA is due in March 2004, and the PA analyses supporting the CRA incorporates revised conceptual models, which address new concerns of the EPA and incorporate new technical information from laboratory and field investigations.

3.0 CONCEPTUAL APPROACH FOR SALADO FLOW ANALYSIS

The conceptual structure for BRAGFLO simulation modeling in 2003 for the WIPP CRA ultimately derives from the regulatory requirements imposed on the facility. The primary

Information Only

regulation determining this structure is the U.S. EPA's standard for the geologic disposal of radioactive waste, *Environmental Radiation Protection Standards for the Management and Disposal of Spent Nuclear Fuel, High-Level and Transuranic Radioactive Wastes* (40 CFR 191) (U.S. EPA 1985, 1993), which is divided into three parts. Subpart A applies to a disposal facility prior to decommissioning and limits annual radiation doses to members of the public from waste management and storage operations. Subpart B applies after decommissioning and sets probabilistic limits on cumulative releases of radionuclides to the accessible environment for 10,000 yr (40 CFR 191.13) and assurance requirements to provide confidence that 40 CFR 191.13 will be met (40 CFR 191.14). Subpart B also sets limits on radiation doses to members of the public in the accessible environment for 10,000 yrs of undisturbed performance (40 CFR 191.15). Subpart C limits radioactive contamination of certain sources of groundwater for 10,000 yr after disposal (40 CFR 191.24). The DOE must provide a reasonable expectation that the WIPP will comply with the requirements of Subparts B and C of 40 CFR 191.

In order to demonstrate compliance with the regulations it is necessary to simulate the flow of brine and gas within the repository and surrounding geologic units. Numerical simulations provide quantitative information about expected flow patterns, pressure histories, and brine saturation near the repository over the 10,000-year regulatory period. This information is an important component in the calculations of the total releases to the accessible environment. Model geometry, initial conditions and boundary conditions must be defined in order to run these numerical simulations. These are discussed in the sections that follow.

3.1 MODEL GEOMETRY

The primary objective in creating the modeling grid for BRAGFLO is to accurately capture the effect of essential hydrologic features with a minimum of computational complexity. This is accomplished in Salado flow modeling by using a vertical, two-dimensional grid system, oriented north to south through the repository and surrounding strata (Figure 3.1.1). The length (Δx), the width (Δz), and the height (Δy) of each grid cell are shown in Figure 3.1.1 as a logical grid (not to scale). This wide variation in grid cell dimensions captures the maximum amount of hydrological detail with the minimum possible number of grid cells. A uniform grid that captured the detail required around boreholes, the shaft, and repository excavations and extended to compliance geographic boundaries would exceed current computing capacity.

The two dimensional BRAGFLO grid captures three-dimensional flow effects by employing "radial flaring." This flaring is visible when looking down on the grid from the top as shown in Figure 3.1.2. In this figure, the width of each grid cell to the north and south of the repository increases with distance away from the center of the waste-filled region. The flaring simulates convergent or divergent flow to the north and south centered on the repository, and laterally away from the repository. The flaring methodology used to create the grid is discussed in a separate memo (Stein, 2002a). This methodology for providing geometric control to BRAGFLO modeling was tested in

Information Only

WIPP PA (1996b) and shown to represent fluid release to the accessible boundaries within system uncertainty.

The Salado flow grid incorporates the repository, the Castile brine reservoir, the Salado Formation, bedded units above the Salado, the shaft, panel seals, and an intrusion borehole. The dimensions of rows and columns of grid blocks, which are indicated in meters along the left and bottom margins of the grid in Figure 3.1.1, have been selected to provide an accurate geometric model of features that affect hydrologic flow and transport and to accommodate calculation mechanics.

3.1.1 Stratigraphic Modeling Units

The stratigraphy used in the CRA is essentially the same as described in the CCA (U.S. DOE, 1996). The definition of hydro-stratigraphic modeling units for Salado Flow Analysis follows the convention of formations and member divisions (Mercer, 1987) except that a further sub-division has been made within the Salado Formation. At the stratigraphic level of the repository, additional modeling units are defined in the grid based upon observed differences in permeability between anhydrite interbeds and the surrounding halite (Webb and Larsen, 1996).

3.1.1.1 Castile Formation

The Castile Formation is located beneath the Salado Formation. It is composed of thickly interbedded halite and anhydrite in the area of the repository, and it is represented in the grid system by an impermeable barrier surrounding a pressurized brine pocket beneath the repository (Anderson et al, 1972). All boreholes in Salado flow modeling are assumed to be drilled through the repository in search of deeper resources. The potential consequences of encountering a pressurized brine pocket are considered by incorporating a borehole into the model that reaches the Castile brine pocket, which is pressurized.

The potential consequence of a borehole that does not encounter pressurized brine is evaluated by terminating the borehole in the modeling grid at the base of the repository. The deeper part of the borehole would have no consequence except possibly to drain brine from the repository. Eliminating the bottom part of the borehole simplifies the management of material properties (Popielak et al, 1983; Freeze and Larsen, 1996; and Powers et al, 1996). Fluid flow between the brine reservoir and the repository in Salado models will only occur in an E1¹ drilling intrusion scenario, because the intervening Castile and Salado evaporites have such a low permeability.

3.1.1.2 Salado Formation

The Salado Formation consists of halite with thin interbeds of anhydrite (Jones et al, 1960). The Salado flow grid includes intact halite surrounding the repository and two

¹ E1 and E2 intrusions are defined in section 4.3.1

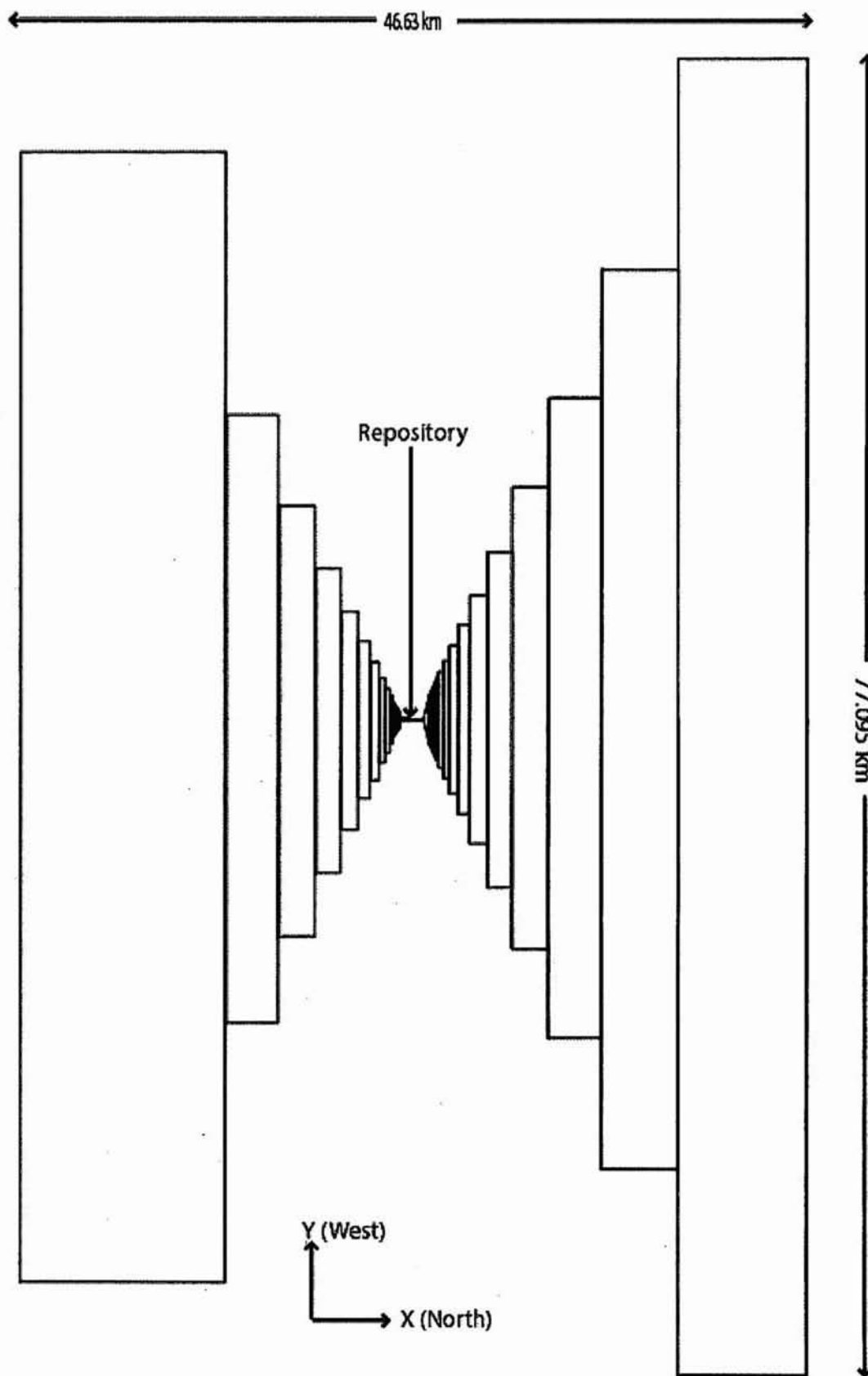


Figure 3.1.2: Top view of CRA logical grid

Information Only

anhydrite interbeds, Marker Bed 138 (S_MB138) and Marker Bed 139 (S_MB139) and a layer that represented two thin interbeds, (Anhydrites A and B) that are combined into one layer for modeling purposes (S_ANH_AB). In addition, the halite immediately above and below the repository is modeled as a disturbed rock zone (DRZ), which has a different set of properties from intact halite due to disturbance from excavation and differential expansion. The DRZ and the marker beds are also allowed to undergo fracturing when repository pressures are sufficiently high. Christian-Frear and Webb (1996) and Webb and Larsen (1996) demonstrated that these materials sufficiently captured the essential elements of the Salado stratigraphy.

3.1.1.3 Hydro-Stratigraphic Units Above the Salado Formation

Stratigraphy above the Salado (Mercer, 1987) is represented in the BRAGFLO modeling grid, from the top down, by the following materials:

- Santa Rosa (Mercer, 1987)- coarse clastic sediments
- Dewey Lake Redbeds
(Lucas and Anderson, 1993) - fine grained clastic sediments
- Rustler Formation (U.S. DOE, 1996)-
 - 49er Member - anhydrite and mudstone
 - Magenta Dolomite Member - dolomite
 - Tamarisk Member - anhydrite and mudstone
 - Culebra Dolomite Member - dolomite
 - Los Medaños Member - anhydrite, mudstone, and sandstone
 (Powers and Holt, 1999)
 (Referred to as "Unnamed" in the WIPP parameter database)

3.1.2 Excavated Modeling Units

The treatment of excavated regions in the Salado Flow modeling grid and changes from previous grids are discussed in Stein and Zelinski (2003). Within the repository and shaft system, BRAGFLO geometry (the modeling grid) preserves the true excavated volumes. Lateral dimensions have been set to preserve volume and to retain important cross-sectional areas and distance between constructed regions. These simplifications overestimate fluid contact with waste, which is a critical factor in determining the quantity of actinides mobilized in the liquid phase. The simplification also overestimates brine flow because 1) all pillars have been removed from the panels resulting in homogenous waste regions through which fluid can flow freely and 2) the panels in the rest of the repository have no pillars and fewer panel closures than are planned, resulting in very large regions of homogenous waste that are assigned a high permeability.

The repository consists of three waste regions. One region represents a single waste panel, which allows more detailed representation of a borehole penetrating a panel during an intrusion scenario. All other non-intruded waste panels are collectively grouped into two waste regions, north rest of repository (RoR) and south RoR. The waste regions are

Information Only

separated by Option D panel closures, which are designed to impede brine and gas flow between panels. The excavated area near the shaft at the north end of the repository is divided into two grid regions, the operations area (OPS_AREA) and the experimental area (EXP_AREA). These two areas are separated in the grid by the concrete monolith of the shaft (CONC_MON), and the working area is separated from the north RoR waste panel by a set of panel closures that represent the two sets of panel closures that will be placed between these two areas.

3.1.3 Borehole Modeling Units

The borehole in Scenarios 2-6 is represented by a column of grid blocks that have a Δx of 0.27575 meters and a Δz of 0.27575 meters. In the undisturbed scenario (Scenario 1), these blocks have the material properties of the neighboring stratigraphic or excavated modeling unit, and there is no designation in the grid of a borehole except for the reduced lateral dimensions of this particular column of grid blocks. In the scenarios for drilling disturbance, these cells start out with the same material properties as in the undisturbed scenario, but at the time of intrusion the borehole grid blocks are reassigned to borehole material properties.

3.1.4 Changes to the BRAGFLO Modeling Grid for CRA

The CRA grid is the same grid that was used in the AP106 analysis (Stein and Zelinski, 2003) and was approved by the Salado Flow Peer Review Panel (Caporuscio, 2003). The CRA grid has been designed to address a variety of issues that have arisen since the CCA. Some of these changes have been evaluated and used in the TBM analysis, and others are new to the CRA (and AP106). The following changes from the CCA grid have been incorporated into the CRA grid:

1. Refinement of grid outside the excavated area to improve computational accuracy and efficiency,
2. Simplification of the shaft seal model,
3. Implementation of Option D Panel closures.
4. Increased Segmentation in Rest of Repository (south RoR and north RoR)

3.1.4.1 Grid Refinement (1)

The number of grid cells has been increased from (x,y) dimensions of 31 by 27 blocks in the CCA grid to 68 by 33 blocks in the CRA grid. The grid blocks to the north and south of the excavated region were refined in the x -direction from the CCA grid. The x -dimension of the grid cells immediately to the north and south of the repository start at 2 m adjacent to the repository and increase by a factor of 1.45 away from the repository. Exceptions to this are made to ensure that the location of the Land Withdrawal Boundary and the total extent of the grid match that in the CCA grid. This refinement factor was chosen to reduce numerical dispersion caused by rapid increases in cell dimensions (Anderson and Woessner, 1992; Wang and Anderson, 1982).

Information Only

In the y-direction the grid spacing within layers representing the Salado has been changed from the CCA. The CCA grid spacing in the Salado was dictated by the thickness of different shaft seal materials, because of the limitation of a finite difference grid, which requires fixed row and column dimensions across the grid. Since the shaft has been simplified, the y spacing in the Salado is now uniform. In addition, two layers were added immediately above and below Marker Bed 139 to refine the grid spacing near this layer. These changes result in a total of 33 y-divisions for the grid.

3.1.4.2 Simplified Shaft Model (2)

A shaft seal model is included in the CRA grid, but it is implemented in a simpler fashion than was used for the CCA and PAVT. A detailed description of the simplified model and its parameters are discussed in AP-094 (James and Stein, 2002) and the resulting analysis report (James and Stein, 2003). The final version of the model used in the CRA is described by Stein and Zelinski (2003). The final version used in the CRA was approved by the Salado Flow Peer Review panel (Caporuscio and others, 2003).

The new model does not alter the conceptual model of the shaft seal components as described in SNL (1996). Rather, it conservatively represents the behavior of seal components in the repository system model. Specifically, the original 11 separate material layers that defined the shaft model for the CCA were reduced to two layers each with properties equivalent to the composite effect of the original materials combined in series. Additionally, the six time intervals that were used to represent the evolution of the shaft seal materials over time were reduced to two intervals. The CRA and CCA shaft models are graphically compared in Figure 3.1.3. The simplified shaft model was tested in the AP-106 calculations (Stein and Zelinski, 2003), which supported the Salado Flow Peer Review. The results of this analysis demonstrated that brine flow through the simplified shaft model was comparable to brine flows seen through the detailed shaft model in the PAVT calculations. The conclusion remains that the shaft seals are very effective barriers to flow throughout the 10,000-year regulatory period.

3.1.4.3 Implementation of Option D Panel Closures (3)

Option D panel closures (Figure 3.1.4) are designed to provide minimal fluid flow between panels. The CRA explicitly represents selected Option D panel closures in the computational grid using a model that was approved by the Salado Flow Peer Review Panel (Caporuscio and others, 2003). First, the CRA grid extends the concrete portion of the Option D panel closures into the upper and lower DRZ (Figure 3.1.1). The CRA panel closure system model divides the panel closure and surrounding materials into four materials in 13 grid cells including:

- Six cells of panel closure concrete represented by the material CONC_PCS,
- One cell above and one cell below the concrete material consisting of marker bed anhydrite,

Information Only

- Two cells of healed DRZ above Anhydrite AB above the panel closure system (PCS) represented by the material DRZ_PCS,
- Three cells of empty drift and explosion wall represented by the material DRF_PCS.

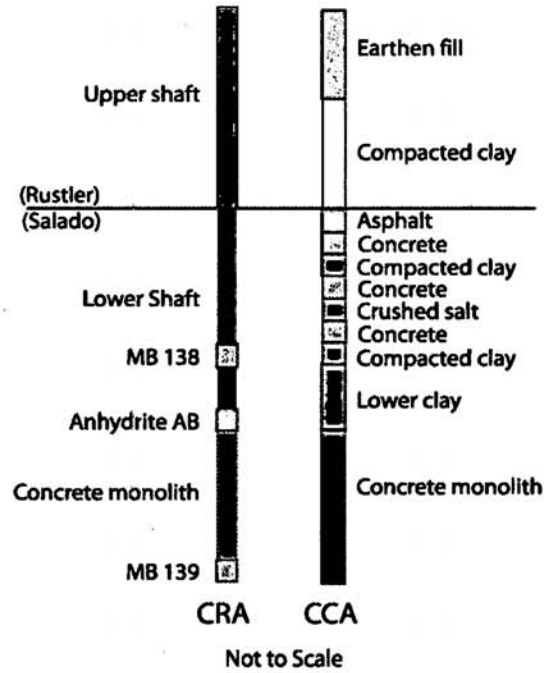


Figure 3.1.3: Comparison Of The Simplified Shaft (CRA) And The Detailed Shaft (CCA) Models

Not To Scale. Shown With Logical Dimensions.

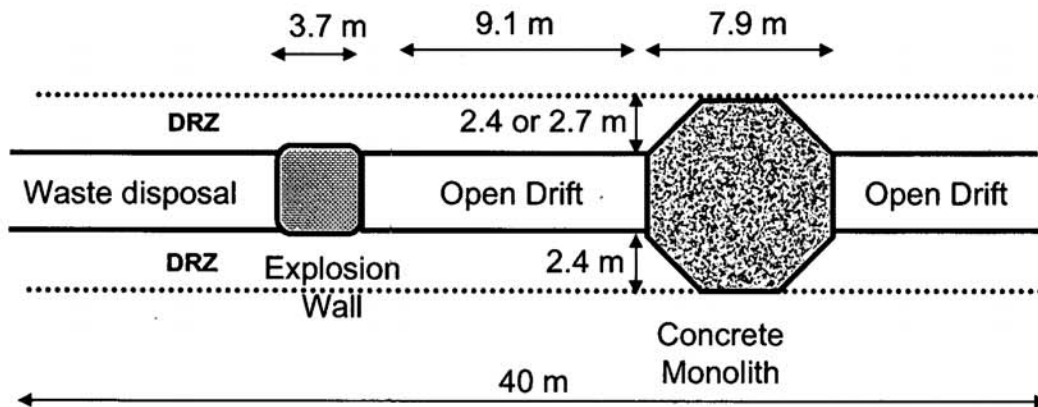


Figure 3.1.4: Schematic Side View of Option D Panel Closure

Information Only

Panel Closure Concrete: The Option D panel closure design requires the use of a salt-saturated concrete, identified as Salado Mass Concrete (SMC), as is required for the shaft seal system. The design of the shaft seal system and the properties of SMC are described in Hurtado et al. (1997). The CRA BRAGFLO grid incorporates the material, CONC_PCS, which is assigned the material properties of undegraded SMC and is used to represent the concrete portion of the Option D panel closure system (Stein, 2002b).

Panel Closure Abutment with Marker Beds: In the CRA grid, we represent regions where the Option D panel closures intersect the Marker Beds as isolated blocks of marker bed material. This representation is warranted for two reasons.

- First, the marker bed material has a very similar permeability distribution (10^{-21} to $10^{-17.1}$ m²) as the concrete portion of the Option D panel closures ($10^{-20.699}$ to 10^{-17} m²), and thus, assigning this material as anhydrite marker bed in the model has essentially the same effect as assuming it behaves as concrete as long as pressures are below the fracture initiation pressure.
- Second, in the case of high pressures it is expected that fracturing may occur in the anhydrite marker beds and flow could go “around” the panel closures out of the 2-D plane considered in the model grid. In this case the flow would be through the marker bed material that is already allowed to fracture. Therefore, assigning these isolated cells as anhydrite marker bed materials is appropriate.

Disturbed Rock Zone Above the Panel Closure: After construction of the concrete portion of the panel closure, the salt surrounding the monolith will be subjected to compressive stresses, which will facilitate the rapid healing of disturbed zones. The rounded configuration of monolith creates a situation very favorable for concrete: high compressive stresses and low stress differences. In turn, the compressive stresses developed within the salt will quickly heal any damage caused by construction excavation, thereby eliminating the DRZ along the length of the panel closure. The permeability of the salt immediately above and below the rigid concrete monolith component of Option D will approach the intrinsic permeability of the Salado halite.

To capture the healed DRZ above the monoliths, the CRA uses the material, DRZ_PCS, in the BRAGFLO grid. The property values assigned to DRZ_PCS are the same as those values used for a similar DRZ-related material (DRZ_1), except for the properties PRMX_LOG, PRMY_LOG, and PRMZ_LOG, the logarithm of permeability in the X, Y, and Z directions, respectively. These permeability values are assigned the same distributions used for the material CONC_PCS. In this instance, the values are based on the nature of the model set-up, and not directly on experimental data (although the general range of the distribution agrees with experimental observations of healed salt). The use of these permeabilities ensures that any fluid flow is equally probable through or around the Option D panel closures and best represents the uncertainty that exists in the performance of the panel closure system.

Information Only

Empty Drift And Explosion Wall Materials: DRF_PCS is the material representing the empty drift and explosion wall. This material has properties equivalent to the material representing the waste panel (except it is not filled with waste) and is used for the three panel closures that are adjacent to waste regions. The creep closure model is applied to this material to be consistent with the neighboring materials. The non-concrete portion of the northernmost panel closure between the operations area and the experimental area is assigned properties equivalent to the operations area. This is done so that the creep closure model is applied consistently to different regions in the grid (the waste regions have the creep closure model applied whereas the operations area is modeled as pre-closed and assigned an initial low porosity for all times). The assignment of a high permeability to this region containing the explosion wall is justified because the explosion wall is not designed to withstand the stresses imposed by creep closure and will be highly permeable following rapid room closure.

3.1.4.4 Increased Segmentation in Rest of Repository (4)

The Option D panel closures are designed to impede brine flow between panels. It is therefore necessary to include greater segmentation within the repository such that the serial effects of these panel closures can be adequately simulated. Consequently, the CRA grid divides the rest of repository into two separate blocks: the south RoR and north RoR. For the CRA, four sets of panel closures were included in the model domain. These panel closures lie in between the following grid regions: the single intruded waste panel, south RoR, north, operations area, and experimental area. The inclusion of four sets of panel closures as compared to the CCA grid, which represented only two sets of panel closures is considered necessary to evaluate the effects of Option D type panel closures.

One example illustrating why greater segmentation is warranted is immediately following a drilling intrusion. In the CCA grid, the intruded panel is separated from a single rest of repository block representing nine panels with no panel closures separating panels within the rest of repository from each other. This representation overestimates the extent to which a single intrusion can depressurize other parts of the repository. The CRA grid places more panel closures between blocks representing waste-filled regions and thus provides a more accurate and conservative representation of the effect of multiple drilling intrusions. In the CRA grid, an intrusion into one panel is less likely to depressurize other parts of the repository that may be separated by as many as four sets of panel closures. This change was accepted by the Salado Flow Peer Review Panel (Caporuscio and others, 2003).

3.2 INITIAL CONDITIONS

BRAGFLO simulation of brine and gas flow in the vicinity of the WIPP site requires the assignment of initial conditions including brine pressure, brine saturation, and concentrations of iron and biodegradable material. These initial conditions are provided

to BRAGFLO through various pre-processing steps during which values are extracted or sampled from the WIPP Parameter Database.

At the beginning of each BRAGFLO run (scenario-vector combination), the model simulates a short period of time representing disposal operations. This portion of the run is called the initialization period and lasts for 5 years (from $t = -5$ to 0 years), corresponding to the time a typical waste panel is expected to be open during disposal operations. All grid blocks require initial pressure and saturation at the beginning of the run ($t = -5$ years). At the beginning of the regulatory period (0 to 10,000 years), BRAGFLO resets initial conditions within the excavated regions and in the shaft.

The initial conditions at -5 years for BRAGFLO modeling are listed below:

- Brine pressure in all non-excavated regions is equal to lithostatic pressure (sampled at one location and assumed hydrostatic at all other locations).
- Pressure within the repository is set to 1.01325×10^5 Pa (1 atm).
- Brine saturation within the non-excavated regions is set to 1.0.
- Brine saturation within the excavated regions is set to 0.0.

During the initialization period brine tends to flow into the excavated areas and the shaft, resulting in decreased pressure and saturation in the rock immediately adjacent to the excavations. At time, $t = 0$, the pressure and saturation in the all the excavations is reset to the initial conditions for the materials used to represent these regions for the regulatory period. This practice is intended to capture the effect of evaporation of brine inflow during the operational period and the transport of this brine up the shaft ventilation system. The material changes at time, $t = 0$, in which the initial conditions are reset are listed below:

- CAVITY_1 is set to WAS_AREA and initial concentration of iron and biodegradable material is set.
- CAVITY_2 is set to REPOSIT and initial concentration of iron and biodegradable material is set.
- CAVITY_3 is set to OPS_AREA and EXP_AREA
- CAVITY_4 is set to panel closure and shaft seal materials

3.3 BOUNDARY CONDITIONS

The boundary conditions assigned for the BRAGFLO calculations are as follows:

- Constant pressure at the north and south ends of the Culebra and Magenta Dolomites.
- Constant pressure (1.01325×10^5 Pa) and saturation (0.08363 dimensionless) conditions at the land surface boundary of the grid.
- No flow conditions at all other grid boundaries.

4.0 SALADO FLOW MODELING METHODOLOGY

The purpose of Salado Flow modeling is to perform two-phase flow analyses of brine and gas in the vicinity of the WIPP repository over a 10,000-year regulatory compliance period. This is the first activity in an integrated WIPP PA process that evaluates the potential for radionuclide transport from the WIPP repository to the accessible environment. The primary software that is used in the Salado Flow Analysis is BRAGFLO 5.0.

The BRAGFLO software models:

- Brine and gas flow
- Creep closure of the waste filled regions within the repository,
- Gas generation due to corrosion of steel and degradation of biodegradable materials (cellulosics, plastics, and rubbers),
- Physical changes (e.g. porosity) in the modeling domain over time,
- The consequences of rock fracturing due to high pressure.

The system of coupled processes in each run of the model (scenario-vector combination) can be very sensitive to small changes in conditions within the model, causing large differences in results. For example, a small increase in pressure may cause fracturing that results in a large increase in brine outflow. However, without sufficient brine inflow to allow gas generation processes to proceed there cannot be large brine outflows.

To capture the variability and uncertainty in future brine and gas flow patterns, the Salado Flow Analyses includes 1,800 separate BRAGFLO runs. The runs are divided into three replicates, each consisting of six different scenarios. Each replicate has 100 sets of sampled input parameters (vectors) that are used in each of its scenarios. Section 4.0 describes how the scenarios and vectors are defined. The analysis of results often collectively considers groups of 100 vectors (a scenario). For the CRA analysis, three replicates are run and the results of each are compared.

4.1 SALADO FLOW MODELING PROCESS

The essential tasks in the Salado Flow modeling process are to:

- Define a numerical modeling grid that adequately represents the functional geometry of important hydrologic features in and around the repository.
- Assign material and property values to regions of the grid.
- Calculate parameters required by BRAGFLO (e.g. gas generation, rock fracturing, and creep closure model parameters) that define the hydrologic environment for flow and transport modeling.
- Perform two-phase flow calculations to model brine and gas flow.
- Convert BRAGFLO results into formats suitable for analysis and for use with other software.

These tasks are accomplished in twelve discrete computer-modeling steps, which are summarized in Table 4.1.1. The Salado Flow modeling process employs the software module, BRAGFLO 5.0 to perform two-phase flow analysis, and eight other software modules to perform essential pre- and post-processing functions.

4.1.1 Data Input and Pre-BRAGFLO Processing

The analyst controls the Salado Flow modeling process by means of ASCII input control files (Table 4.1.1) that specify how input information is to be acquired and prepared and how modeling steps are to be performed. Instructions are provided in the pre-BRAGFLO processing steps 1) GENMESH(GM), 2) MATSET(MS), 3) PRELHS (LHS1), 6) ICSET(IC), 7) ALGEBRACDB (ALG1), and 8) PREBRAG(BF1). In most steps, a binary, computational database (.CDB) file is read in from the previous step and new data is added to the file and a new binary file is produced which contains all of the information added in all previous steps.

4.1.1.1 Grid Generation

The first step in the BRAGFLO modeling process (Step 1 in Table 4.1.1) is the definition of the modeling grid using the application, GENMESH (WIPP PA, 1995a). The parameters required to define the mesh include grid cell dimensions and region definitions. The analyst supplies these parameters in the input control file. This analysis uses an adaptation of the TBM grid (Hansen et al., 2002) with changes (Stein and Zelinski, 2003) that have been approved by the Salado Flow Peer Review Panel (Caporuscio, 2003). The GENMESH input file used for the CRA is located in the CMS library, LIBCRA1_GM.

4.1.1.2 MATSET: Fixed Data Input

Details of the functionality of MATSET are discussed in the Users Manual (WIPP PA, 2000). MATSET is the first step for assigning the material property values needed by BRAGFLO (Step 2 in Table 4.1.1). The GENMESH output file, which is input into MATSET, provides the initial material map. All materials and properties that are used in BRAGFLO modeling should be specified in this modeling step, although the values may be changed in subsequent steps. For example, the parameters that are assigned sampled values by the LHS software module in modeling Steps 3 through 5, must be assigned initial values by MATSET in order to create a slot to receive the sampled values.

Each property assignment requires specification of both the material (e.g. Salado halite) and the property (e.g. bulk compressibility) to be associated with that material. For PA analysis, MATSET extracts the information from the WIPP Parameter Database (Section 4.3) according to instructions in the user-supplied input control file. If the database contains information defining a distribution of values for a material/property pair,

MATSET retrieves the median value. At the end of this step all material assignments have been made and initial values have been assigned to all associated properties. Constant values are used with no changes. Selected values with distributions are assigned sampled values in the next modeling steps (Section 4.1.1.3) by the software applications, PRELHS, LHS, and POSTLHS. The median values of parameters with distributions are used in BRAGFLO calculations if they have not been selected for sampling. The MATSET input file used for the CRA is located in the CMS library, LIBCRA1_MS.

4.1.1.3 LHS: Sampled Data Input

Modeling Steps 3-5 (Table 4.1.1) employ the software module, PRELHS, LHS, and POSTLHS to generate repeatable sets (corresponding to vectors) of random values for selected input parameters. The WIPP application of the LHS software uses the Latin Hypercube Sampling (LHS) method (Iman and Shortencarier, 1984), and the theory and implementation of LHS is explained in the users manual (WIPP PA, 1996a). LHS provides 100 sets of sampled values, one per vector, based upon distribution information that is drawn from the WIPP Parameter Database. LHS supports a variety of data distributions including: normal, lognormal, uniform, loguniform, cumulative, triangular, and student-T distributions. Each sample set is repeatable because it is based upon a seed number supplied by the user.

The PRELHS code requires sampling control information supplied by the user in an ASCII input control file. The code queries the WIPP Parameter Database for the parameters that define the distributions for each sampled variable. The LHS code generates the 100 samples for each parameter. The POSTLHS code requires the output file from MATSET and generates 100 output CAMDAT files in which the initial median values have been replaced with the sampled parameters. Table 4.1.2 summarizes the parameters that are assigned sampled values by the LHS software. The independent variable name in the right hand column of the table is used in the analysis of BRAGFLO. Leading up to the analysis activities, all values are assigned according to a material/property pairings (e.g. MB138/log of permeability). The PRELHS input files used for the CRA are located in the CMS library, LIBCRA1_LHS.

TABLE 4.1.1: BRAGFLO CALCULATIONS STEPS

Modeling Step	Software Application	Version	W/PP Prefix	Function	Interaction
1)	GENMESH	6.08	GM	Generates the modeling grid and defines groups of cells as regions that are stored as material "blocks" in the output file.	User Input Control File
2)	MATSET	9.00	MS	Defines additional material blocks and extracts properties from the WIPP database and assigns material-property values.	User Input Control File & Input from GENMESH
3)	PRELHS	2.30	LHS1	Identifies correlated properties. Retrieves property distribution data from WIPP database. User identifies properties to be sampled. Accepts user specified "seed" number that is used by LHS2 to randomly select values of sampled variables.	User Input Control File & Input from MATSET
4)	LHS	2.41	LHS2	LHS sampling is performed creating 100 "vectors" of sampled data. Each vector is defined by a set of randomly generated values for sampled variable based upon the distribution information retrieved by LHS1 from the WIPP database.	No direct user interaction. Input from LHS1.
5)	POSTLHS	4.07	LHS3	Generates 100 CAMDAT output files (one for each vector).	No direct user interaction. Input from LHS2.
6)	ICSET	2.22	IC	Sets selected initial conditions such as initial brine saturation, and initial pressure in the Culebra and Magenta units at the edge of the grid. Other initial conditions are set in the next step.	User Input Control File & Input from LHS3
7)	ALGEGRACDB	2.35	ALG1	User can use ALGEBRACDB to calculate values for specified material properties from other input information (e.g. log permeability to permeability, bulk compressibility to pore compressibility, etc.).	User Input Control File & Input from ICSET

Information Only

Modeling Step	Software Application	Version	WIPP Prefix	Function	Interaction
				Calculations defining initial pressures, steel and biodegradable concentrations, gas generation rates, etc. are made.	
8)	PREBRAG	7.00	BF1	User specifies temporal parameters for BRAGFLO including drilling location and time and changes in material properties over time. This is the step where each scenario is defined.	User Input Control File & Input from ALG1
9)	BRAGFLO	5.00	BF2	Performs calculations for gas generations and gas/brine flow in a porous medium.	No direct user interaction. Input from BF1.
10)	POSTBRAG	2.40	BF3	Converts BF2 binary output file into the binary WIPP database format.	No direct user interaction. Input from BF2.
11)	ALGEBRACDB	2.35	ALG2	User defines time-integrated output variables used in the analysis of results (e.g. volume averaged pressures and saturations).	User Input Control File & Input from BF3.
12)	SUMMARIZE	2.20	SUM	Generates ASCII tables of output variables.	User Input Control File & Input from ALG2
13a)	SPLAT	1.02		Creates plots of output variables for each vector (usually 100)	User Input control File & Input from SUMMARIZE
13b)	PCCSRC	2.21		Performs correlation and regression analyses	User Input control File & Input from SUMMARIZE & LHS

Steps with user interaction are indicated with bold lettering

TABLE 4.1.2: LIST OF SAMPLED MATERIAL/PROPERTY PAIRS WITH DISTRIBUTION TYPE

INDEPENDENT VARIABLE	MATERIAL	PROPERTY	DISTRIBUTION	DESCRIPTION
ANHBCEXP	S_MB139	PORE_DIS	STUDENT	Brooks-Corey pore distribution parameter for anhydrite (dimensionless).
ANHBCVGP	S_MB139	RELP_MOD	cumulative	Pointer variable for selection of relative permeability model for use in anhydrite.
ANHCOMP	S_MB139	COMP_RCK	STUDENT	Bulk compressibility of anhydrite (Pa ⁻¹).
ANHPRM	S_MB139	PRMX_LOG	STUDENT	Logarithm of intrinsic anhydrite permeability (m ²).
ANRBR SAT	S_MB139	SAT_RBRN	STUDENT	Residual brine saturation in anhydrite (dimensionless).
ANRGSSAT	S_MB139	SAT_RGAS	STUDENT	Residual gas saturation in anhydrite (dimensionless).
BHPERM	BH_SAND	PRMX_LOG	UNIFORM	Logarithm of intrinsic borehole permeability (m ²).
BPCOMP	CASTILER	COMP_RCK	TRIANGULAR	Logarithm of bulk compressibility of brine pocket (Pa ⁻¹).
BPINTPRS	CASTILER	PRESSURE	TRIANGULAR	Initial pressure in brine pocket (Pa).
BPPRM	CASTILER	PRMX_LOG	TRIANGULAR	Logarithm of intrinsic brine pocket permeability (m ²).
CONBCEXP	CONC_PCS	PORE_DIS	cumulative	Brooks-Corey pore distribution parameter for the concrete portion of PCS (dimensionless).
CONBR SAT	CONC_PCS	SAT_RBRN	cumulative	Residual brine saturation in the concrete portion of PCS (dimensionless)
CONGSSAT	CONC_PCS	SAT_RGAS	UNIFORM	Residual gas saturation in the concrete portion of PCS (dimensionless)
CONPRM	CONC_PCS	PRMX_LOG	TRIANGULAR	Logarithm of concrete permeability (m ²). Of the DRZ above a panel closure
DRZPCPRM	DRZ_PCS	PRMX_LOG	TRIANGULAR	Logarithm of concrete the permeability (m ²).
DRZPRM	DRZ_1	PRMX_LOG	UNIFORM	Logarithm of DRZ permeability (m ²).
HALCOMP	S_HALITE	COMP_RCK	UNIFORM	Bulk compressibility of halite (Pa ⁻¹).
HALPOR	S_HALITE	POROSITY	cumulative	Halite porosity (dimensionless).
HALPRM	S_HALITE	PRMX_LOG	UNIFORM	Logarithm of halite permeability (m ²).
PLGPRM	CONC_PLG	PRMX_LOG	UNIFORM	Logarithm of concrete plug permeability (m ²).
SALPRES	S_HALITE	PRESSURE	UNIFORM	Initial brine pressure, without the repository being present, at a reference point located in the center of the combined shafts at the elevation of the midpoint of MB 139 (Pa).
SHLPRM2	SHFTL_T1	PRMX_LOG	cumulative	Logarithm of intrinsic permeability of the lower portion of the simplified shaft (0-200 years)(m ²).
SHLPRM3	SHFTL_T2	PRMX_LOG	cumulative	Logarithm of intrinsic permeability of the lower portion of the simplified shaft (after 200 years)(m ²).

Information Only

SHUPRM	SHFTU	PRMX_LOG	cumulative	Logarithm of intrinsic permeability of the upper portion of the simplified shaft (m ²).
SHURBRN	SHFTU	SAT_RBRN	cumulative	Residual brine saturation of the upper portion of the simplified shaft (dimensionless)
SHURGAS	SHFTU	SAT_RGAS	UNIFORM	Residual gas saturation of the upper portion of the simplified shaft (dimensionless)
WASTWICK	WAS_AREA	SAT_WICK	UNIFORM	Increase in brine saturation of waste due to capillary forces (dimensionless).
WFBETCEL	CELLULS	FBETA	UNIFORM	Scale factor used in definition of stoichiometric coefficient for microbial gas generation (dimensionless).
WGRCOR	STEEL	CORRMCO2	UNIFORM	Corrosion rate for steel under inundated conditions in the absence of CO ₂ (m/s).
WGRMICH	WAS_AREA	GRATMICH	UNIFORM	Microbial degradation rate for cellulose under humid conditions (mol/kg's).
WGRMICI	WAS_AREA	GRATMICI	UNIFORM	Microbial degradation rate for cellulose under inundated conditions (mol/kg's).
WMICDFLG	WAS_AREA	PROBDEG	cumulative	Pointer variable for microbial degradation of cellulose.
WRBRNSAT	WAS_AREA	SAT_RBRN	UNIFORM	Residual brine saturation in waste (dimensionless).
WRGSSAT	WAS_AREA	SAT_RGAS	UNIFORM	Residual gas saturation in waste (dimensionless).

Information Only

4.1.1.4 ICSET: Initial Conditions

Initial conditions required by BRAGFLO include pressure, saturation, and steel and biodegradable concentrations. From a data management perspective initial conditions are properties associated with the first numerical time step. Modeling Step 6 (Table 4.1.1) uses the application, ICSET to define some of these initial conditions. The functionality of ICSET is described in the users manual (WIPP PA, 1996c). The code requires a user-supplied input control file defining how initial conditions are to be set and the POSTLHS binary (.CDB) file from Step 5. ICSET updates the input CDB file with the user supplied initial conditions creating a new output CDB file. This step includes the definition of some initial conditions derived from MATSET and others set by the user:

- Initial brine saturation in the Santa Rosa and the unsaturated portion of the Dewey Lake is set to unsaturated conditions using values (from WIPP Parameter Database) at -5 years.
- Initial brine saturation is set to 0.015 in the material DRF_PCS and the waste areas at time zero.
- Initial brine saturation is set to zero in all excavated areas at time -5 years.
- Initial brine saturation is set to zero in non-waste excavated areas at time zero.
- Initial brine saturation in all portions of the grid, except for the repository and the unsaturated formations is set to 1.0 at -5 years.
- Initial steel and biodegradable concentrations throughout the grid are set to 0.0 at -5 years. (These values will be changed in the next step (4.1.1.5) when steel and biodegradable materials are introduced.)

The ICSET input file used for the CRA is located in the CMS library, LIBCRA1_IC.

4.1.1.5 ALGEBRACDB: Data Modification and Calculation of New Modeling Parameters

Modeling Step 7 (Table 4.1.1) employs the software module, ALGEBRACDB, which is used to manipulate data from the binary (.CDB) output file from ICSET. ALGEBRACDB is capable of performing most common algebraic manipulations and evaluating most common transcendental functions (trigonometric, logarithmic, exponential, etc.). Its functionality is discussed in the users manual (WIPP PA, 1996d).

ALGEBRACDB reads its instructions from a user-supplied ASCII input control file that employs an algebraic syntax that is similar in appearance to normal FORTRAN syntax. It then executes the mathematical instructions to modify input data from ICSET and to calculate new input parameters for the BRAGFLO software. The results are written to a new binary (.CDB) output file. Files associated with this step are designated with ALG1 in the filename, because ALGEBRACDB is also used in post-BRAGFLO processing.

Calculations performed in this step include:

- Calculation of inventories of steel and degradable organic material.
- Conversion between units stored in the WIPP Parameter Database and units required by BRAGFLO.

- Assignment of parameters sampled for one material to another material (e.g. hydraulic properties are sampled for MB 139 and assigned to the other marker beds in the model).
- Assignment of gas generation parameters including initial concentration, humid and inundated gas generation rates that depend on inventory and sampled parameters.
- Calculation and application of the 1° stratigraphic dip of the Salado Formation.

The ALGEBRACDB input file used for the CRA is located in the CMS library, LIBCRA1_ALG.

4.1.1.6 PREBRAG: Changes in Modeling Parameters Over Time

The final pre-processing step for BRAGFLO modeling (Step 8 in Table 4.1.1) employs the application PREBRAG, which accepts the binary (.CDB) output file from ALGEBRA (ALG1). The functionality of PREBRAG is discussed in the users manual (WIPP PA, 2003b). The user supplies instructions in an ASCII input control file to specify changes in modeling conditions at different times and to identify what information should be calculated and written by BRAGFLO to the output files. This is the modeling step in which "scenarios" are defined by specifying changes in materials and properties at different times (e.g. "create" a borehole at 350 or 1000 years by redefining the material map at that time in the simulation). The PREBRAG input files used for the CRA are located in the CMS library, LIBCRA1_BF.

4.1.2 BRAGFLO Calculations

Quantification of the effects of gas and brine flow on radionuclide transport for undisturbed and disturbed conditions requires use of a two-phase flow (brine and gas) code. For WIPP PA, the DOE uses the two-phase flow code, BRAGFLO, to simulate gas and brine flow as well as to incorporate the effects of disposal room consolidation and closure, gas generation, and rock fracturing in response to gas pressure (Step 9 in Table 4.1.1). Its functionality and the theory on which it is based are discussed in the users manual (WIPP PA, 2003a). The results of BRAGFLO include calculated values for variables at times and grid locations that are specified in the PREBRAG input control file. The output data is written to ASCII and binary output files. Only the binary files are used for Salado Flow analysis and for input to subsequent WIPP PA activities (e.g. NUTS modeling). The ASCII input files are stored in CMS in the libraries: LIBCRA1_BFR#S#, where the #-symbols are replaced by replicate and scenario numbers.

4.1.3 Post-BRAGFLO Processing

4.1.3.1 POSTBRAG

The post-BRAGFLO processing application, POSTBRAG, is used to convert the BRAGFLO binary output file (.BIN) into the binary format (.CDB) that is used by other WIPP PA software tools (Step 10 in Table 4.1.1). The software ALGEBRACDB is used to calculate cumulative and/or volume-averaged values for specific regions in the grid. The output is written to a binary (.CDB) file (modeling Step 11 in Table 4.1.1). Files associated with post-BRAGFLO processing using ALGEBRACDB are identified with ALG2 in their names.

4.1.3.2 ALGEBRACDB: Post-Processing of BRAGFLO Results (ALG2 Step)

In this post-processing step the software module, ALGEBRACDB is used to process BRAGFLO results that vary in time and space. In this step various quantities are calculated, including: volume-averaged pressure and saturation in different regions of the grid and cumulative fluxes of brine across certain boundaries. The ALGEBRACDB input file used for the CRA is located in the CMS library, LIBCRA1_ALG.

4.1.3.3 SUMMARIZE

The software module, SUMMARIZE (Step 12 in Table 4.1.1) is used to extract data from the binary output files (.CDB) from POSTBRAG or ALGEBRACDB (ALG2) to produce ASCII tables organized according to analytical needs. One common step is to create a table of output variables with values for 100 vectors reported at specified time intervals. In this case, SUMMARIZE will linearly interpolate output values at specific times from the nearest times in the binary file. This is necessary because BRAGFLO uses a variable time-step and thus vectors do not have output at exactly the same times. Previous to this step, output is organized with a separate file for each vector.

Tables from SUMMARIZE are used to make plots of variables over time (e.g. horsetail plots) using the plotting software module, SPLAT. These plots show the values of output variables for each of the 100 vectors in a scenario over time (usually the full 10,000 year regulatory period).

4.1.3.4 SPLAT

The application, SPLAT, is used to generate plots of output variables for selected vectors (usually all 100 in a scenario) from SUMMARIZE tables (one table per vector). SPLAT extracts the selected variable from each vector file, and produces a plot with one line per vector.

4.1.3.5 Sensitivity Analysis

Several approaches are used in the Salado Flow Analysis to evaluate the effects of sampled input parameters on BRAGFLO results. The simplest method is to use scatter plots to visually evaluate relationships of an output variable with a single input parameter (or another output variable).

Excel is used to calculate Pearson sample correlation coefficients for pairings of variables and input parameters. Pearson correlation coefficients were calculated to determine the relative importance of various input parameters to annualized brine outflow rates during this stage. The Pearson correlation coefficient, r , for two arrays, X and Y containing n elements is:

$$r = \frac{n(\sum XY) - (\sum X)(\sum Y)}{\sqrt{[n\sum X^2 - (\sum X)^2][n\sum Y^2 - (\sum Y)^2]}}$$

Pearson correlation coefficients vary from -1.0 to 1.0 and indicate the extent of a linear relationship between the two arrays.

The application, PCCSRC, is a systematic approach to identifying the most important input parameters (WIPP PA, 1995b). PCCSRC produces plots of correlation statistics for selected output variables (dependent variables) relative to sampled input parameters (independent variables). Partial rank correlation coefficients (PRCC's) are used in the Salado Flow Analysis, because some relationships may be non-linear over the full range of conditions represented in 100 vectors. These correlation calculations are performed on the ranks of the variables rather than their values, reducing problems due to non-linear relationships. Partial correlation coefficients are calculated by excluding the influence of all other parameters. Each PRCC explains how much of the ranking for the output variable can be explained by the ranking of the input variable with the linear effects of the other variables removed (Helton et al, 1998).

PRCC's are calculated at selected times to produce plots of PRCC's over an extended period of time. A cutoff of 0.25 is usually used for the PRCC in the Salado Flow Analysis, and only the top five PRCC's are plotted. The correlations may be positive or negative, and the absolute value of the PRCC indicates the relative importance of each input parameter to the uncertainty in the output variable.

4.1.4 Methods of Analysis

Methods of analysis are selected for each variable according to the nature of the modeling results. No one method is useful for all output variables, because distributions, trends, and dependencies differ. For example, cumulative values at 10,000 years are used frequently in the Salado Flow Analysis to evaluate results from a regulatory compliance perspective. They provide a simple measure of how modeling results compare to regulatory requirements for variables involving volume fluxes (e.g., brine flow).

The Salado Flow Analysis examines multiple of interactive process models (e.g., brine inflow, gas generation, fracturing and brine outflow). An analysis of annual rates (e.g., brine outflow in m^3/yr) can be a useful technique in specific circumstances (e.g., brine flow after the borehole connection to pressurized brine in the Castile has been sealed for E1² intrusions).

The calculation of median values for 100 vectors in a scenario is the most common approach to collective analysis in the Salado Flow Analysis. The median has the advantage of weighting the impact of every vector equally. However, the median over time does not represent a single vector, since different vectors may be at the median at different times over the 10,000-year regulatory period. Median values are not useful when half or more of the vectors have zero values (e.g., microbial gas generation).

In contrast, averages are strongly impacted by highly anomalous values, and they may not be representative for the entire population of results (e.g., cumulative brine outflow in S2 with a maximum of 156,000 m^3 and a median of 5,000 m^3). Average values are used occasionally if there are no highly anomalous values or if the number of zero-values is constant across the scenarios.

^{2 2} E1 and E2 intrusions are defined in section 4.3.1

Maximum values for an output variable are sometimes presented to evaluate dependencies and associations for the most extreme results. Again, different vectors may have the maximum value at different times. Groups of anomalous vectors are sometimes considered separately to isolate the causes, which may not be apparent in the whole population, because the primary dependencies are operative in a limited range of circumstances (e.g., fracturing at high pressure and brine flow at high borehole permeabilities).

4.1.5 Execution and Run control

Digital Command Language (DCL) scripts, referred to here as EVAL run scripts, are used to implement and document the running of all software codes. These scripts, which are the basis for the WIPP PA run control system, are stored in the CRA1_EVAL CMS library. All inputs are fetched at run time by the scripts, and outputs and run logs are automatically stored by the scripts in class CRA1 of the CMS libraries (Long, 2003).

4.2 DATA FOR THE SALADO FLOW ANALYSIS

There are three sources for input into the Salado Flow Analysis:

- WIPP Parameter Database
- Input control files supplied by the analyst
- The ASCII file from SANTOS containing the porosity closure surface.

4.2.1 WIPP Parameter Database

The WIPP Parameter Database is the primary repository for validated input data to WIPP PA activities. The database includes 1) numerical results from investigations performed under the WIPP Quality Assurance (QA) Program and 2) references to document validation of the data for usage in regulated analyses including the 2003 WIPP PA. Each input parameter has been investigated and evaluated under the WIPP Quality Assurance (QA) Program to assess the values or ranges of values that are appropriate for Salado Flow Analyses and subsequent WIPP PA activities.

Most parameters have discrete values (e.g. the acceleration due to gravity) in the WIPP Parameter Database, but some are described by a distribution of possible values with associated probabilities. Parameter distributions are appropriate for describing variability in the geological environment and for representing uncertainty due either to limitations of measurements or unpredictability of changes over the 10,000-year regulatory period.

4.2.2 Input Control Files

User-supplied input files are required in many steps of the Salado Flow modeling process (Table 4.1.1). These files contain the instructions that control the computational processes. Some of the most prominent tasks specified in these input files include:

- specification of dimensions for the BRAGFLO logical grid.
- assignment of values to properties and materials (constants, median values, and sampled values).
- calculation of new input values in pre-BRAGFLO processing.
- timing of changes in the modeling domain (e.g., borehole intrusion).
- calculation of integrated results for analyses in post-BRAGFLO processing

For a list of files used in the 2003 CRA, see Long (2003).

4.2.3 Porosity Surface From SANTOS

In addition, BRAGFLO version 5.0 requires information defining the porosity surface for the repository in the format of an ASCII input file. This table is generated by the analysis of creep closure results from the SANTOS software. At present, only one porosity surface is validated for use in PA analyses (WIPP PA, 2003a).

4.2.4 Transfer of Information Between Software Modules

The BRAGFLO modeling process involves the use of several software modules, which have been integrated into a continuous BRAGFLO modeling process. Output files from one module often become input files for a subsequent modeling step. However, this is an automated process controlled by scripts that are preserved in class CRA1 in LIBCRA1_EVAL of CMS, and intermediate output files are preserved in class CRA1 of the relevant CMS library.

4.3 UNCERTAINTY IN SALADO FLOW ANALYSIS

Evaluation of the risks of uncertainty are addressed in three ways in the Salado Flow Analysis:

- Scenarios representing possible future events (drilling intrusions) are modeled to evaluate the potential consequences.
- Latin hyper-cube (random) sampling of key input parameters is used to evaluate uncertainty and variability of input data.
- Comparison of results from three different replicates (100 vectors per replicate) provide a means for assessing statistical uncertainty.

4.3.1 Uncertainty of Future Events - Scenarios

Drilling intrusion is a likely human activity to affect flow and transport near the repository during the 10,000-year regulatory compliance period. Six scenarios capture the effects of a potential drilling intrusion, and the events modeled in each scenario are summarized in Table 4.3.1.

TABLE 4.3.1: BRAGFLO MODELING SCENARIOS

SCENARIO	DESCRIPTION
S1	Undisturbed Repository
S2	E1 intrusion at 350 years
S3	E1 intrusion at 1000 years
S4	E2 intrusion at 350 years
S5	E2 intrusion at 1,000 years
S6	E2 intrusion at 1,000 years; E1 intrusion at 2,000 years.

E1: Borehole penetrates through the repository and into a hypothetical pressurized brine reservoir in the Castile Formation.

E2: Borehole penetrates the repository, but does not encounter brine in the Castile

The long-term effects of penetration by an exploratory borehole are calculated for two intrusion times, 350 years and 1,000 years following repository closure. The earlier time (350 years) is representative of intrusions for which a significant amount of americium exists and more time is available for Culebra ground water transport. The later intrusion time (1,000 years) is representative of the repository after the pressure has stabilized. The choice of just two intrusion times is a compromise dictated by the massive computational effort required in PA calculations.

Salado Flow modeling only considers the effects of an intrusion on brine and gas flow. Analyses of radionuclide transport and potential for release are analyzed in subsequent PA activities using brine flow fields calculated by BRAGFLO.

4.3.2 Variability and Uncertainty of Input Parameters

There are a variety of reasons for uncertainty concerning input parameters to the Salado Flow Model, including: geological variability, changes in the physical/chemical environment over the 10,000-year regulatory period, and limitations on measurements and sampling. Analysis of uncertainty for input parameter values is accomplished by sampling values for selected input parameters from distribution ranges that are stored in the WIPP Parameter Database using the LHS software (Section 4.1.1.3). Thirty-three input parameters have been designated as having ranges of values that should be sampled to provide input for Salado Flow Analysis. Other parameters are also sampled at the same time, but these values are only used in subsequent WIPP PA modeling activities and do not impact the Salado Flow Model.

Most of the sampled variables (Table 4.1.1) are assumed to be uncorrelated. However, the pairs (ANHCOMP, ANHPRM), (HALCOMP, HALPRM) and (BPCOMP, BPPRM) are assumed to

have rank correlations of -0.99 , -0.99 and -0.75 , respectively. These correlations result from a belief that the underlying physics implies that a large value for one variable in a pair should be associated with a small value for the other variable in the pair.

4.3.3 Statistical Uncertainty - Replicates

There are three replicates in the Salado Flow Analysis, and each consists of 100 sets of sampled parameters. Thus each scenario is actually modeled in 300 vectors, 100 in each replicate. Comparison of results between the three replicates provides an indication of statistical reliability.

For notational convenience, the replicates are designated R1, R2, and R3. The most extensive analysis was performed on replicate R1. The other two replicates were used for comparison purposes to confirm the statistical validity of R1.

5.0 MODELING RESULTS

Numerical results from the Salado Flow Analysis are stored in the binary (.CDB) files that reside in class CRA1 of the CMS libraries: LIBCRA1_BFR#S#, where the #-symbols are replaced with replicate and scenario numbers. These results include detailed and summarized information about:

- Creep closure of the excavated areas of the repository.
- Gas generation by corrosion of metal and microbial decomposition of organic material.
- Pressure.
- Fracturing of rock due to high pressure
- Permeability.
- Brine and gas saturation.
- Brine and gas flow.

Other output data may be selected by the user, but this may require adjustments to pre- and post-processing steps. The Salado Flow output data are preserved for all cells and areas of the grid at incremental times between 0 and 10,000 years.

The application, ALGEBRACDB, is used to post-process numerical output from BRAGFLO resulting in data that are more useful for analysis. The output variables from ALGEBRACDB are listed in Appendix A.

Graphics are used extensively to demonstrate observations, relationships, and dependencies. "Horsetail" plots, which are produced using the application, SPLAT, plot values of individual variables for all vectors in a scenario as a function of time for the entire 10,000-year regulatory compliance period. These plots are an effective method for demonstrating the potential range and behavior of results. "Composite" plots display the statistics for a replicate over time (e.g., median, mean, 10th and 90th percentiles for 100 vectors in a scenario). These plots are used to

collectively view results for comparison purposes (e.g., comparing trends for two different output variables). The VMS application, PCCSRC, is used to correlate output variables with sampled input parameters and to generate plots displaying the most prominent partial correlation coefficients (PRCC) over time.

5.1 EXCEPTION VECTORS

The ASCII input control file to PREBRAG includes a series of input numerical control parameters that influence the way BRAGFLO performs calculations. The standard settings optimize calculations under most circumstances, but occasionally BRAGFLO does not complete the calculations for individual vectors, which are referred to as exception vectors. The most common failure is that BRAGFLO calculations do not reach 10,000 years within the maximum number of time steps prescribed (10,000 time steps). Exception vectors usually result from the combination of extreme conditions of coincident sampled variables and very small grid cells (e.g., the intersection of the borehole or shaft with a marker bed). These circumstances can lead to extreme spatial or temporal gradients within the model domain that exceed tolerances specified in the input control file. These conditions cause BRAGFLO to shorten its time step. For most vectors this automatic time-step control is sufficient to solve the short-lived numerical problem, however for exception vectors it is not and it is necessary to relax, tighten, or otherwise adjust BRAGFLO input numerical control parameters in order to complete the calculations.

The capability to make such adjustments is a normal part of any numerical modeling study including the BRAGFLO modeling process. The input control parameters are included in BRAGFLO code to permit the analyst to make adjustments for circumstances that fall outside of the normal range of modeling conditions and allow a difficult calculation to complete. Description of adjustments to input control parameters for exception vectors are included in the discussion of results for each scenario.

Changing the value of the input control parameter, ICONVTEST, is the most common adjustment to BRAGFLO to allow the completion of calculations for "exception" vectors. The following excerpt from the users manual (WIPP PA, 2003a) explains when the standard value, "1", should be changed to "0".

"ICONVTEST: Flag specifying whether *either* or *both* convergence criteria must be satisfied before a solution is considered to have converged. Recommended value: 1. Requiring both convergence criteria to be met should result in a more accurate solution. However, prohibitively small time steps are sometimes required because the convergence tests tend to over-emphasize the importance of small grid blocks in which small changes can result in relatively large mass balance errors. To get BRAGFLO to run to completion when such problems occur, it may be necessary to relax one of the criteria that must be met. Generally, this has been found to have little impact on gross results. However, in some instances, important short-lived transient results can differ greatly depending on whether either or both convergence criteria are met. Therefore, whenever possible, ICONVTEST = 1 should be used.

- = 0: Satisfy *either* EPSNORM or FTOLNORM. (described next, on Lines 6.10 and 6.14).
- = 1: Satisfy *both* EPSNORM and FTOLNORM. (described next, on Lines 6.10 and 6.14)."

5.1.1 Replicate 1

In Replicate 1, BRAGFLO calculations for eight vectors did not run to completion using standard input control values. Calculations for two of these ("1" in Table 5.1.1) were completed by changing the value for ICONVTEST from "1" to "0". This is discussed in Section 5.1 and in the users manual (WIPP PA, 2003a). Vector 98 (2 in Table 5.1.1) in all six scenarios, also required changing the value of the input parameter, FTOLNORM(1), from 1.0E-2 to 1.0E-3. This change reduced the error tolerance allowed between iterations and prevented the development of uncontrolled oscillations in the solution in subsequent time steps. The following excerpt from the BRAGFLO users guide explains the adjustment to this parameter (WIPP PA, 2003a):

"FTOLNORM(1): [kg gas in residual/kg gas in grid block]. For gas saturation, the value of the residual is normalized by dividing by the amount of gas present in the grid block, $\phi(\rho_g S_g + C_{gb} \rho_b S_b)$, where ϕ is the porosity, ρ_g and ρ_b are the gas and brine densities at local conditions, S_g and S_b are the gas and brine saturations, and C_{gb} is the mass fraction of gas in the brine phase ($C_{gb} = 0.0$ if no dissolved gas is present). The minimum of this normalized residual value is compared with FTOLNORM(1). If ICONVTEST = 0 and the normalized residual is less than FTOLNORM(1), convergence is accepted".

The adjusted value for FTOLNORM(1) is still within the recommended range. "Tightening" this input control parameter prevented the calculation of residual gas saturation from diverging further than before the change and thus time step length did not need to be reduced as much to reach convergence.

TABLE 5.1.1: EXCEPTION VECTORS, REPLICATE 1

Vector	S1	S2	S3	S4	S5	S6
18					1	
79		1				
98	2	2	2	2	2	2

5.1.2 Replicate 2

Eleven vectors were rerun with modified input control parameters in order to have BRAGFLO complete the calculations. Calculations for ten of these ("1" in Table 5.1.2) were completed by changing the value for ICONVTEST from "1" to "0". Vector 56 in Scenario 1 also required that EPS_NORM(1) be changed from 3.0 to 2.0 ("3" in Table 5.1.2). The following excerpt from the users manual confirms that this parameter is still within the recommended range.

EPSNORM(1): Number of digits of accuracy to the right of the decimal in the change in gas saturation. This parameter limits the change in gas saturation when saturations are very small, in which case DDEPMAX(1) is too easily satisfied. Recommended value range: 2 to 5 with a best estimate of 3.

TABLE 5.1.2: EXCEPTION VECTORS, REPLICATE 2

Vector	S1	S2	S3	S4	S5	S6
13	1		1		1	
56	3	1	1	1	1	1
71				1		
99						1

5.1.3 Replicate 3

Five vectors were rerun with modified input control parameters in order to have BRAGFLO complete the calculations. All five exception vectors ("1" in Table 5.1.3) were completed by changing the value for ICONVTEST from "1" to "0".

TABLE 5.1.3: EXCEPTION VECTORS, REPLICATE 3

Vector	S1	S2	S3	S4	S5	S6
20	1					
27	1			1		1
28	1					

5.2 OVERVIEW OF THE SALADO FLOW ANALYSIS

Repository behavior is characterized by interactions among creep closure, gas generation, and fluid and gas flow. The Salado Flow Analysis is divided into three replicates, and each is comprised of the same six modeling scenarios. Replicate 1 is the primary subject for analysis, and the other two are used to confirm the results for the most important output variables and to demonstrate statistical confidence in the results. Each scenario consists of 100 vectors that are defined by a unique set sampled input values (modeling Step 3-5/Table 4.1.1).

5.2.1 Organization

The discussion of results is organized by scenario or pair of scenarios as follows:

- Section 5.3: Undisturbed (Scenario 1)
- Section 5.4: Disturbed (Scenarios 2 and 5)
- Section 5.5: Comparison of replicates

Each of the sections listed above includes an analysis of the following:

- *Halite Creep.* The plastic flow of salt causes the pore volume of the repository to decrease over time by gradually filling the empty space.
- *Brine Inflow.* Availability of brine is required for gas generation and for fluid flow away from the repository.
- *Gas Generation.* In some scenarios, gas generation results in high pressures within the repository.
- *Pressure.* High pressure within the repository can increase permeability of wall rock by causing hydro fracturing. This is a primary output variable to subsequent PA analyses (e.g., spallings, direct brine release).
- *Brine Saturation.* This affects the rate of steel corrosion. This is also a primary output variable to subsequent PA analyses (e.g., direct brine releases).
- *Rock Fracturing.* Caused by high gas pressure. Rock fracturing can increase permeability of the wall rock in the DRZ and of anhydrite in the marker beds providing a conduit for local brine migration (e.g., around the panel closures and into the shaft).
- *Brine Outflow.* Brine outflow to the accessible environment is a potential carrier for radionuclide transport. Brine flow up the borehole is an input variable to analysis of radionuclide flow and transport in the Culebra.
- *Comparison of results* among the replicates.

5.2.2 Halite Creep

Creep closure of the excavated regions begins immediately because of excavated-induced loading. As rooms close waste consolidation will occur and continue until back stresses imposed by compressed waste resist further closure or until fluid pressure becomes sufficiently high due to gas generation.

BRAGFLO calculates the porosity of materials that undergo creep closure by interpolating over a "porosity surface." The porosity surface consists of porosity as a function of time and pressure and was obtained by modeling deformation of a waste-filled room using the code, SANTOS (Butcher et al., 1995 and Stone 1995). The creep closure porosity surface is provided to BRAGFLO via the ASCII file, BF2_CRA1_CLOSURE.DAT, which resides in the CRA1 class of the CMS library: LIBCRA1_BF.

5.2.3 Summary of Gas Generation Factors

The rate of gas generation strongly influences repository pressurization and fluid flow along potential pathways for radionuclide migration. Gas generation may occur as a result of 1) anoxic corrosion of steel-based waste and waste containers, and 2) biodegradation of organic materials (cellulosics, plastics, and rubbers) in waste and waste containers. It is assumed that there is a probability of 1.0 that gas is generated by anoxic corrosion of steel and that there is a probability of 0.5 that microbial degradation of organic material will occur.

The anoxic corrosion of steel-based metals is assumed to consume brine as part of the reaction, and therefore brine must be present in the waste regions for corrosion reactions to proceed. Moreover, it is assumed that inundated conditions are necessary for corrosion; the humid rate of corrosion is set to zero. The rate of corrosion is zeroth-order and is sampled (Step 3-5 in Table 4.1.1) and remains fixed for the 10,000-year regulatory period.

The potential for gas generation by microbial action in the repository is uncertain so three possibilities are considered in Salado Flow models. WMICDFLG is a sampled input parameter that controls the amount of biodegradable material that is available to the microbes for gas generation. Possible values of WMICDFLG are: 0, 1, and 2 where:

- "0" implies no microbial degradation of cellulose (50% probability)
- "1" implies microbial degradation of only cellulose only (25% probability)
- "2" implies microbial degradation of cellulose, plastic and rubber (25% probability).

Gas generation by microbial degradation occurs in both inundated and humid conditions. The inundated rate is a sampled parameter, WCRMICI, and the humid rate calculated by multiplying the inundated rate by a sampled parameter, WGRMICH (factor < 1; median = 0.634). Microbial gas generation requires brine to be present, but it is assumed the microbes do not consume or produce water. The rate of total gas generation is directly dependent upon brine saturation. It declines until brine saturation becomes zero at which time all microbial gas generation ceases.

5.2.4 Coupling of Gas Generation and Brine/Gas Flow

Gas generation and brine and gas flow are related. Since moisture is required for both corrosion and microbial gas generation processes and it is consumed by the corrosion of steel, the rate of brine inflow into the repository affects the total rate of gas generation. However, generally brine inflow decreases as pressure increases, and brine may eventually be expelled from the repository if pressure exceeds brine pressure in the surrounding formation. One result of this might be the slowing or even stopping of the gas generation process in some vectors. In addition, if pressures exceed the fracture initiation pressure, additional brine may flow into the repository from the surrounding DRZ.

Similarly, gas may flow away from the waste into areas with lower pressure, which may include the northern experimental and operations areas, the DRZ, the anhydrite interbeds and the shaft. Gas flow into intact halite is not significant because of the high threshold pressure of halite.

5.3 MODELING RESULTS FOR UNDISTURBED PERFORMANCE (R1S1)

Previous analyses (U.S. DOE, 1996; PAVT, 1997; Helton et al., 1998; and Hansen et al., 2002) have identified two potential pathways for brine flow and radionuclide transport away from the repository in the undisturbed scenario. In the first pathway, brine may migrate through the panel seals and drifts or through the disturbed rock zone (DRZ) surrounding the repository to the shaft and then upwards towards the Culebra Dolomite Member of the Rustler Formation. The quantity of brine reaching the Culebra is important, because lateral groundwater transport can carry radionuclides towards the subsurface land withdrawal boundary. In the second pathway, brine may migrate from the repository through the DRZ and laterally towards the subsurface land withdrawal boundary through the anhydrite interbeds of the Salado formation.

In addition, pressure and brine saturation in the undisturbed scenario are important variables because conditions in this scenario are used as initial conditions that are required by codes used to calculate direct releases from the first intrusion into the repository. Subsequent intrusions use to conditions calculated for the disturbed scenarios.

5.3.1 Sequence of Events

There is only one change to material properties specified in the PREBRAG input control file for Scenario 1. This is a change in lower shaft materials 200 years after closure to reflect compaction that is applied to all scenarios.

Scenario 1

200 years - change in lower shaft material properties to reflect compaction. Material SHFTL_T1 is replaced by material SHFTL_T2.

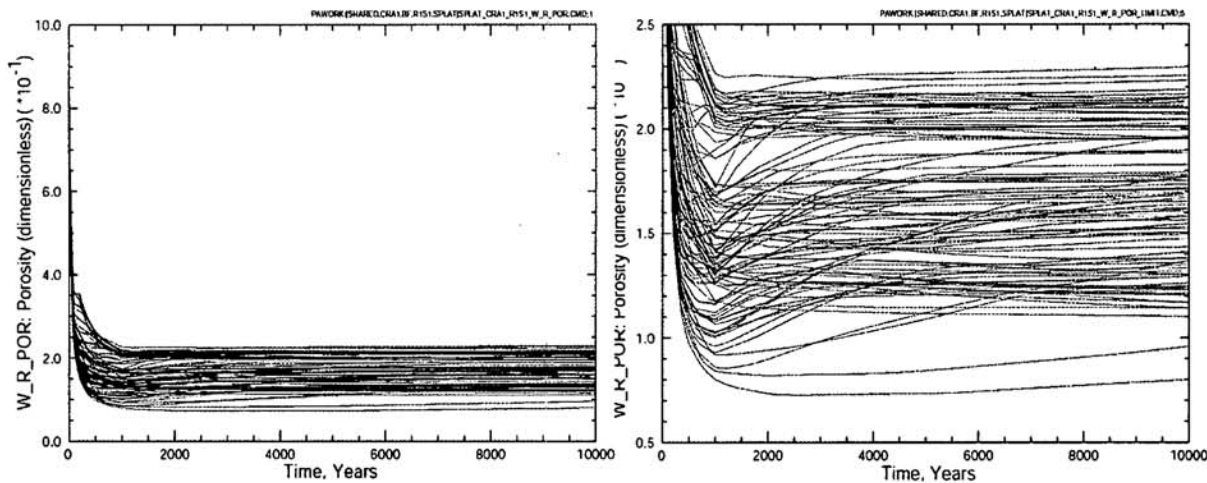
5.3.2 Porosity and Halite Creep

Halite creep causes the pore volume (void space), of the waste filled regions of the repository to decrease over time as halite flows to fill the excavated space and compresses the waste. Porosity is calculated by dividing the pore volume by total volume, and it can be expressed as a fraction or as pore volume percent of total volume. Creep closure trends are also summarized in Appendix B.

The output variable, W_R_POR, is the volume-averaged porosity for all waste areas. The values of W_R_POR, over the 10,000-year modeling period, are plotted for all 100 vectors of Scenario 1 in Figure 5.3.1a. Figure 5.3.1b shows the same data plotted on a reduced porosity range (5% to 25%) to better illustrate the trends of individual vectors. The porosity in all vectors drops from its initial value of 84.8% to a minimum value that ranges from 8% to 23% at 10,000 years. However, much of the reduction in pore volume (35% and 53%) occurs during the first 50 years. Increasing pressure within the repository often causes temporary reversal periods when porosity increases for some time. Five vectors, 24, 35, 38, 51, and 56, in Scenario 1 do not show a reversal in creep closure (an increase in pore volume after the initial decrease in response to

increased pressure). Fifty vectors have increases in porosity from their minimum values that range from 1.0% to 7.6% increases.

Figure 5.3.2 displays plots for input parameters that have the highest partial rank correlation coefficients (PRCC) with volume-averaged porosity in all waste areas, W_R_POR. The positive correlations of gas generation factors, WMICDFLG, WASTWICK, WGRCOR, HALPOR, and WGRMICI reflect reduced creep closure by increasing pressure resulting from gas generation.



a) Porosity range displayed = 0 to 1.0

b) Porosity Range Displayed = 0.05 To 0.25

Figure 5.3.1: R1S1 - Volume Averaged Porosity In All Waste Regions Over 10,000 Year

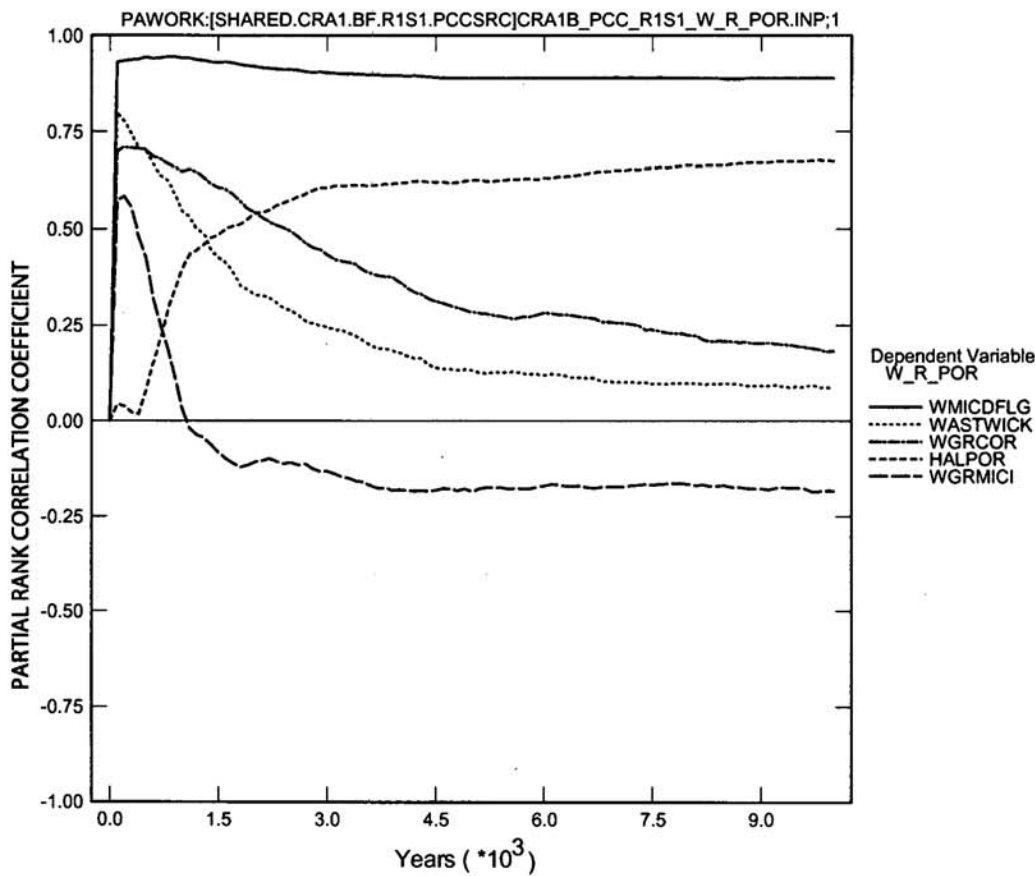


Figure 5.3.2: R1S1 - Primary Correlations Of Porosity In The Waste Regions (W_R_POR) With Sampled Input Parameters

5.3.3 Brine Inflow

In the undisturbed scenario, brine can only come into contact with the waste by flowing through or from the DRZ into the repository, and the only significant external source of brine to the DRZ is from the anhydrite marker beds. There may also be a substantial volume of in situ brine within the DRZ that is available for flow into the repository depending upon the porosity of halite (HALPOR), which is a sampled value, and the permeability of the DRZ, which can be increased by high pressure within the repository due to fracturing. The output variable, BRAALIC, is the cumulative total brine inflow from all marker beds into the DRZ (Figure 5.3.3a) and BRNREPTC is the cumulative total brine flow into the repository (Figure 5.3.3b). Horsetail plots for BRAALIC and BRNREPTC in Scenario 1 are plotted at the same scales in Figure 5.3.3 to illustrate how brine flow from the marker beds into the DRZ is less than the brine flow from the DRZ into the repository.

A scatter plot of BRAALIC versus BRNREPTC indicates no prominent relationship between the two brine flows, indicating that brine flow into the DRZ from the anhydrite marker beds is not the primary source for brine flow into the repository (Figure 5.3.4a). However, a scatter plot of halite porosity, HALPOR, versus BRNREPTC shows a generally linear relationship indicating that in situ brine within the DRZ is the primary source for brine flow into the repository in the undisturbed scenario (Figure 5.3.4b).

Brine inflow statistics for BRAALIC and BRNREPTC are summarized in Tables 5.3.1 and 5.3.2. The median cumulative brine inflow from all marker beds into the DRZ, $\sim 1,200 \text{ m}^3$, is only 16% of the median cumulative brine inflow into the repository, $\sim 7,200 \text{ m}^3$. Vector 22 has the largest cumulative brine flow into the repository, $49,000 \text{ m}^3$, but it has only 850 m^3 of cumulative brine inflow from the marker beds into the DRZ. Table 5.3.2 contains brine inflow values for the 10 vectors with the largest BRAALIC values and for the 10 vectors with the highest BRNREPTC values. It indicates that high brine flows into the repository are not correlated with brine flow into the DRZ, but high brine flows into the DRZ are generally associated with brine flow into the repository that are average or above average.

TABLE 5.3.1: STATISTICS FOR CUMULATIVE BRINE INFLOW AT 10,000 YEARS

	BRAALIC (m^3)	Vector	BRNREPTC (m^3)
max	22,194	V048	34,201
min	23	V018	439
	BRNREPTC	Vector	BRAALIC
max	49,258	V022	854
min	77	V090	120

Note: BRAALIC - total brine inflow from all marker beds into the DRZ
 BRNREPTC - total brine flow into the repository

TABLE 5.3.2: HIGH BRINE INFLOW AT 10,000 YEARS

Vector	BRNREPTC (m ³)	BRAALIC (m ³)
22	49,258	854
48	34,201	22,194
29	31,662	1,195
34	30,508	1,667
87	28,947	3,012
75	27,657	566
6	26,597	184
63	26,187	628
41	25,466	350
9	24,778	2,164
48	34,201	22,194
97	13,560	18,947
84	7,552	18,302
31	17,876	10,181
17	4,728	9,575
96	11,808	8,937
91	11,483	8,672
28	23,312	7,844
33	10,369	7,749
81	7,459	7,141
Avg	10,775	2,296
Med	7,232	1,195

The plot of prominent PRCC's for BRNREPTC also shows that HALPOR has the dominant influence on brine inflow, because it determines how much brine is stored in the DRZ (Figure 5.3.5). HALPOR is followed in importance by the permeabilities of the DRZ (DRZPRM), anhydrite (ANHPRM), and halite (HALPRM), because they influence the rate of brine flow.

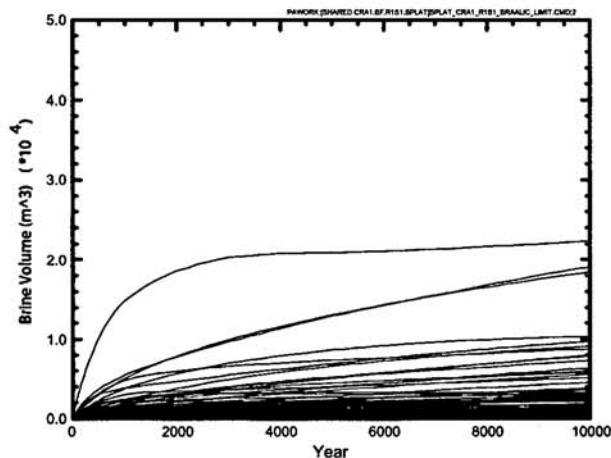
The anhydrite marker beds (Figure 3.1.1) provide the only significant pathways by which brine can flow from the Salado Formation into the DRZ, (BRAALIC). The DRZ and anhydrite permeabilities, DRZPRM and ANHPRM, have positive PRCC's with BRAALIC, and the microbial gas generation flag (WGMICDFLG) has a comparable negative PRCC (Figure 5.3.6). Higher permeability favors brine flow and higher gas generation results in higher pressure that resists brine inflow. Table 5.3.3 shows results of cumulative brine inflow from all marker beds into the DRZ at 10,000 years. The largest brine inflows occur through MB 139, and almost no inflow occurs through MB 138. More brine flows into the DRZ from the north end of the repository, because this is up the local stratigraphic gradient (Table 5.3.3).

Salado Flow results indicate that the shaft is not a significant potential source of brine inflow into the repository. Figure 5.3.7 shows that the maximum cumulative flow of brine down the shaft (at the base of the Culebra) is $\sim 66 \text{ m}^3$ compared to the median cumulative brine flow into the repository of $7,232 \text{ m}^3$.

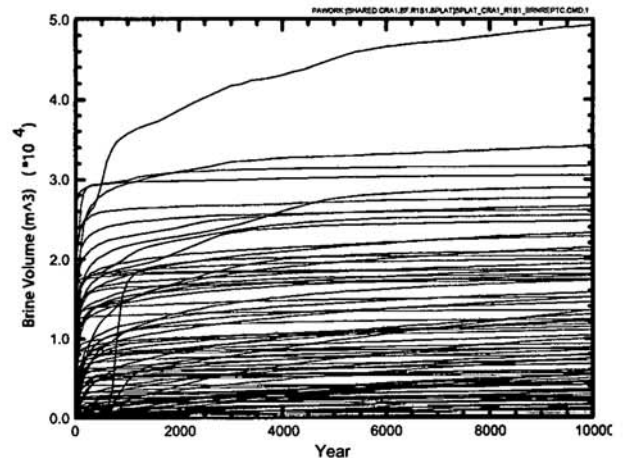
TABLE 5.3.3: SUMMARY OF CUMULATIVE BRINE INFLOW FROM ALL MARKER BEDS INTO THE DRZ AT 10,000 YEARS

Output Variable	BRM39NIC	BRM39SIC	BRAABNIC	BRAABSIC	BRM38NIC	BRM38SIC
Flow path	MB39 North	MB39 South	Anhy AB North	Anhy AB South	MB38 North	MB38 South
max	9,889	6,139	5,002	2,248	67	762
min	1	7	0	1	0	0
avg	1,110	671	465	273	5	74
med	513	314	186	118	1	17

Note: cumulative brine flows in m^3 .



a) Cumulative Brine Inflow From All Marker Beds Into the DRZ



b) Cumulative Brine Inflow Into the Repository

Figure 5.3.3: R1S1 - Cumulative Brine Inflow

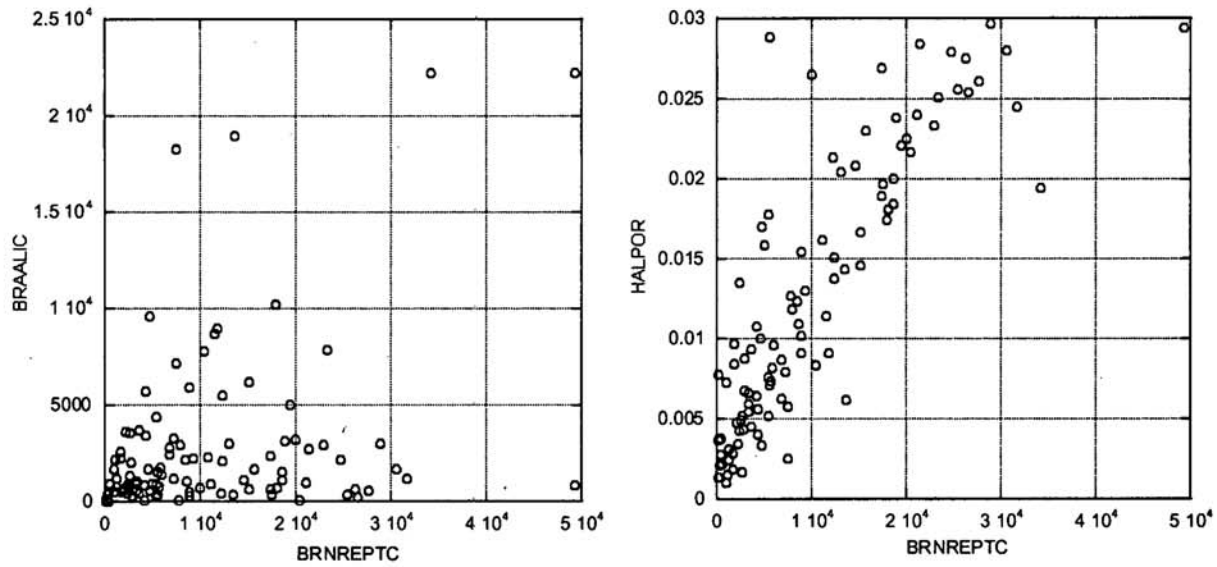


Figure 5.3.4: R1S1 - Scatter Plots For Total Cumulative Brine Flow Into the Repository with a) BRAALIC and b) HALPOR

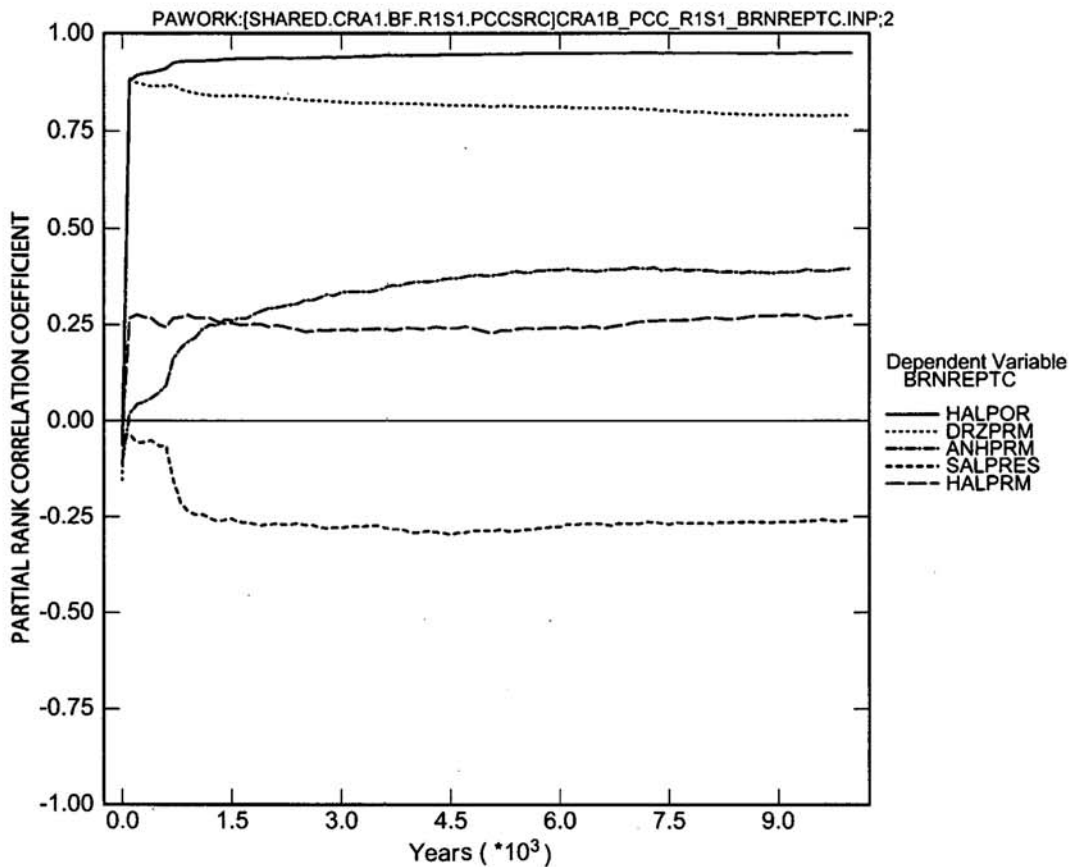


Figure 5.3.5: R1S1 - Primary Correlations for BRAGFLO Brine Inflow (BRNREPTC) Towards the Repository

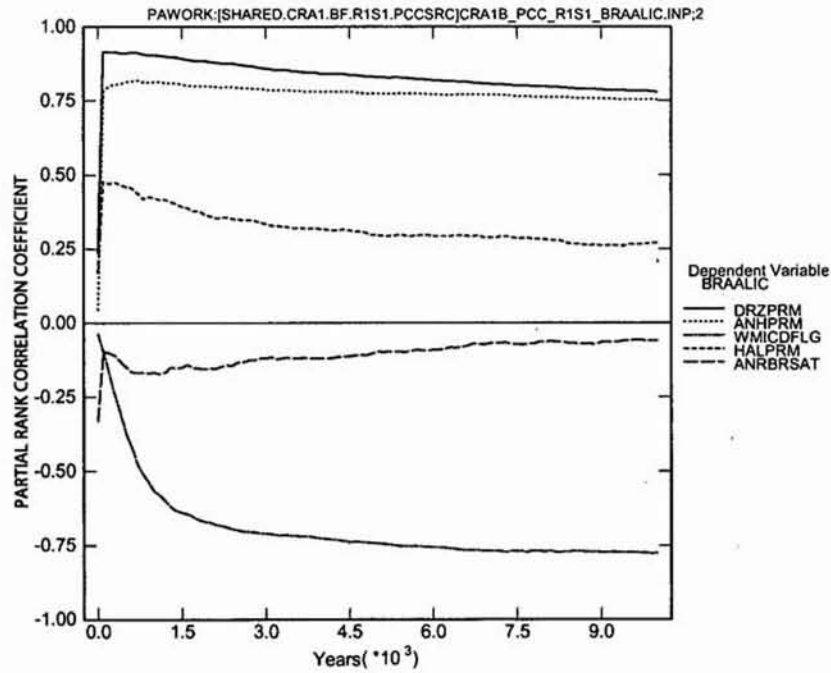


Figure 5.3.6: R1S1 - Primary Correlations for BRAGFLO Brine Inflow (BRAALIC) Into the DRZ

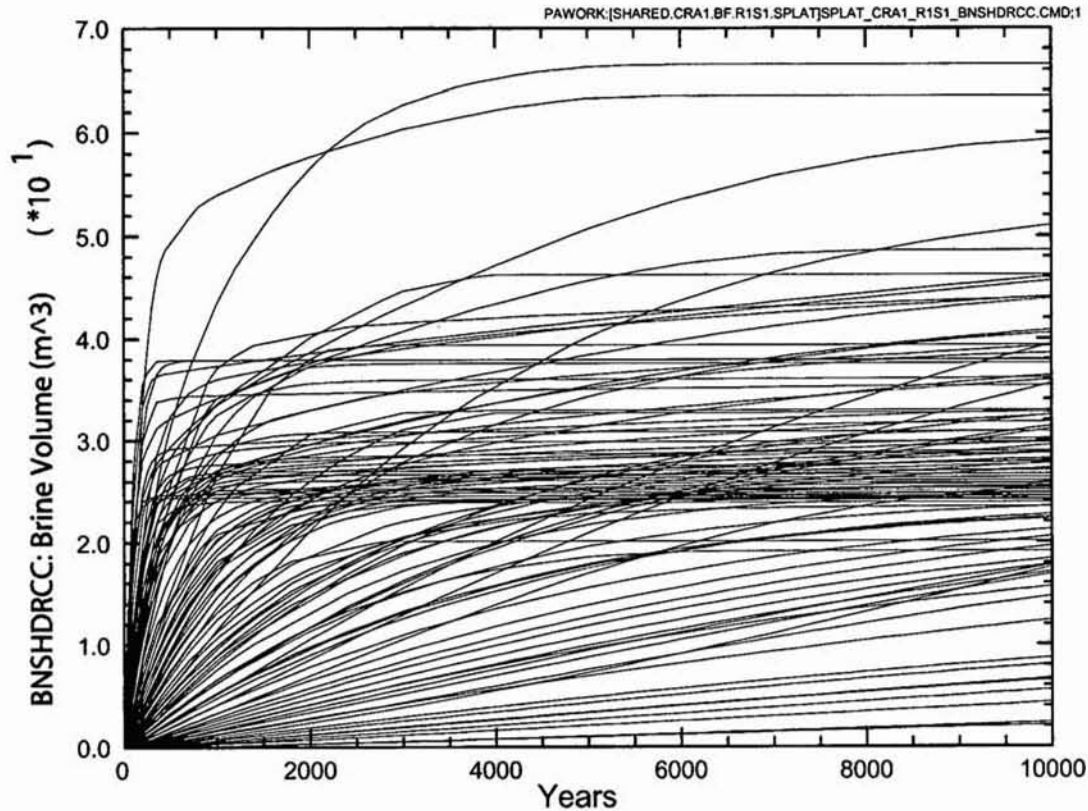


Figure 5.3.7: Cumulative Brine Flow Down the shaft at the Base of the Culebra

Information Only

5.3.4 Brine Saturation

Brine saturation is an important result of the Salado Flow model, because (1) gas generation processes require the availability of brine to proceed and (2) Direct Brine Releases (DBR), which are modeled in another PA activity, depend on the brine saturation in the waste regions calculated by BRAGFLO. Statistics for volume-averaged brine saturation in different regions of the repository are summarized in Table 5.3.4. Brine saturation in the Waste Panel, WAS_SATB, ranges from near zero to 0.98. Generally, brine saturation (average and median values) is greater in the Waste Panel than in the RoR areas, because the Waste Panel 1) is down the stratigraphic dip and 2) has direct contact with the Marker Beds (Figure 5.3.8). Likewise brine saturation is much higher in the Operations Area than in the Experimental Area, because 1) the Operations area is down the local stratigraphic gradient and 2) the intervening barrier, CONC_MON, is relatively permeable (10^{-14} m^2).

TABLE 5.3.4: VOLUME-AVERAGED BRINE SATURATION AT 10,000 YEARS

Material	Output Variable	min	10 th percentile	med	avg	90 th percentile	max
Waste Panel	WAS SATB	5.96E-08	2.26E-06	1.13E-02	8.71E-02	2.68E-01	9.80E-01
RoR South	SRR SATB	0.00E+00	2.19E-07	1.27E-05	2.52E-02	7.51E-02	4.61E-01
RoR North	NRR SATB	0.00E+00	2.38E-07	1.28E-05	2.36E-02	7.44E-02	4.60E-01
Operations Area	OPS SATB	1.51E-02	3.01E-02	3.02E-01	4.12E-01	1.00E-00	1.00E+00
Experimental Area	EXP SATB	5.02E-03	2.46E-02	6.05E-02	8.52E-02	1.36E-01	7.35E-01

Brine saturation increases rapidly in all excavated areas, but the amount of the initial increase is determined by factors such as the permeability of the DRZ, DRZPRM, and the porosity of halite, HALPOR. Initially there is a large pressure differential between the DRZ and the excavated regions, and the relatively high permeability of the DRZ, compared to undisturbed halite, permits the rapid influx of brine. Brine inflow slows as the pressures equalize, as brine saturation in the DRZ decreases, as gas generation gradually increases the pressure in many vectors. Brine saturation begins to decrease in vectors with sufficiently high pressure as brine inflow is impeded, and eventually, brine may be forced out of the excavated areas if pressure rises sufficiently.

The Waste Panel has the widest range of volume-averaged brine saturation with values at 10,000 years (Figure 5.3.8a) ranging from a low of 6×10^{-8} to a high of 0.98 (Table 5.3.4). Many vectors show a sharp increase in brine saturation during the first 500 years when pressure is relatively low. Then brine saturation declines in most vectors to 10,000 years due to continuing gas generation by corrosion, which increases the pressure in some vectors (Figure 5.3.8).

The range of brine saturation in the RoR areas is 0.0 to 0.46 (Figure 5.3.8b & c). These areas, which are up the hydrological gradient from the Waste Panel, have the lowest average and median brine saturation values due to consumption of brine by corrosion, to increased pressure by gas generation, and to reduced brine inflow due to the presence of excavated areas on both sides (Table 5.3.4).

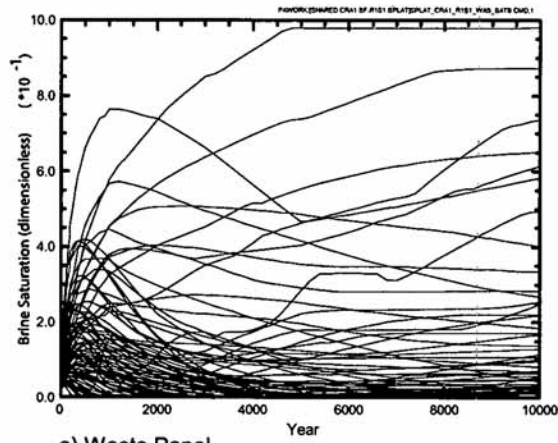
The Experimental and Operations non-waste areas, at the north end of the grid, have higher median and average brine saturations than the waste-filled areas (Table 5.3.4). These two non-waste areas are separated in the CRA modeling grid by the concrete-filled portion of the shaft (CONC_MON), which is relatively permeable. Consequently brine migrates quickly from the Experimental area down dip into the Operations areas. The result is high brine saturation in the Operations Area (avg = 0.46) versus the Experimental Area (avg = 0.09) (Figure 5.3.9). The waste-filled and non-waste areas are separated by Option D panel closures, which block the flow of brine to and from the Operations Area, BNRRNFLW and BNRRSFLW respectively. As in the waste-filled areas of the repository, there is a sharp increase in brine saturation during the first 500 years, but the maximum saturations are much lower than in the waste-filled areas, not exceeding 0.4 for most vectors (Figure 5.3.8d), because there is less fracturing of the DRZ adjacent to the non-waste areas to release in situ brine.

The relationship between brine saturation and pressure changes as a function of pressure. At low pressures, which commonly occur early in the modeling period, there is a positive correlation between brine saturation and pressure, because increases in saturation accelerate the rate of gas generation, which results in increasing pressure. However, at higher pressures, which develop as a consequence of gas generation, the correlation decreases and become negative, because increasing pressure tends to impede brine inflow. Eventually, high pressure drives brine out of the repository thereby reducing brine saturation. Figure 5.3.10 illustrates both correlations for vector 100. The crossover from positive to negative correlation between brine saturation and pressure occurs at about 11.4 MPa for Vector 100 in Figure 5.3.10, but this change varies greatly according to conditions influenced by the interaction of a variety of sampled input parameters. The coupling of brine inflow, brine consumption and pressure in the low and high-pressure ranges obscure the importance of individual input parameters at each end of the pressure spectrum. It is difficult to segregate the two regimes because the transition is gradual, and other factors effect brine saturation and gas generation.

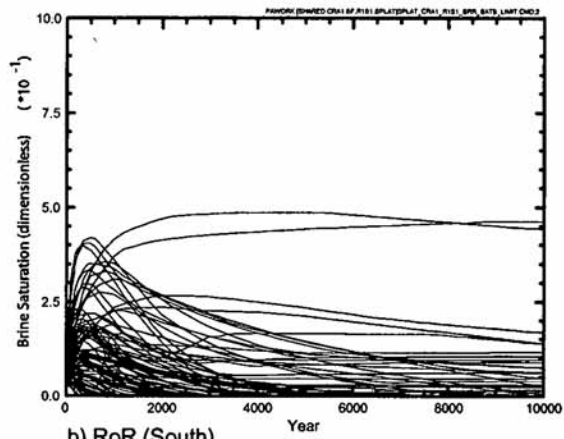
The PRCC's for brine saturation in the Waste Panel, WAS_SATB, show positive correlations with halite porosity, HALPOR, and DRZ permeability, DRZPRM (Section 5.3.3). There are also negative PRCC's with the gas generation factors, corrosion rate, WGRCOR, the wicking factor which influences corrosion, WASTWICK, and the microbial gas generation flag, WMICDFLG, because gas generation increases pressure, limiting brine inflow (Figure 5.3.11).

The PRCC's for brine saturation in the combined non-waste areas are significantly different due to its separation from gas generating processes in the waste by Option D panel closures (Figure 5.3.12). The two non-waste areas are considered jointly for brine saturation analysis, because the low permeability of the barrier between them permits the rapid migration of brine to the lowest excavated space. There are positive PRCC's with HALPOR and DRZPRM and a negative PRCC for WMICDFLG as in the Waste Panel. However, halite permeability, HALPRM, and anhydrite permeability, ANHPRM, have significant positive PRCC's in the non-waste areas, because increased permeability favors brine flow into the repository. The effects of gas generation are reduced because of the Option D panel closures.

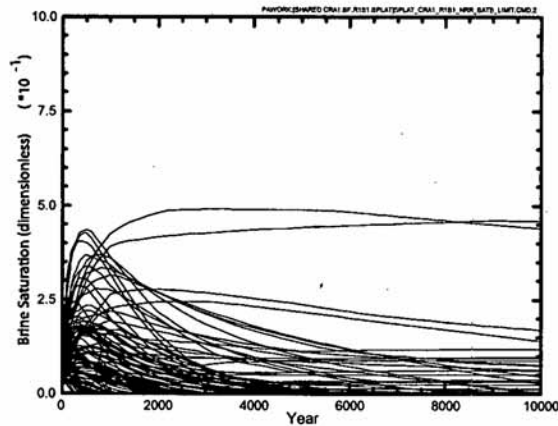
Information Only



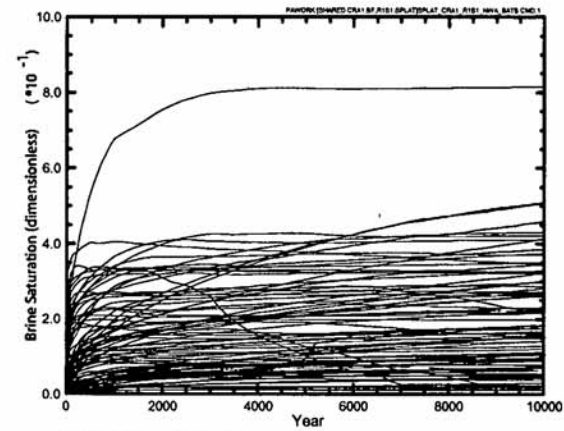
a) Waste Panel



b) RoR (South)



c) RoR (North)



d) non-waste areas

Figure: 5.3.8: R1S1 – Volume-Averaged Brine Saturation

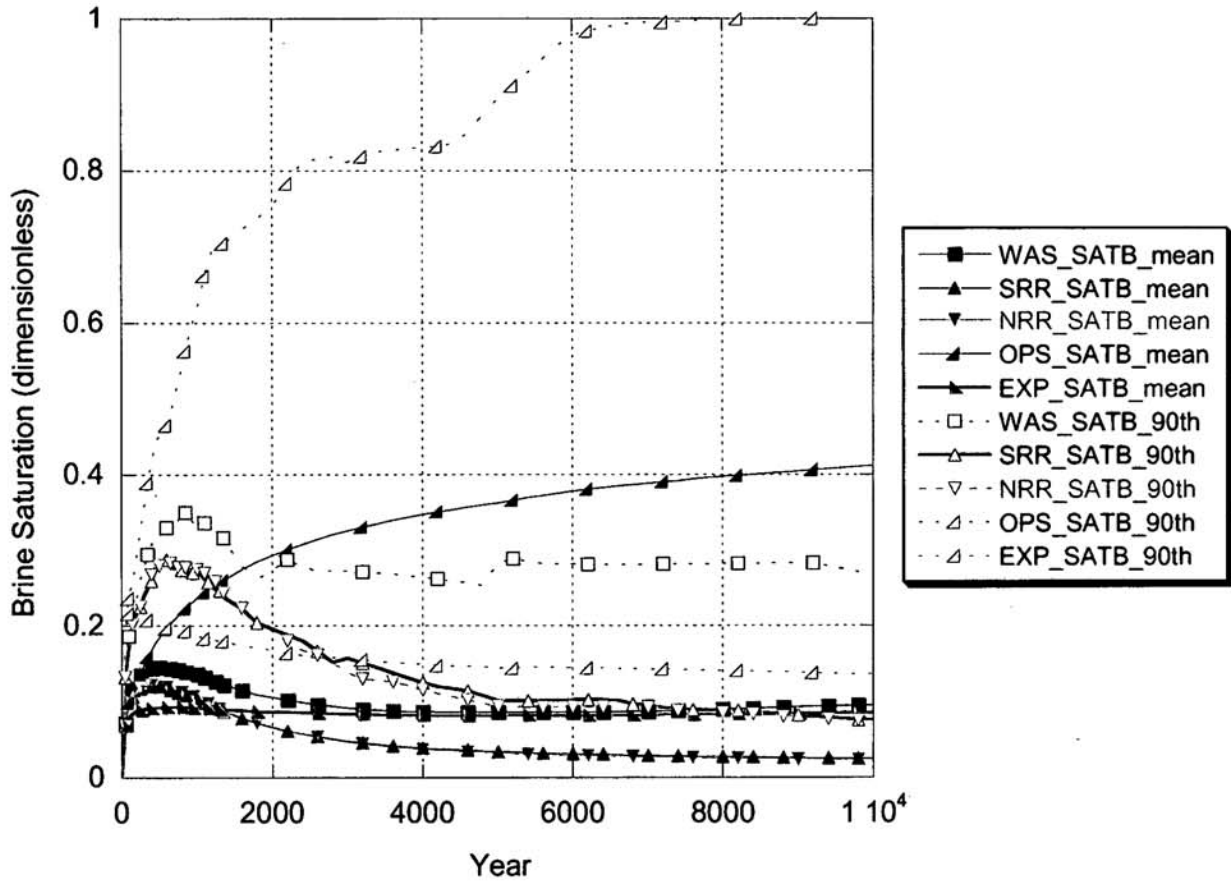


Figure 5.3.9: R1S1 - Brine Saturation in Excavated Areas

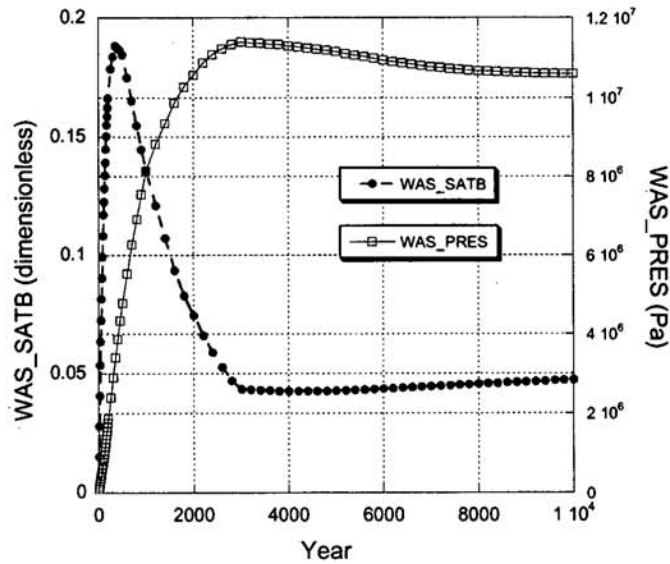


Figure 5.3.10: R1S1, Vector 100 Brine Saturation and pressure in the Waste Panel

Information Only

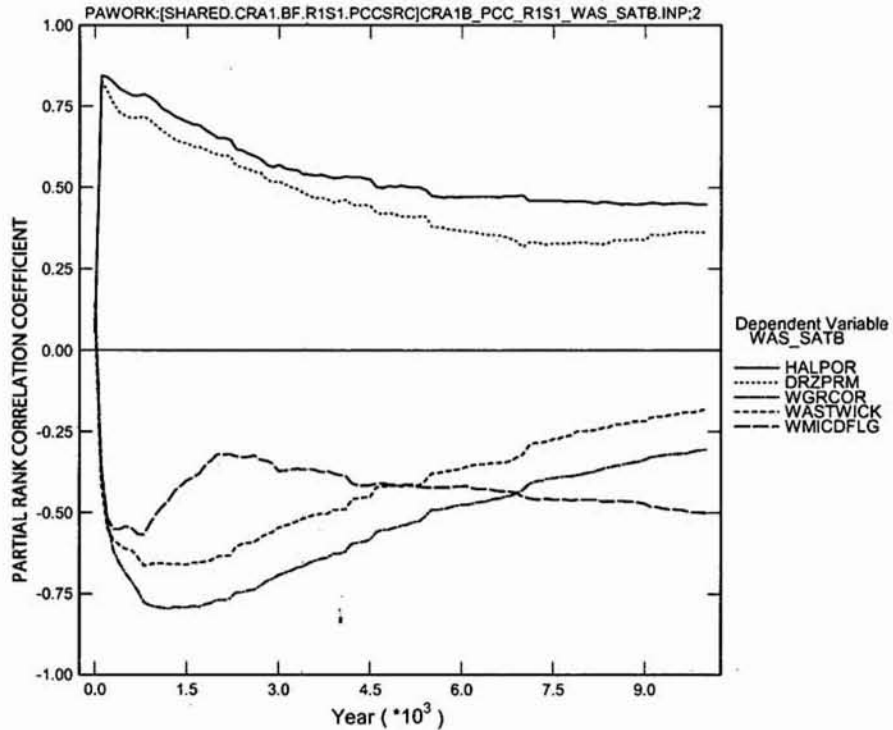


Figure 5.3.11: R1S1 - Primary Correlations of Brine Saturation in the Waste Panel, WAS_SATB, with Input Parameters in the Waste Panel

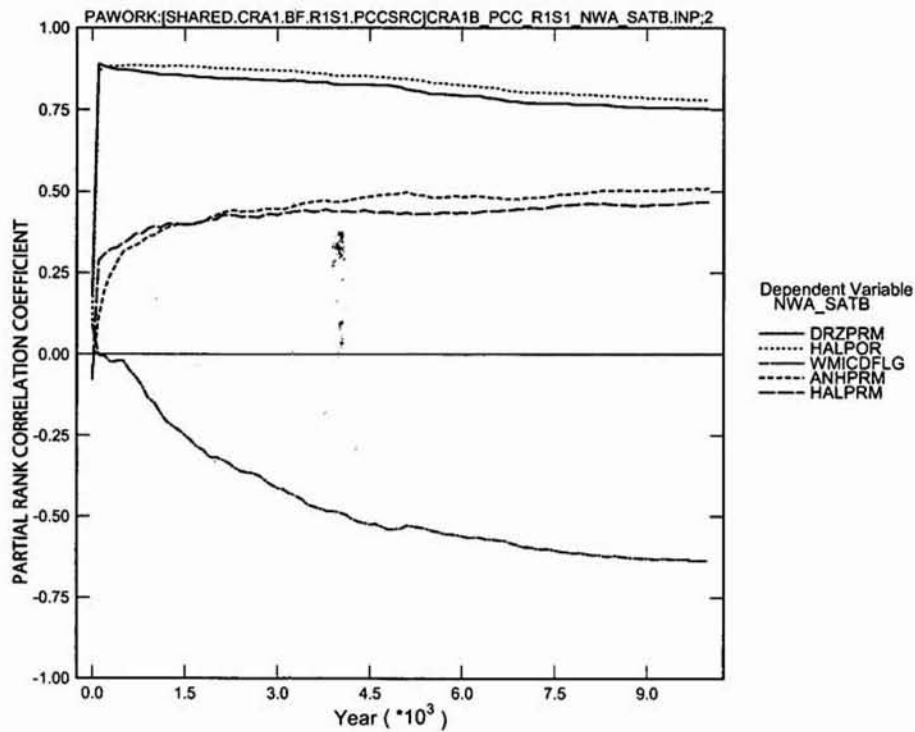


Figure 5.3.12: R1S1 - Primary Correlations of Brine Saturation in Non-Waste Areas, NWA_SATB, with Input Parameters

Information Only

5.3.5 Gas Generation

There are two potential sources for gas generation in the Salado Flow Model. The corrosion of steel, in the presence of brine, generates hydrogen gas, and microbial degradation of organic material in the waste, including cellulose, rubber, and plastic, may yield methane, CO₂ and other gases. However, all gas is assumed to have the properties of hydrogen in BRAGFLO. The CO₂ portion of the gas produced by microbial degradation is assumed to be sequestered by MgO and is thus not released into the repository.

5.3.5.1 Gas Generation by Corrosion

Gas generation by corrosion continues until all steel or all brine is consumed. On average, gas generation by corrosion declines rapidly after 1,000 years, but it continues at a relatively slow rate in many vectors to the end of 10,000 years (Figure 5.3.13). Cumulative gas generated by corrosion is not limited by the availability of steel (Figure 5.3.14) since at least 30% of the steel remains in all vectors at 10,000 years. Brine availability is the limiting factor for gas generation by corrosion for many vectors (Figure 5.3.15).

Brine is consumed in the corrosion process, and increasing pressure, which impedes brine inflow, further reduces brine availability. At high pressure, brine can be driven out of the repository. Figure 5.3.15 shows that brine volume in the repository declines rapidly approaching zero in many vectors by 3,000 years.

Initially, the corrosion rate parameter, WGRCOR, and the wicking factor, WASTWICK, have high positive correlations with gas generation by corrosion. Both determine the rate of corrosion, but halite porosity, HALPOR, becomes the dominant input parameter at about 1,600 years as brine availability becomes the factor determining how long corrosion continues (Figure 5.3.16).

5.3.5.2 Gas Generation by Microbial Activity

The nature of microbial gas generation is determined by the microbial gas generation parameter, WMICDFLG. Fifty percent of all vectors have no gas generation by microbial activity. Twenty-five percent of vectors have microbial gas generation by degradation of cellulose only and the other twenty-five percent have gas generation by degradation of cellulose, rubber, and plastic. Most microbial gas generation occurs in the first 1,000 years, and its cessation is indicated by horizontal lines depicting cumulative moles of gas generated (Figure 5.3.17). The higher level (about 5.3×10^8 moles) represents vectors with degradation of cellulose, rubber, and plastic, and the lower level (about 1.8×10^8 moles) represents vectors with cellulose degradation only. The flattening of each vector to a horizontal line usually results from the complete degradation of available organics (Figure 5.3.18).

Six vectors in Scenario 1 (Figure 5.3.17) show that microbial degradation has all but stopped before all decomposable organic material is consumed. For these vectors, brine saturation has dropped to levels very close to zero, and the sampled humid degradation rate is also low (Fig. 5.3.16). Consequently, some decomposable organic material survives to the end of the 10,000-year regulatory period for these vectors (Figure 5.3.18).

Figure 5.3.19 shows the five most prominent correlations of microbial gas generation to sampled input parameters. The positive correlation of microbial gas generation with WMICDFLG is nearly 1.0 from time zero to 10,000 years, because this parameter determines whether there is microbial degradation in each vector and what type of material (cellulosics or cellulose, plastics, and rubbers) is degraded. The influence of the other parameters is not significant. Since the PRCC of WMICDFLG is nearly one and microbial degradation goes to completion in most vectors, WMICDFLG accounts for virtually all of microbial gas generation.

When brine saturation is zero, microbial gas generation ceases, and if brine saturation is greater than zero microbial gas generation rate is calculated as the weighted average of two rates, the inundated rate and the humid rate. The fraction of organic material in the waste that is subjected to inundated degradation is equal to the brine saturation of the area, and the fraction that is subjected to humid degradation is equal to the gas saturation. (Brine and gas saturation add to 1.0.) Thus, as brine saturation becomes very small (e.g., 10^{-6}), microbial gas generation approaches the humid rate. Conversely, when a grid cell is totally saturated, microbial degradation proceeds at the inundated rate. Overall, more microbial gas generation (more than 80% for most vectors) takes place under inundated than humid conditions. Microbial degradation of inundated organics proceeds quickly in the first few hundred years when brine saturation is relatively high in many vectors due to the initial influx of brine after closure of the repository. There is usually enough brine present to permit complete degradation of organics.

5.3.5.3 Total Gas Generation

Total gas generation (Figure 5.3.20) is obtained by combining gas generation due to corrosion (Figure 5.3.13) and gas generation due to microbial degradation (Figure 5.3.17). On average, total cumulative gas generation by corrosion is almost twice as much as the average gas generation by microbial degradation (Figure 5.3.21). However, 50% of all vectors have no microbial gas generation.

Rates of gas generation provide insight concerning the dynamics of BRAGFLO modeling (Figure 5.3.22). Microbial gas generation peaks in the first 200 years and declines to virtually zero by 1,000 years. Gas generation by corrosion starts at a lower rate, but it continues in most vectors at a very low rate to the end 10,000 years. After about 300 years the corrosion gas generation rate is greater than microbial gas generation.

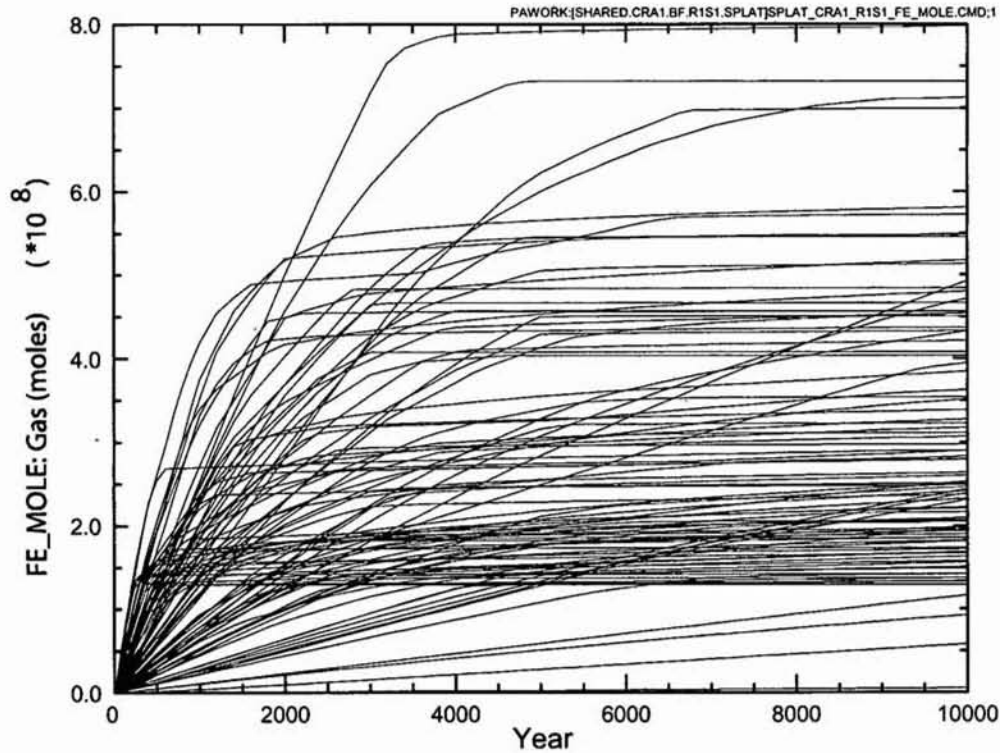


Figure 5.3.13: R1S1 - Cumulative Gas Generation Due to Corrosion of Steel

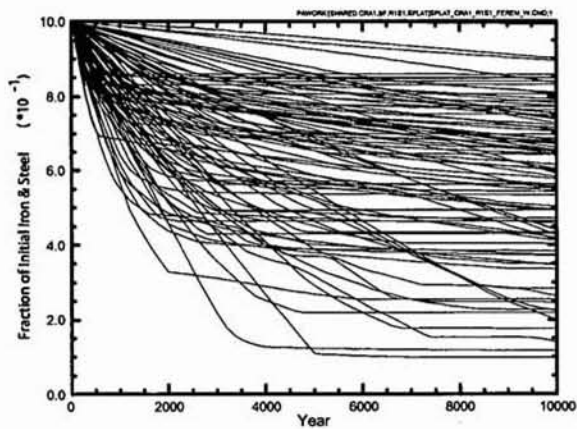


Figure 5.3.14: R1S1 - Fraction of Steel Remaining in the Waste Panel

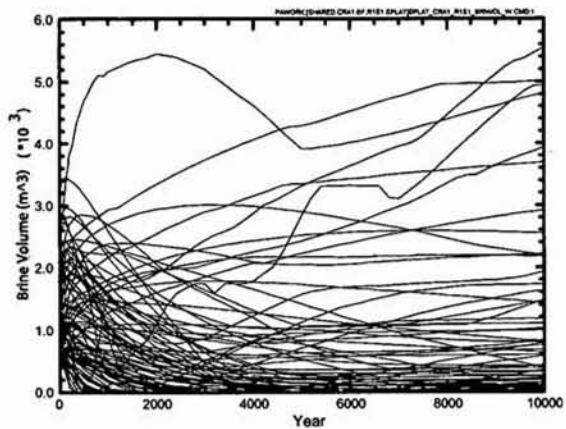


Figure 5.3.15: R1S1 - Brine Volume Remaining in the Waste Panel

Information Only

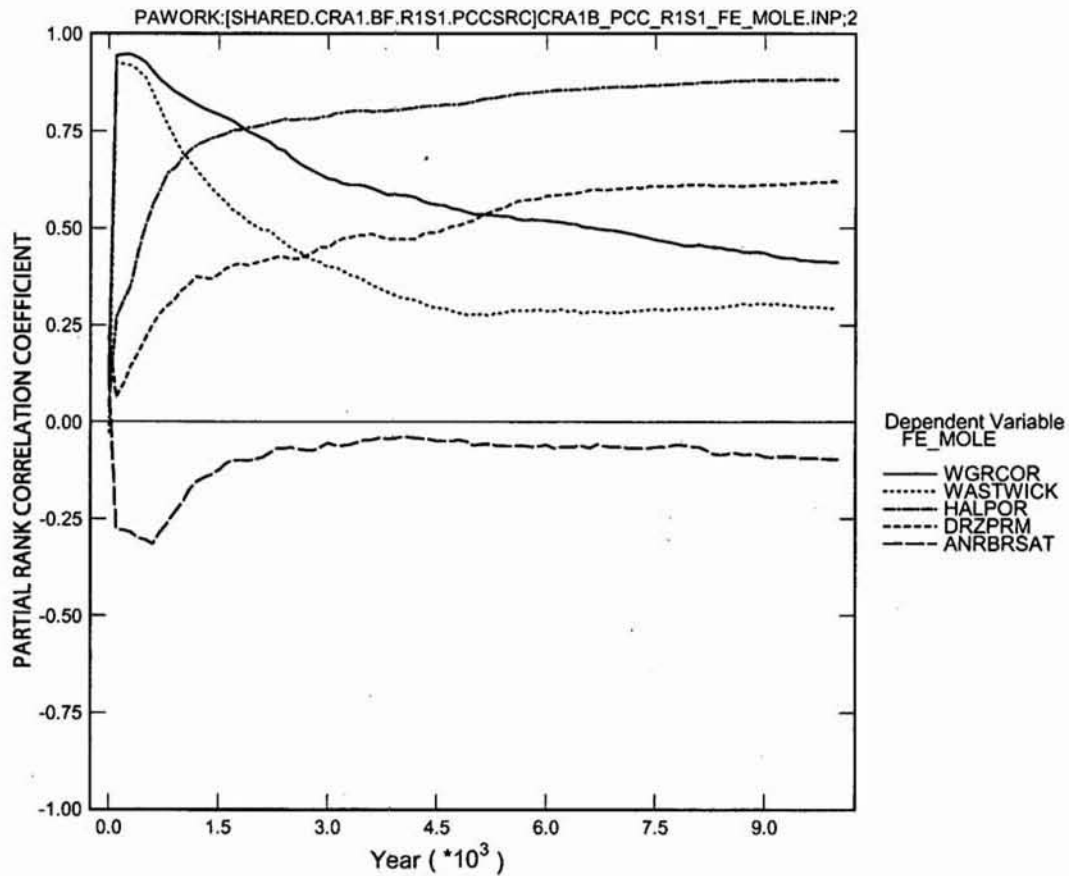


Figure 5.3.16: R1S1 - Primary Correlations of Gas Generation by Corrosion, FE_MOLE, with Input Parameters

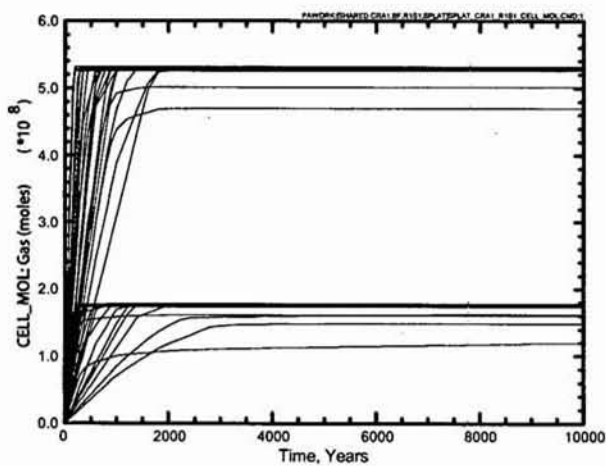


Figure 5.3.17: R1S1 - Cumulative Gas Generation Due to Microbial Activity

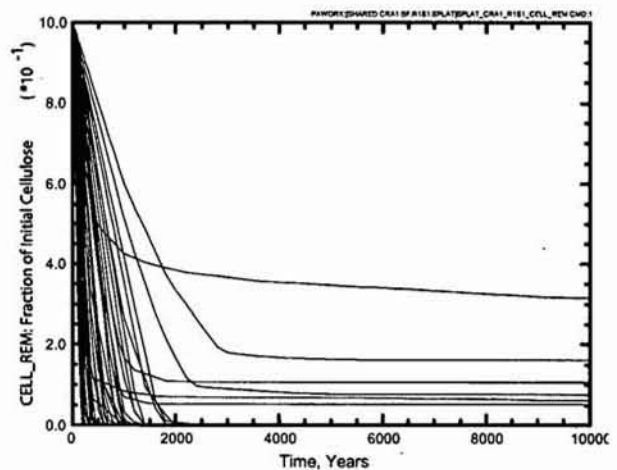


Figure 5.3.18: R1S1 - Remaining Fraction of Cellulosics

Information Only

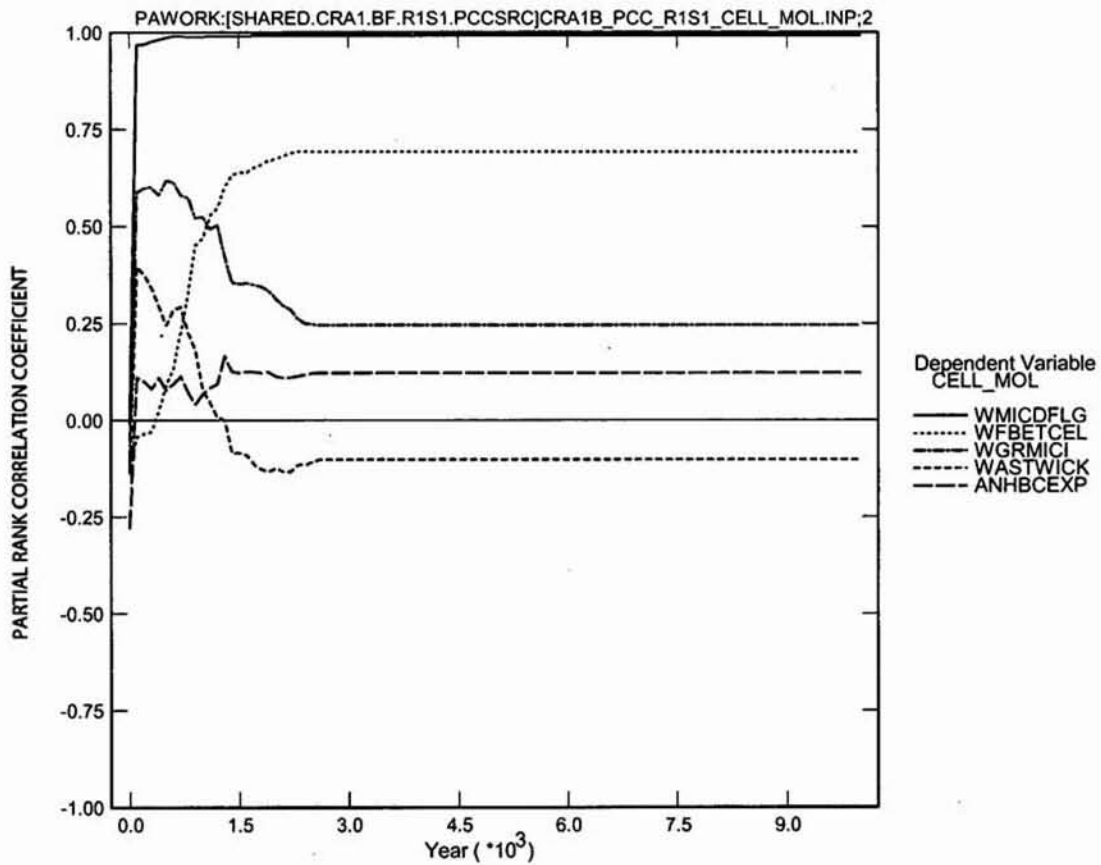


Figure 5.3.19: R1S1 - Primary Correlations of Cumulative Microbial Gas Generation with Input Parameters

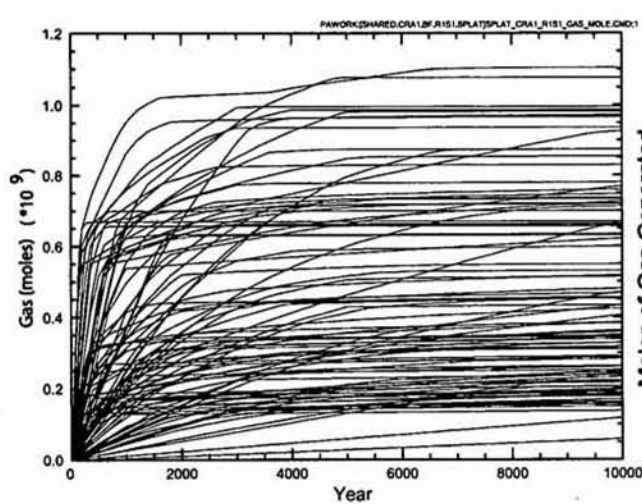


Figure 5.3.20: R1S1 - Total Cumulative Gas Generation

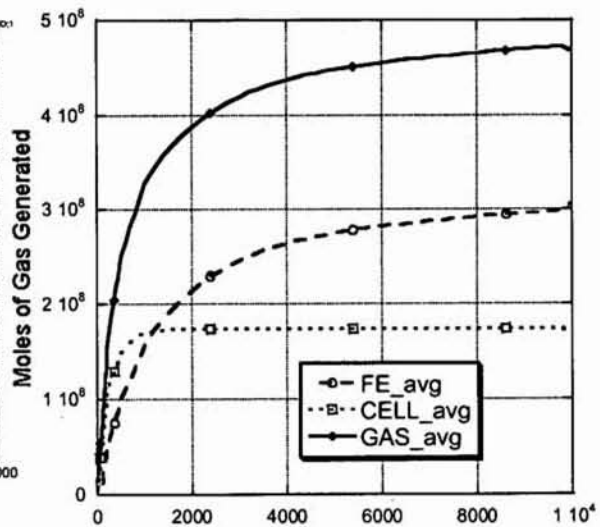
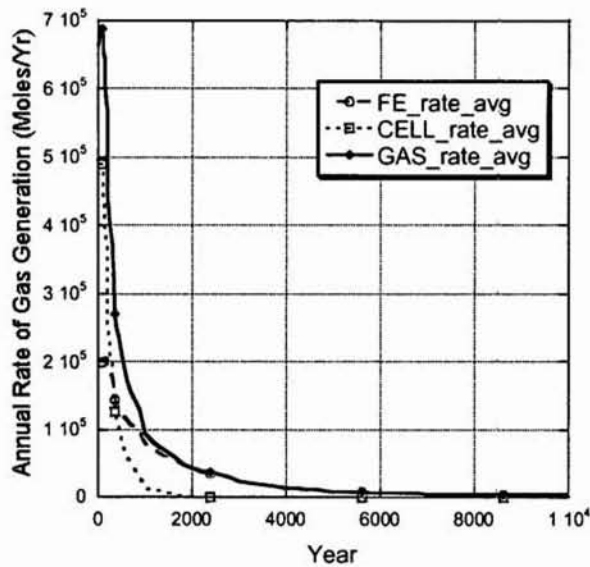
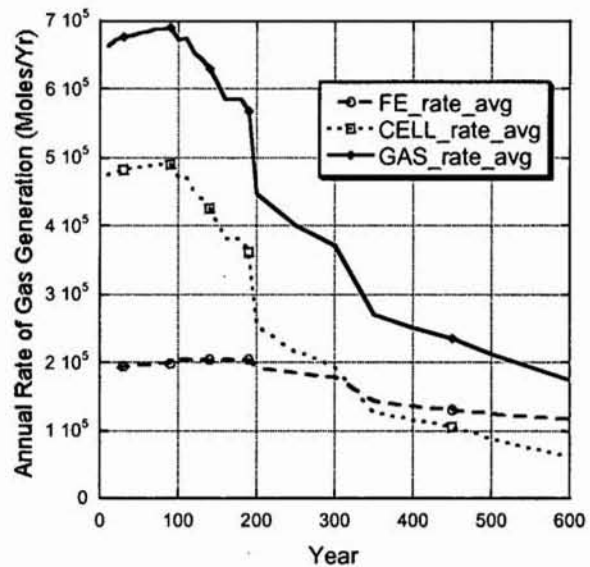


Figure 5.3.21: R1 S1 - Average Total Cumulative Gas Generation

Information Only



a) 10,000 years



b) First 600 Years

Figure 5.3.22: R1S1 - Total Annual Gas Generation

5.3.6 Pressure

Pressure within the repository is particularly important, to WIPP PA, because the release mechanisms, Spallings and Direct Brine Release (DBR), are sensitive to this variable. In addition, pressure strongly influences the extent to which contaminated brine can migrate from the repository into the marker beds. Pressure within the three waste areas, the Waste Panel, RoR – South, and RoR – North, are very similar due to parallel gas generation processes (Figure 5.3.23a, b, & c). The pressures in the two non-waste areas, the Operations Area and the Experimental Area, are virtually identical, because the concrete monolith separating them is relatively permeable. Pressure in some vectors is lower than in the waste-filled areas (Figures 5.3.23d).

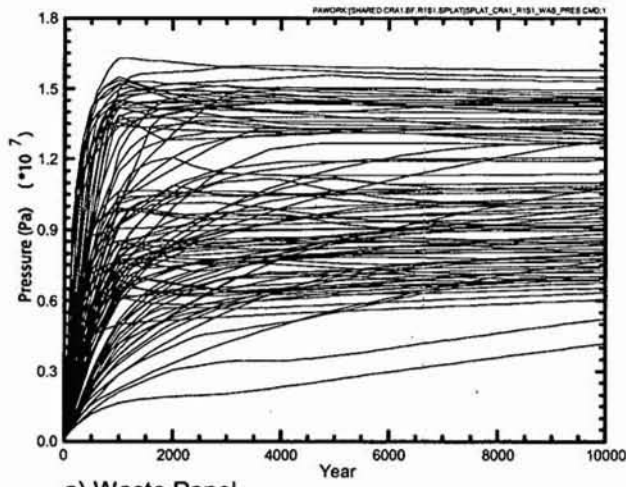
In the first 1,000 years, repository pressure tends to increase rapidly 1) due to higher rates of gas generation in vectors with microbial degradation of organic material, 2) creep closure, and 3) corrosion proceeded at inundated. Later, pressure either approaches an asymptote, or in a few vectors with sufficient brine, it shows a continued but modest rate of increase due to continuing gas generation by corrosion (Figure 5.3.23a, b, & c). The rapid initial increase in pressure up to 1,000 years is due to 1) rapid microbial gas generation in 50% of vectors and 2) the availability of brine in most vectors for corrosion during that period.

The distribution of pressure in the excavated areas is illustrated by plots of average and 90th-percentile values in each area (Figure 5.3.24). Pressure in the two non-waste areas, Operations and Experimental, are coincident due to the relatively high permeability of the intervening concrete monolith so only pressure in the Operations Area is plotted for 100 vectors (Figure 5.3.23d). Also, average pressure in the non-waste area lags behind the waste areas by as much as 1,500 years and 3 MPa due to their separation by Option D panel closures. The average pressure in the three waste areas is similar because gas generation processes are active in each of these areas. However, there is a small consistent pattern of declining pressure from the Waste Panel through RoR-South to RoR North reflecting slow migration of gas towards the non-waste areas. The 90th-percentile pressures level off between 14 and 15 MPa indicating equilibrium between gas generation, which increases pressure, and pressure relief processes (e.g., fracturing, outward migration of fluids, and increased porosity of the excavated areas).

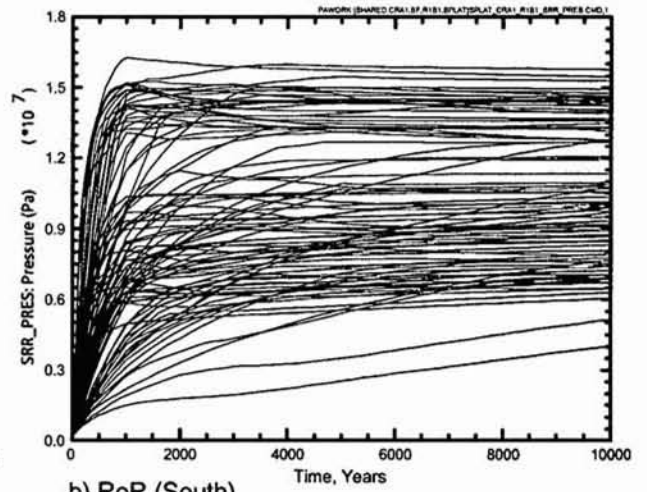
Although pressure tends to increase from gas generation and creep closure, it is also limited by processes that increase available pore volume (e.g., fracturing of the DRZ/marker beds and inflation of the excavated area) or by processes that involve migration of fluids away from the repository (e.g., gas flow up the shaft or brine flow out the marker beds). The relationship between gas generation and pressure is well illustrated by Vector 45, which has the highest pressure attained in Scenario 1 (Figure 5.3.25). Increasing pressure is consistent with gas generation to about 1,000 years. Then pressure levels off between 15 and 16 MPa, but cumulative gas generation increases by another 25 to 30%.

Pressure is primarily dependent upon the sampled input parameter, WMICDFLG, which determines the amount of microbial gas generation (Fig 5.3.26). The PRCC for WMICDFLG is greater than 0.85 though most of the 10,000-year modeling period. The other PRCC's are not very significant, because they explain small portions of the remaining 15%.

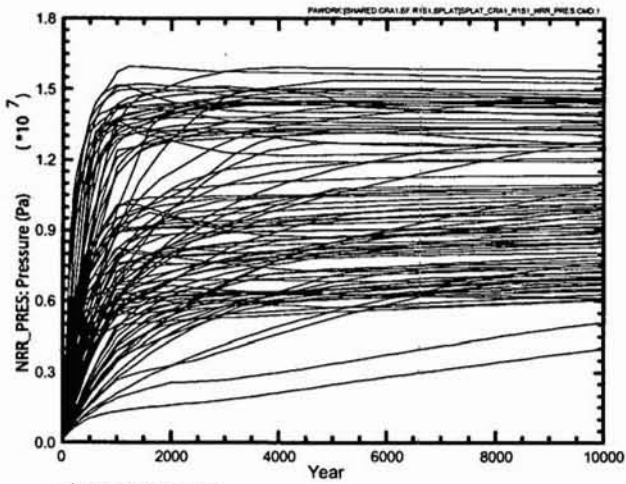
There is a slightly non-linear curve to the plot of moles of gas generated versus pressure in the Waste Panel (Figure 5.3.27). The upward bend is due to the migration of gas at high pressure into adjacent areas and into fractures in the marker beds and DRZ. A scatter plot of WMICDFLG versus WAS_PRES shows a broad positive relationship (Figure 5.3.28). Since WMICDFLG accounts for so much of the variability in pressure, other parameters do not have a significant influence over pressure in the Waste Panel. For example, scatter plots of WGRCOR (Figure 5.3.29) and WASTWICK (Figure 5.23.30) at 10,000 years show no prominent trend.



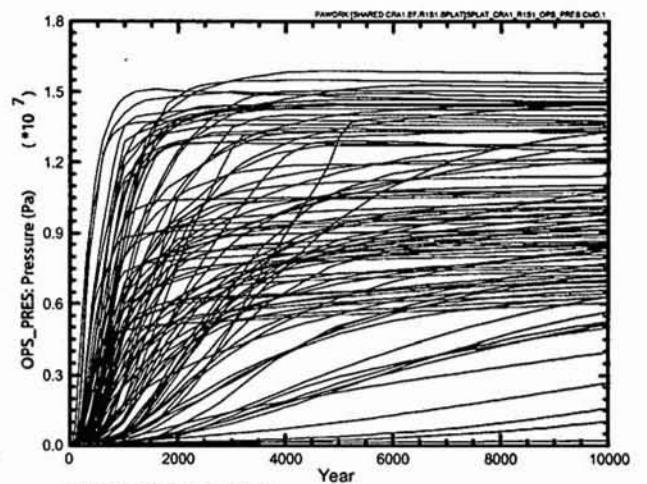
a) Waste Panel



b) RoR (South)



c) RoR (North)



d) Operations Area

Figure 5.3.23: R1S1 – Pressure in the Excavated Areas

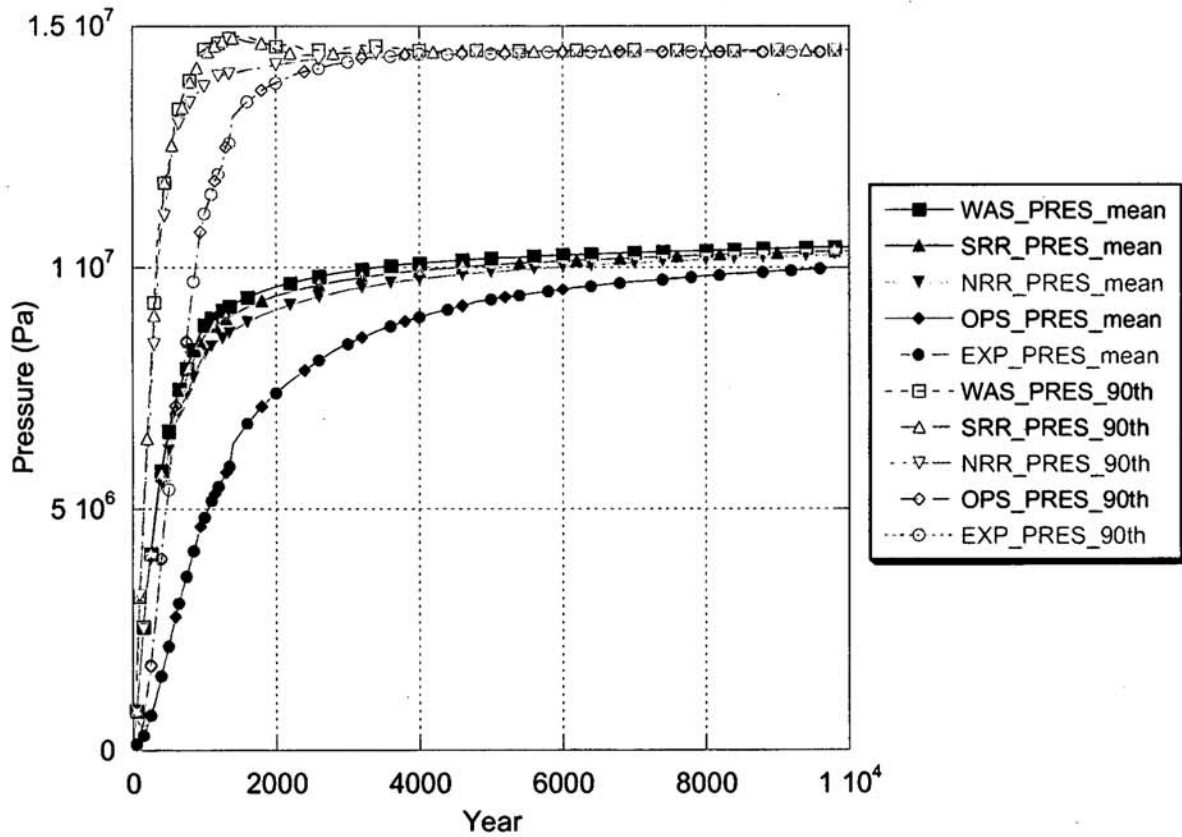


Figure 5.3.24: RIS1 - Pressure in Excavated Areas

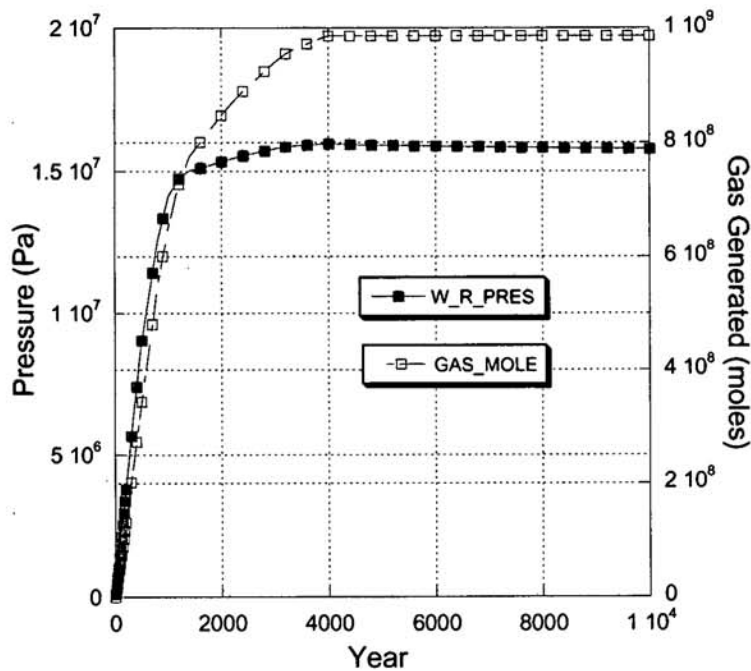


Figure 5.3.25: RIS1 V045 - Pressure and Total Gas Generated in the Waste-Filled Area

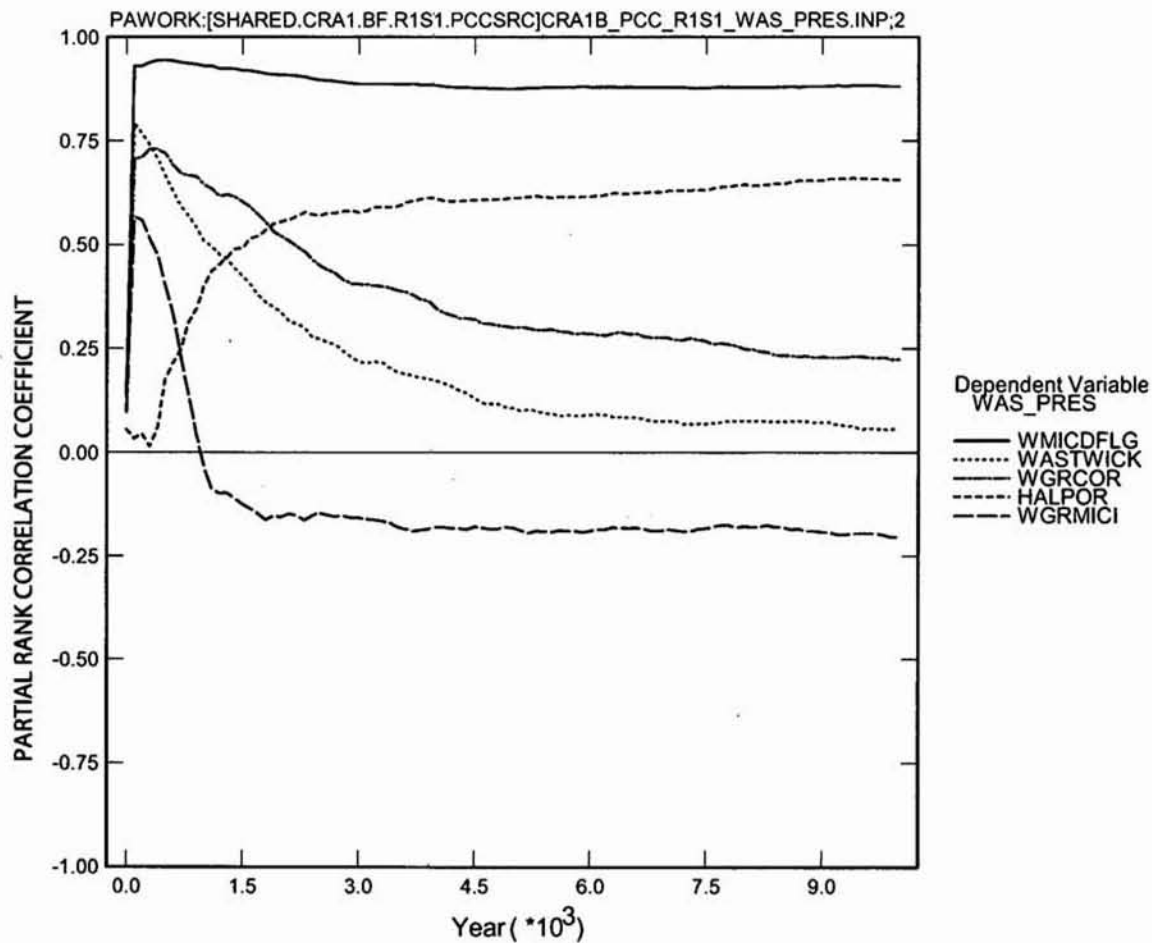


Figure 5.3.26: R1S1 - Primary Correlations of Pressure in the Waste Panel with Input Parameters

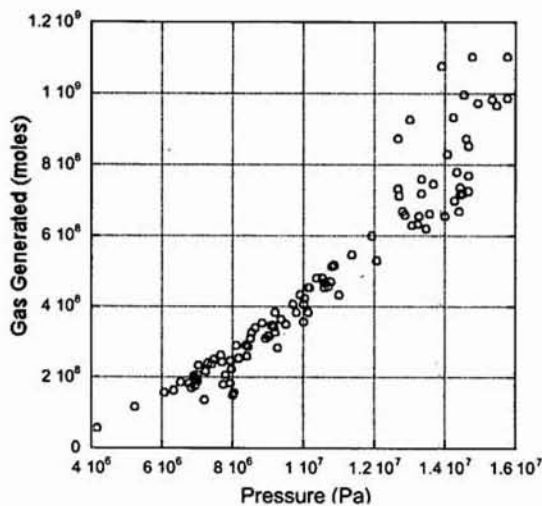


Figure 5.3.27: R1S1 - Scatter Plot of Pressure Versus Total Gas Generation in the Waste Panel at 10,000 Years

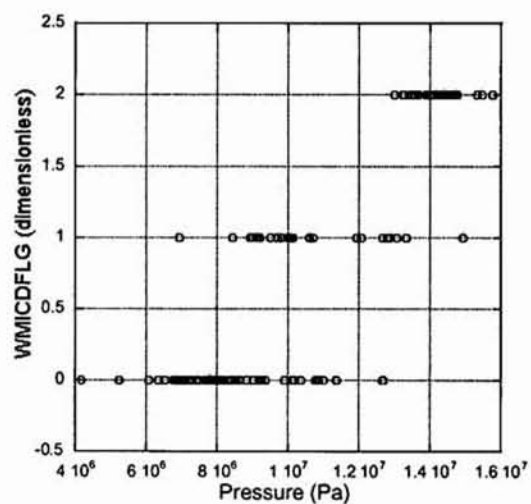


Figure 5.3.28: R1S1 - Scatter Plot of WMICDFLG Versus Pressure in the Waste Panel at 10,000 Years

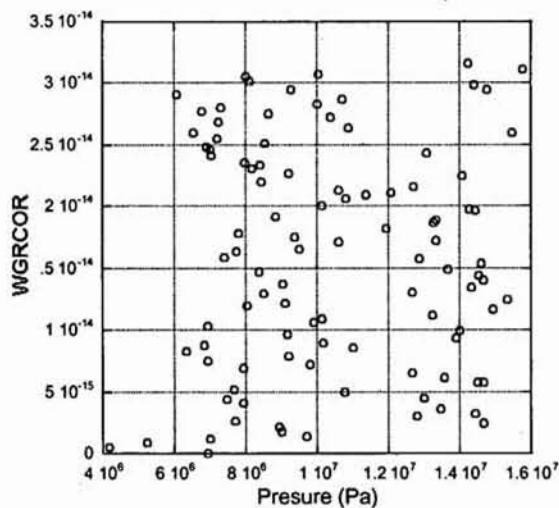


Figure 5.3.29: R1S1 - Scatter Plot of Pressure Versus Gas WGRCOR in the Waste Panel at 10,000 Years

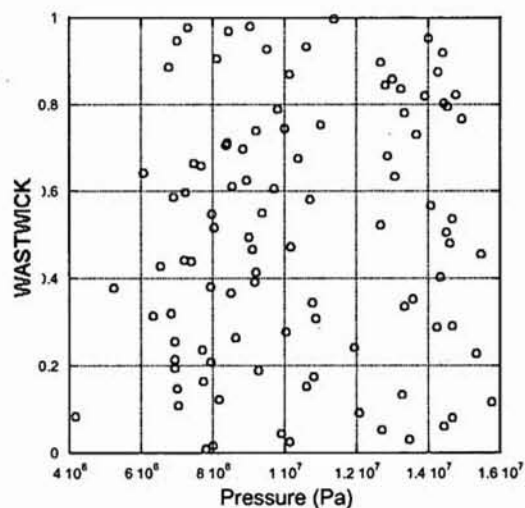


Figure 5.3.30: R1S1 - Scatter Plot of WASTWICK Versus PRESSURE in the Waste Panel at 10,000 Years

5.3.7 Rock Fracturing

If pressures in the DRZ or in the anhydrite marker beds exceed 0.2 MPa above the initial lithostatic pressure, the material is assumed to be fractured and porosity/permeability of the material increases according to the fracture model described in the BRAGFLO users manual (WIPP PA, 2003a). Fracturing occurs within the marker beds in 22% of vectors in the undisturbed scenario (Figure 5.3.31) but fracturing varies among the marker beds from 4 vectors with fracturing in MB138-North to 19 vectors in MB139-South. We define the length of fracturing as the length of marker bed from the repository to the exterior edge of furthest grid cell where permeability has doubled from its initial value. The distribution of fracturing in the six marker bed domains (138 N & S, 139 N & S, and AB N & S) is evaluated by considering plots of the maximum fracture volume (Figure 5.3.32) and fracture length (Figure 5.3.33) over time since only a small percentage of vectors have any fracturing. The marker beds north and south of the repository are considered separately, because north is up-dip and south is down-dip from the repository. These plots show a stair-step pattern, because each cell is either entirely fractured or unfractured so there are intervals of constant fracture volume/length punctuated by sharp jumps when another cell becomes fractured. Fracturing is most extensive in Marker bed 139.

Input dependencies were examined by considering the total fracture volume of the marker beds because this variable is continuous and represents total fracturing in all marker beds. The highest correlation (positive) is with WMCIDFLG, the input control parameter that determines which organic materials, if any, are available for microbial degradation (Figure 5.3.34). WMCIDFLG is also an important input parameter for pressure in the repository, and the importance of pressure to fracturing is illustrated in a scatter plot of

pressure in the Waste Panel, WAS_PRES, versus total fracture volume in all marker beds, VFRACTMB, (Figure 5.3.35). WMICDFLG has the strongest influence on pressure, and it has the highest PRCC (about 0.7), with VFRACTMB (Figure 5.3.36). HALPOR has the second highest PRCC (about 0.45), but its scatter plot shows a very weak correlation with VFRACTMB (Figure 5.3.37). Other individual gas generation factors are even less significant to fracturing.

Vector 45, which has the highest pressure in Scenario S1, illustrates the relationship between pressure and fracturing (Figure 5.3.38). Pressure begins to stabilize at about 1,000 years, when extensive fracturing of the marker beds begins. There is no fracturing below 12 MPa (Figure 5.3.35), and the pressure does not rise in any vector above 16 MPa. Fracturing limits the pressure that would otherwise continue to increase with continuing gas generation.

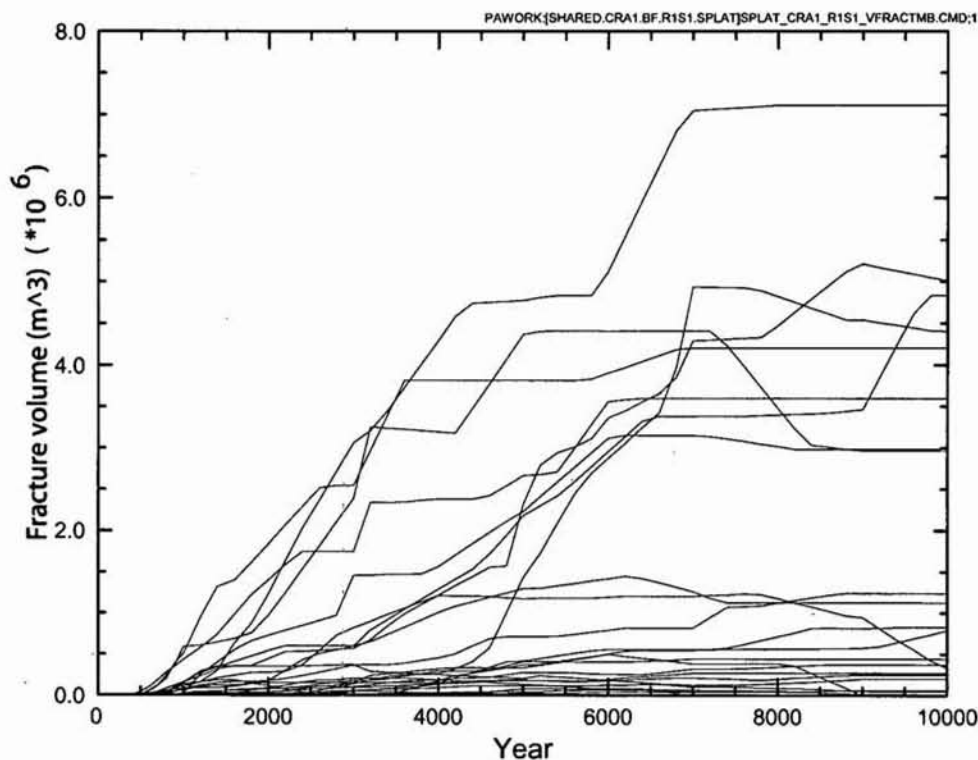


Figure 5.3.31: R1S1 – Total Fracture Volume of the Marker Beds

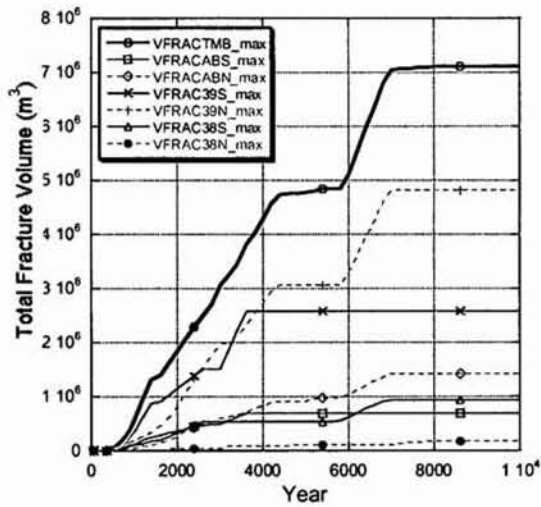


Figure 5.3.32: R1S1 – Fracture Volume of Individual Marker Beds

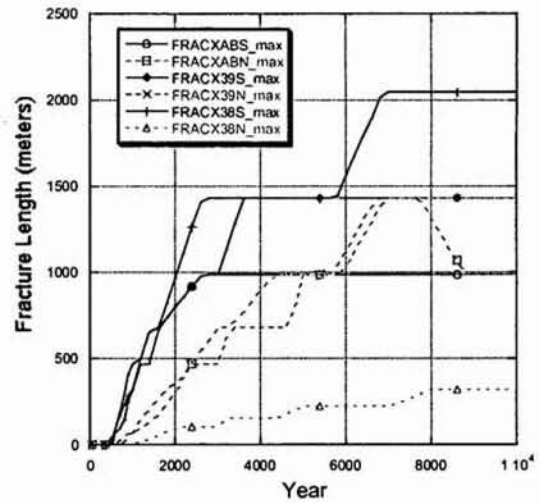


Figure 5.3.33: R1S1 – Fracture Length of Individual Marker Beds

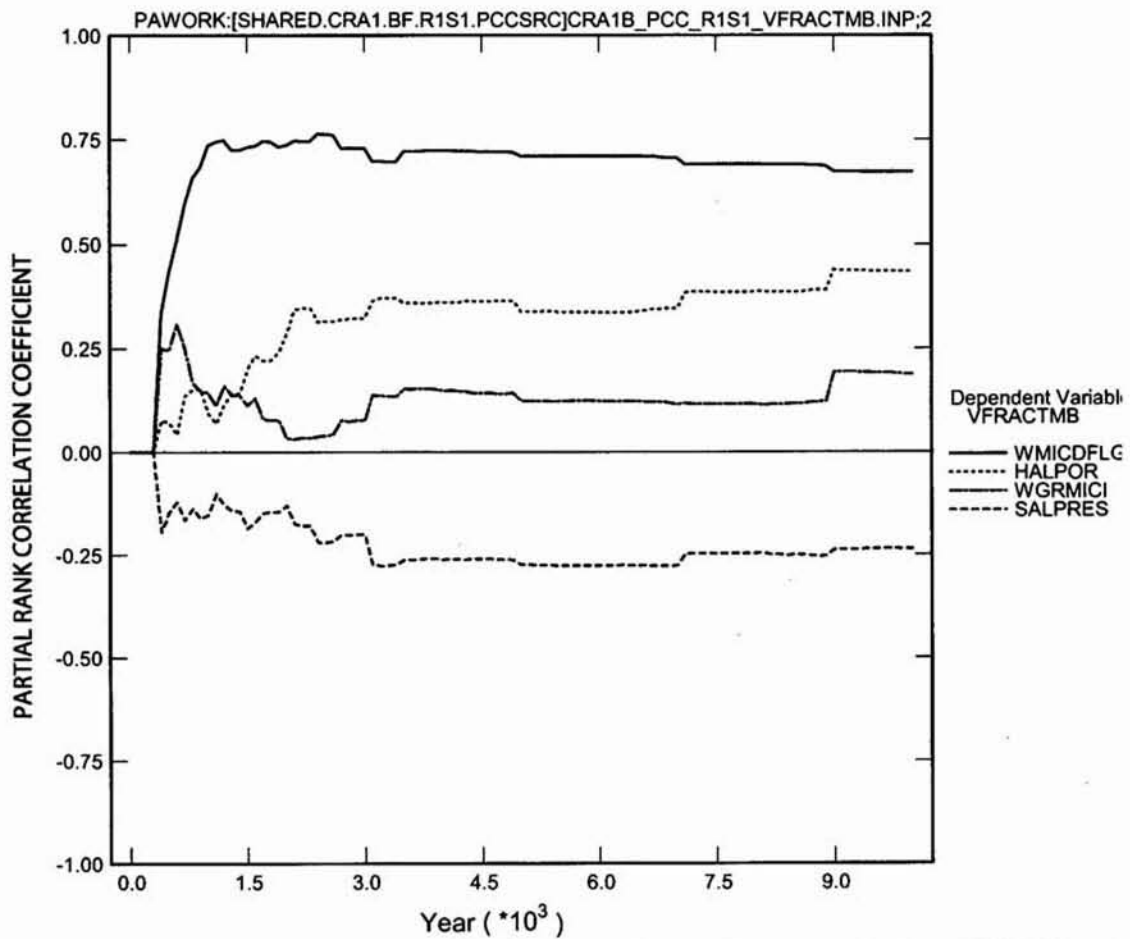


Figure 5.3.34: R1S1 - Primary Correlations of Total Fracture Volume With Input Parameters

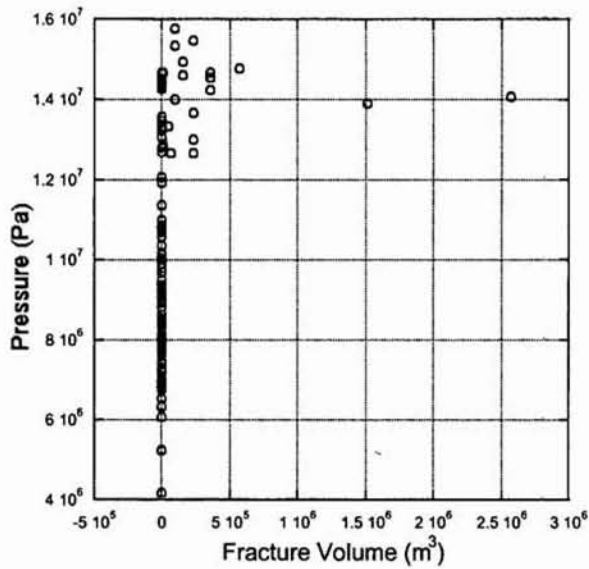


Figure 5.3.35: R1S1 - Pressure in the Waste Panel versus Fracture Volume

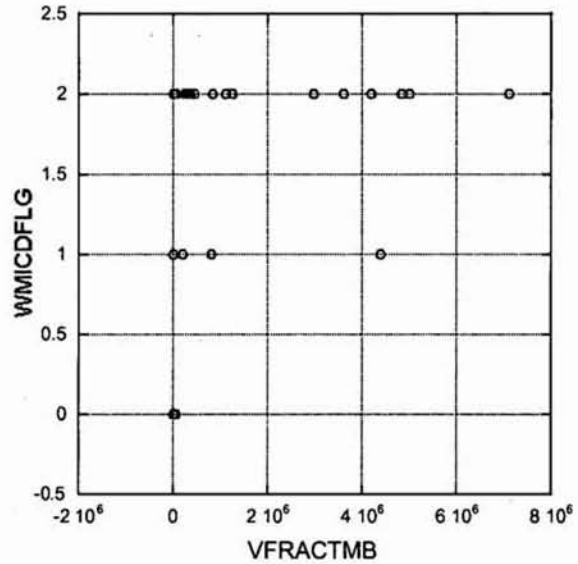


Figure 5.3.36: R1S1 - WMICDFLG versus VFRAC TMB

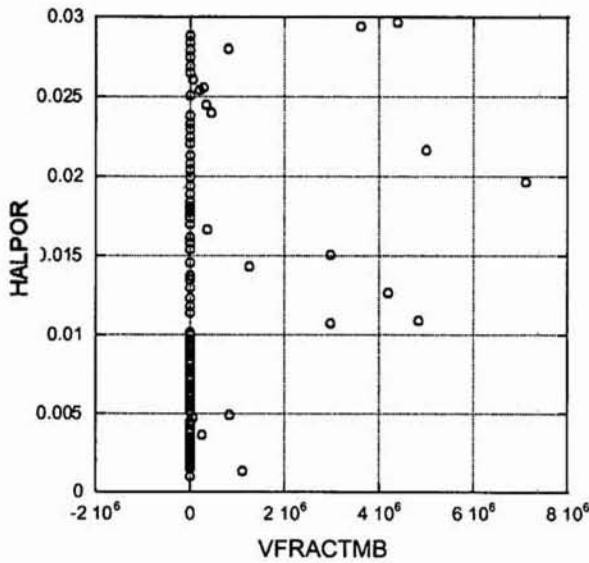


Figure 5.3.37: R1S1 - HALPOR versus VFRAC TMB

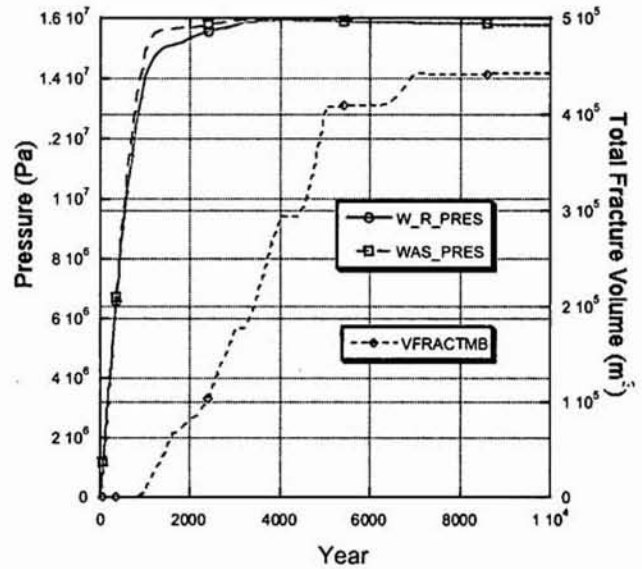


Figure 5.3.38: R1S1 V045 - Pressure in the Waste Panel and the Total Volume of

5.3.8 Brine Outflow

The anhydrite marker beds provide possible pathways by which brine can flow away from the repository in the undisturbed scenario. Such flow is important, because it counts as a release to the accessible environment if contaminated brine crosses the Land Withdrawal Boundary (LWB) within 10,000 years. Total cumulative brine outflow exceeds 3,000 m³ in three vectors (Figure 5.3.39), but these vectors have brine outflows that are several times greater than any other vector (Table 5.3.5). Only a few vectors show any brine outflow at the LWB (Figure 5.3.40), and the greatest cumulative outflow is about 466 m³, which is several orders of magnitude less than the volume of the marker beds between the repository and the LWB.

Brine flow up the shaft is a potential pathway for brine outflow, but only a few vectors show any outflow from the shaft at the base of the Culebra (Figure 5.3.41). The maximum cumulative brine outflow up the shaft over 10,000 years is 50 m³, which is far too small to be significant for releases.

The distribution of brine flow along the potential outflow paths varies somewhat among the vectors, but typically outflow along Marker Bed 139 to the South accounts for 90% of total brine outflow in the undisturbed scenario (Table 5.3.7). MB 139 is down the local stratigraphic dip, and being the lowest outflow pathway, it is most frequently saturated. The dominance of Marker Bed 139 to the south as the primary path for brine outflow is illustrated in Figure 5.3.42, which displays a plot of the maximum brine outflow volumes for each marker bed pathway.

Table 5.3.6 compares selected output variables for Vector 22, which has the greatest brine outflow, with the maximum values for all vectors. The elevated brine inflow is essential to high brine outflow. Moreover, pressure and gas generation are also at or near to the maximum for the 100 vectors in the undisturbed scenario.

Brine outflow is not a uniform process. A plot of the annual rate of brine outflow for Vector 22 shows spikes in brine outflow particularly during the first 2,000 years (Figure 5.3.43). Elevated brine outflow occurs during relatively short periods of time punctuated by longer periods of reduced brine flow. These focused periods of brine outflow are either due to fracturing in the marker bed carrying the brine or the outflow events cease when fracturing in other marker beds result in temporarily lower pressures in the repository.

TABLE 5.3.5: HIGHEST CUMULATIVE BRINE OUTFLOWS FOR THE UNDISTURBED SCENARIO AT 10,000 YEARS

Vector	Brine Outflow (m ³)	Rank and Volume of Fracturing (m ³)
V022	19,600	6 th 3.60E+06
V049	9,800	14 th 3.37E+05
V048	8,600	NA 0.0

TABLE 5.3.6: PROMINENT OUTPUT VALUES -VECTOR 22 AND MAXIMUM

Output Variable	V022 Value	Maximum Value	Vector with Max
Brine Outflow (m ³)	19,567	19,567	V022
Brine Inflow (m ³)	49,258	49,258	V022
Pressure in Waste Areas (Pa)	1.48E+07	1.58E+07	V045
Total Gas Generation (moles)	1.10E+09	1.10E+09	V022
Fracturing MB39South (m)	466	1,429	V079

TABLE 5.3.7: VOLUME OF BRINE OUTFLOW BY VARIOUS POTENTIAL PATHWAYS (M³)

Pathway for Brine Outflow	V022	Maximum	
MB38 North	3	432	V082
MB38 South	6	1,567	V090
AB North	0	0	N/A
AB South	0	5	V082
MB39 North	1,326	1,832	V082
MB39 South	12,828	12,828	V022
Shaft (base of Culebra)	0	50	V053

PRCC's for total cumulative brine flow away from the repository, BRNREPOC, are shown in Figure 5.3.44. Initially, the strongest relationship is with CONPRM, the log of the permeability for concrete. The positive PRCC indicates that increased flow through concrete corresponds to increased outflow from the repository, because the brine can pass more quickly through internal barriers within the repository. By about 1,500 years the residual brine saturation of waste, WRBRNSAT, which has a negative PRCC, becomes the dominant input parameter. Higher values of WRBRNSAT result in a narrower saturation range in which the waste is permeable to brine. The other hydrological factors in Figure 5.3.44, DRZPRM, HALPOR, and CONBCEXP also have weak positive correlations with BRNREPOC.

Many input parameters have competing effects on brine outflow that reduce their significance to total cumulative results. For example, under differing circumstances, higher pressure can either drive brine outflow or it can prevent brine inflow thereby reducing outflow. Thus, sometimes there is no clear correlation with parameters that control many processes in the BRAGFLO model.

Linear correlation analyses do not always reveal the importance of input parameters when multiple coupled processes are involved. The sequence of processes is also important. For example, there can be no outflow without inflow first. If pressure increases rapidly, brine inflow is impeded or stopped thereby decreasing the potential for brine outflow.

However, if pressure increases slowly there can be more brine inflow, and then when pressure is sufficiently high, increased brine outflow can occur.

Information Only

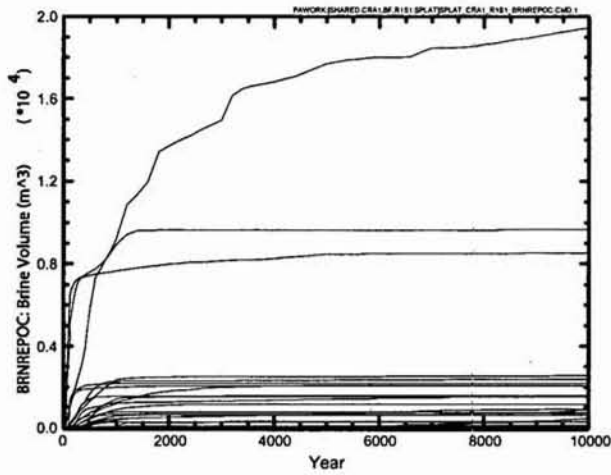


Figure 5.3.39: R1S1 – Brine Flow Away from the Repository, BRNREPOC

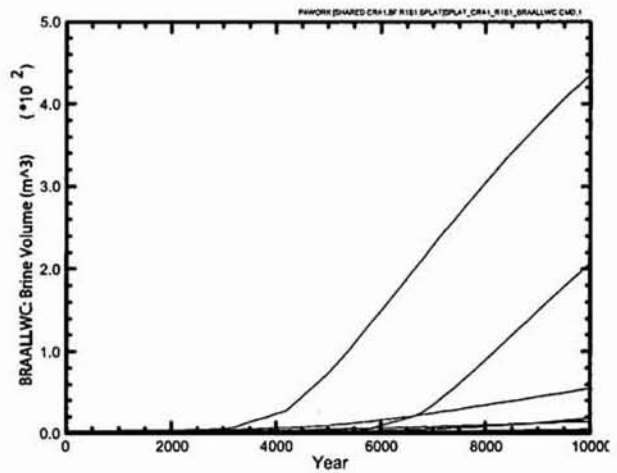


Figure 5.3.40: Brine Outflow at the Land Withdrawal Boundary, BRAALWC

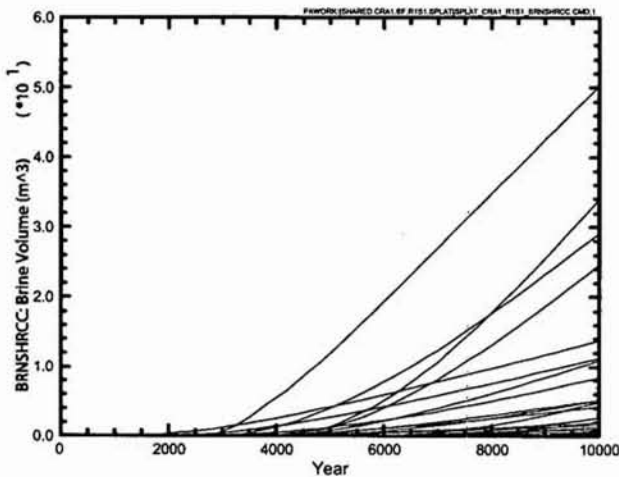


Figure 5.3.41: R1S1 – Cumulative Brine Flow Away Up the Shaft

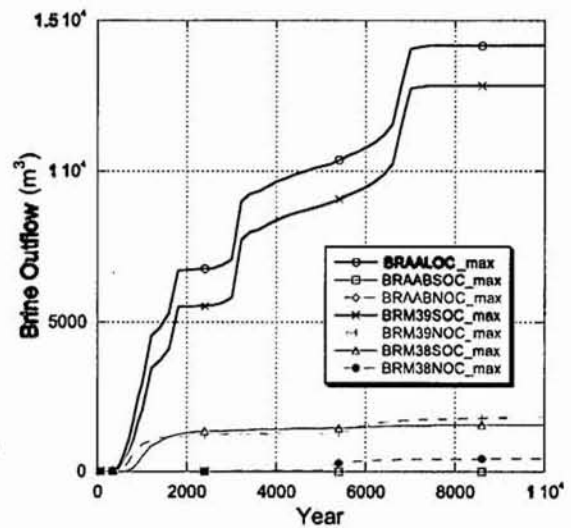
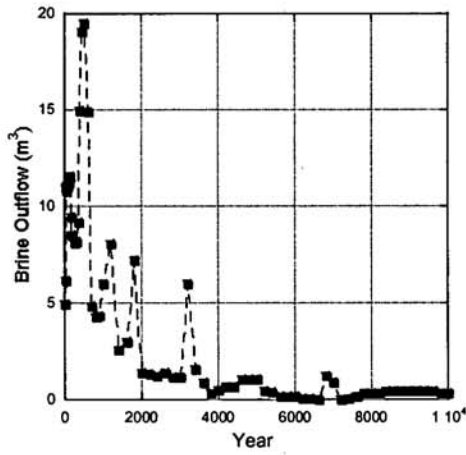
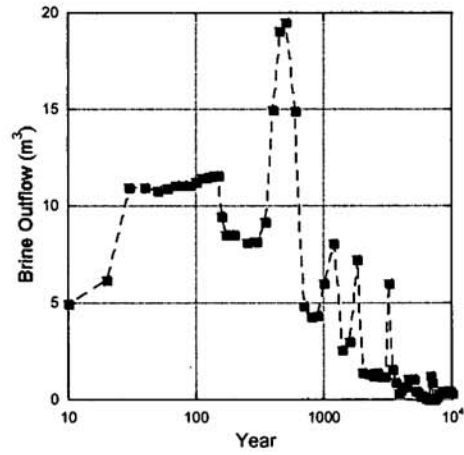


Figure 5.3.42: R1S1 - Cumulative Brine Outflow from the Repository Via Each Marker Bed Pathway



a) linear time scale



b) log time scale

Figure 5.3.43: R1S1 V022- Annual Rate of Brine Flow Away from the Repository

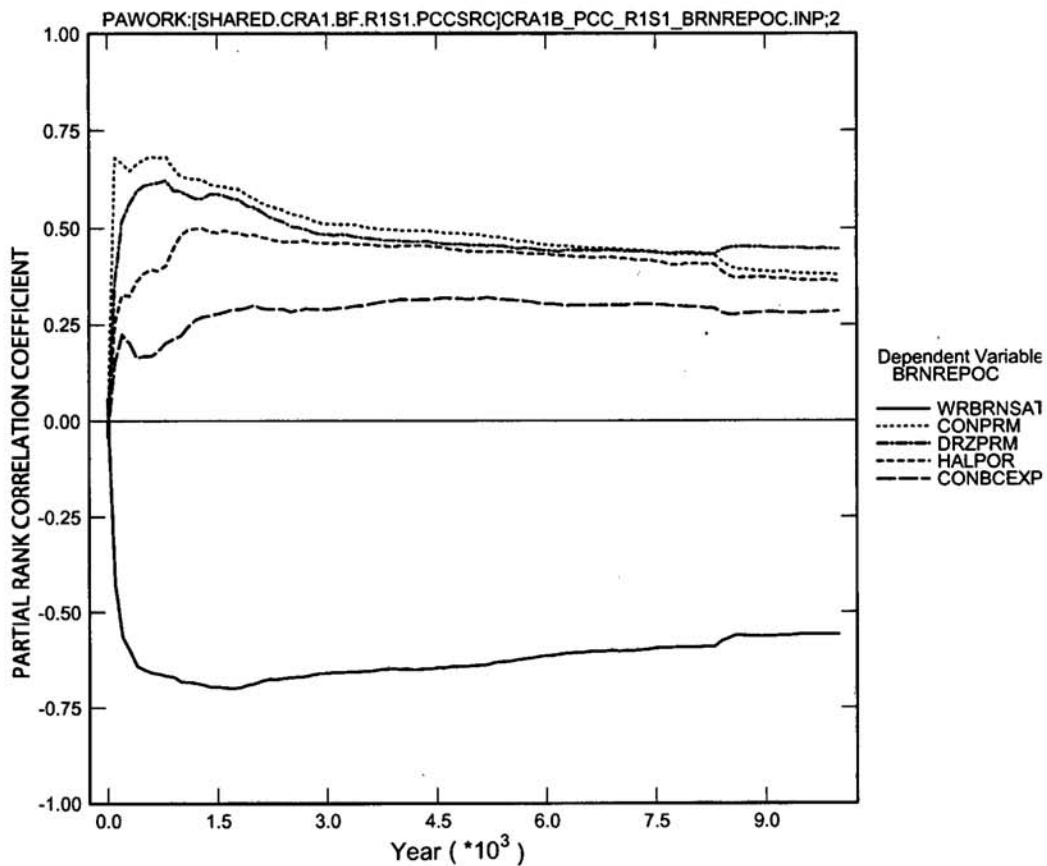


Figure 5.3.44: R1S1 - Primary Correlations of total Cumulative Brine Flow Away from the repository With Input Parameters

5.4 DRILLING DISTURBANCE SCENARIOS (2, 3, 4, 5 & 6)

Scenarios 2 through 6 evaluate the possible results of drilling intrusions into the repository. It is assumed that all boreholes in the Salado Flow Analysis are drilled through the repository in search of deeper resources. The potential consequences of encountering a pressurized brine pocket in the Castile (an E1 event) are considered in Scenarios 2 and 3. Boreholes that do not encounter pressurized brine (S4 & S5) are modeled in the Salado Flow grid as terminating at the base of the repository (an E2 event). Scenario 6 evaluates an E2 event followed by an E1 event. The specific sequences of material property changes in the model are listed in the following section.

This analysis will focus on Scenario 2, which produced the most extreme brine outflow results. The other scenarios will be included, as needed, to complete the Salado Flow analysis.

5.4.1 Sequence of Events

Five drilling disturbance scenarios are considered in this part of the Salado Flow Analysis. The sequence of events for each is summarized below:

Scenario 2 (E1 event)

- 200 years: change in lower shaft material properties. Material SHFTL_T1 is replaced by material SHFTL_T2.
- 350 years: borehole intrusion (E1) through the Waste Panel into a hypothetical pressurized brine reservoir in the underlying Castile Formation. Concrete borehole plugs are immediately emplaced in the borehole at the Culebra and at the surface.
- 550 years: Borehole plugs fail and the borehole (top to bottom) is assumed to have properties equivalent to sand (material: BH_SAND).
- 1,550 years: the permeability of the borehole between the repository and the Castile Formation decreases due to creep closure of the salt (material: BH_CREEP).

Scenario 3 (E1 event)

- 200 years: change in lower shaft material properties.
- 1,000 years: borehole intrusion (E1) through the Waste Panel into a hypothetical pressurized brine reservoir in the underlying Castile Formation. Concrete borehole plugs are immediately emplaced in the borehole at the Culebra and at the surface.
- 1,200 years: Borehole plugs fail and the borehole (top to bottom) is assumed to have properties equivalent to sand (material: BH_SAND).
- 2,200 years: the permeability of the borehole between the repository and the Castile Formation decreases due to creep closure of the salt (material: BH_CREEP).

Scenario 4 (E2 event)

- 200 years: change in lower shaft material properties.
- 350 years: borehole intrusion (E2) through a Waste Panel terminating at the base of the DRZ in the modeling grid (no connection to the underlying Castile Formation). Two plugs are present in the upper part of the borehole.
- 550 years: Borehole plugs fail and the borehole (top to bottom) is assumed to have properties equivalent to sand (material: BH_SAND).

Scenario 5 (E2 event)

- 200 years: change in lower shaft material properties.
- 1,000 years: borehole intrusion (E2) through a Waste Panel terminating at the base of the DRZ in the modeling grid (no connection to the underlying Castile Formation). Two plugs are present in the upper part of the borehole.
- 1,200 years: Borehole plugs fail and the borehole (top to bottom) is assumed to have properties equivalent to sand (material: BH_SAND).

Scenario 6 (E2,E1 events)

- 200 years: change in lower shaft material properties.
- 1,000 years: borehole intrusion (E2) through a Waste Panel terminating at the base of the DRZ in the modeling grid (no connection to the underlying Castile Formation) Borehole filled with sand.
- 2,000 years: borehole intrusion (E1) through a Waste Panel into a hypothetical pressurized brine reservoir in the underlying Castile Formation
- 2,200 years: Borehole plugs fail and the borehole (top to bottom) is assumed to have properties equivalent to sand (material: BH_SAND).
- 3,200 years: the permeability of the borehole between the repository and the Castile Formation decreases due to creep closure of the salt (material: BH_CREEP).

The two-intrusion scenario, S6, performs like an E1 scenario after the E1 drilling event, and it is considered with S2 and S3 throughout this analysis.

5.4.2 Halite Creep

Drilling intrusions have relatively little effect on the range of porosities in the repository compared to the undisturbed scenario, because most creep closure occurs prior to the drilling event (Figure 5.4.1). However, there is less inflation of the repository after the initial decrease in pore volume, because the borehole connection to the ground surface results in lower pressure for the high-pressure vectors in which inflation occurs in the undisturbed Scenario 1. The average porosity at 10,000 years is decreased from about 0.175 in the undisturbed scenario to about 0.14 in the E1 scenarios (S2, S3, and S6) and to about 0.12 in the E2 scenarios (S4 and S5).

Individual vectors in the various Salado Flow modeling scenarios show variation in detail (Figure 5.4.2), but porosity trends are similar in all six scenarios. Porosity drops from an initial value of 0.85 to less than .50 in the first 50 years in all vectors of all six scenarios, and it stabilizes between

0.05 and .25 from 1,000 years to the end of the regulatory compliance period at 10,000 years. The average at 10,000 years ranges from 0.12 in Scenarios 4 and 5 to 0.17 in Scenario 1.

Many vectors in the E1 scenarios (S2 and S3) show an upward spike in porosity (about 0.1) in response to a pressure increase caused by the borehole connection to the Castile (Figure 5.4.2). When the borehole plugs fail, the pressure decreases forming an upward spike in the horsetail plots. Other vectors with high repository pressure show no change at the time of the intrusion, but there is a drop of about 0.1 when the borehole plugs fail. The pressure differential between the Castile and the repository determines whether or not there is a temporary increase in porosity. The corresponding porosity plots for an E2 drilling intrusion at 1,000 years (Figure 5.4.2) show no change at the time of the intrusion, but there is a decrease of about 0.1 in many vectors due to the resulting drop in pressure when the borehole plugs fail 200 years later. The horsetail plot for Scenario 6 shows a decrease in porosity after the E2 drilling intrusion and a subsequent increase after the E1 event forming a trough in the horsetail plots. Some vectors are not affected, because the drilling event does not cause a sufficient change in pressure within the Waste Panel to change the pore volume.

PRCC's for porosity in the Waste Panel, WAS_POR, are shown in Figure 5.4.3. The permeability of the borehole fill material, BHPERM, is the most important input variable with a PRCC below -.75 after the drilling intrusion when BHPERM becomes the primary input parameter influencing Waste Panel porosity in Scenario 2. Higher borehole permeability allows fluids, primarily gas, to migrate more quickly out of the repository thereby reducing pressure in the Waste Panel. The result is increased brine inflow from the Castile thereby increasing brine saturation. Initial pressure in the Castile has the second most significant PRCC ranging from 0.4 to 0.5 during most of the post-drilling period. The scatter plot of BHPERM versus WAS_POR at 10,000 years shows a broad negative correlation (Figure 5.4.4), but the plot of BPINTPRS, versus WAS_POR shows only a vague positive correlation (Figure 5.4.5). BHPERM accounts for most of the variability in porosity in the Waste Panel after the drilling intrusion.

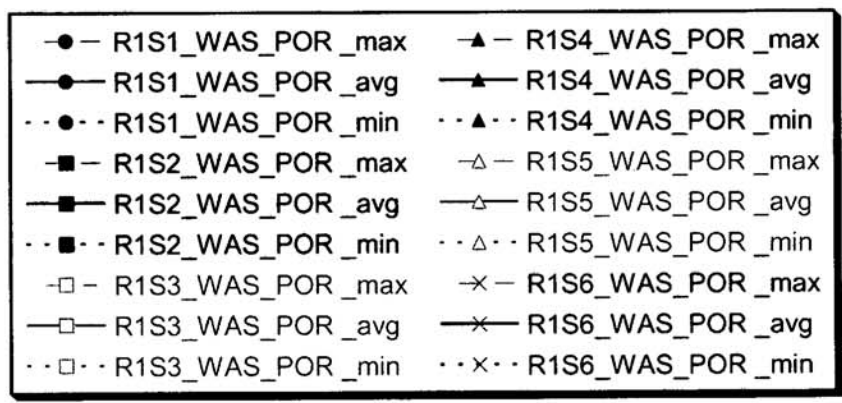
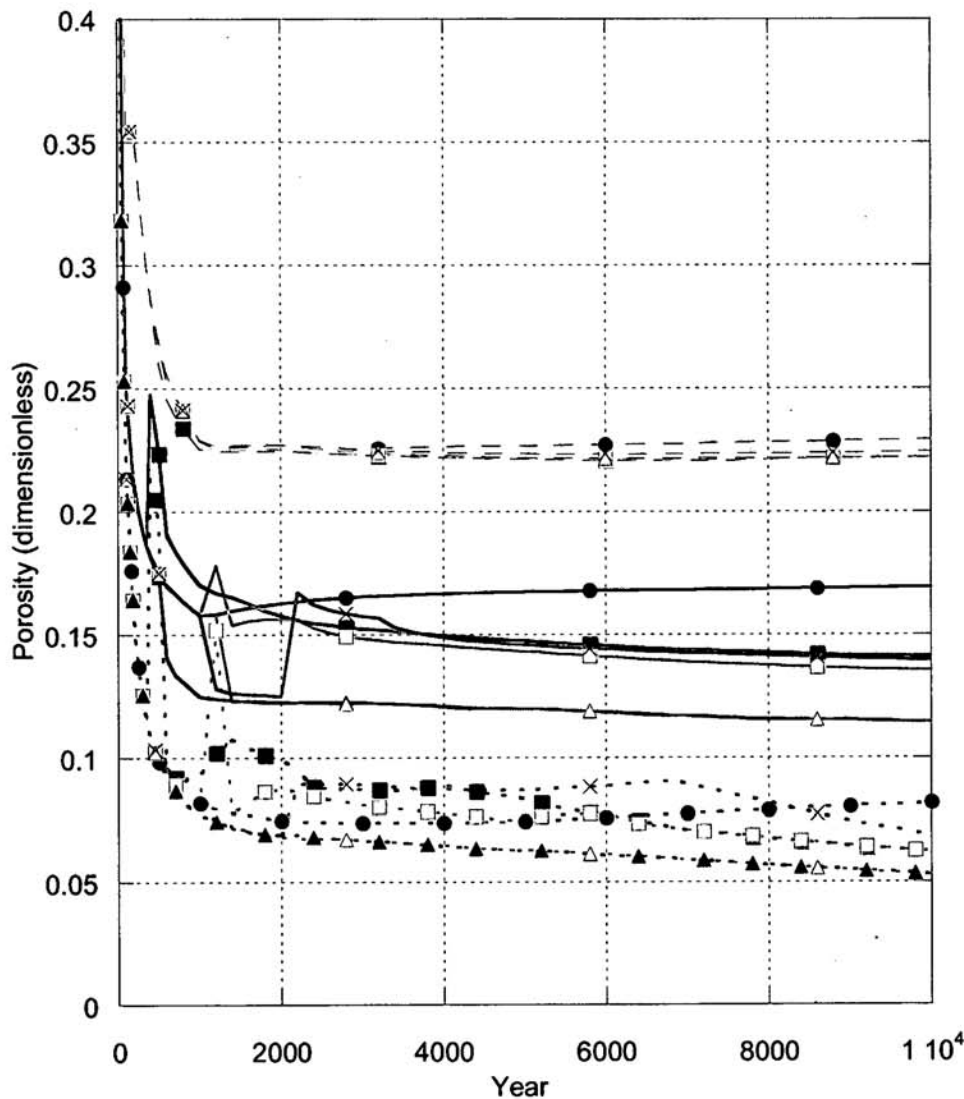
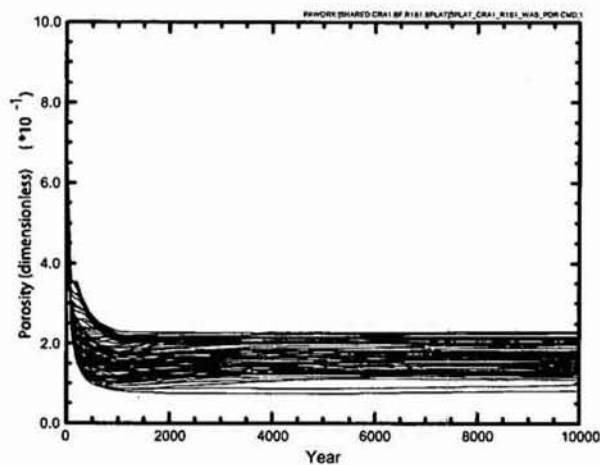
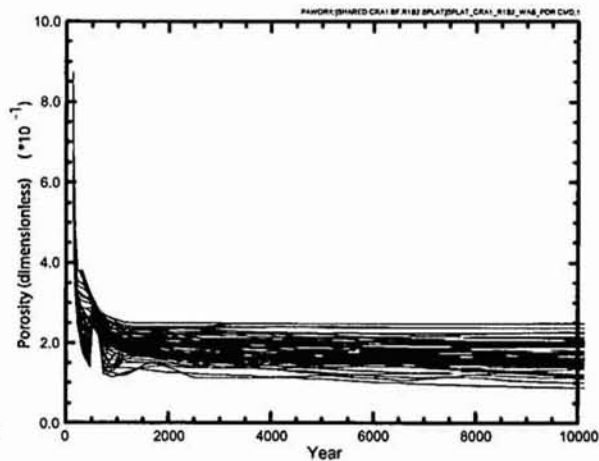


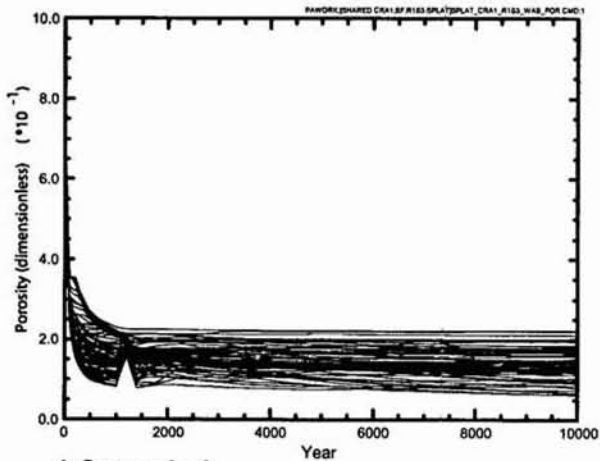
Figure 5.4.1: R1: Porosity of the Waste Panel in Six Scenarios



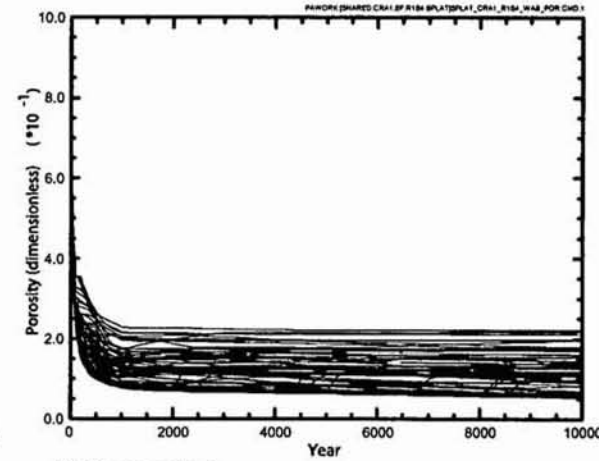
a) Scenario 1



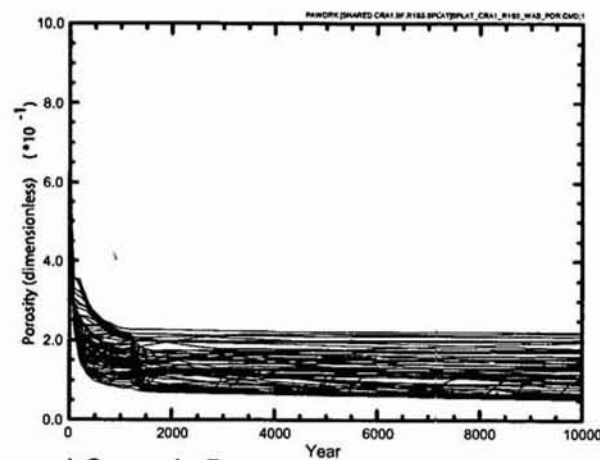
b) Scenario 2



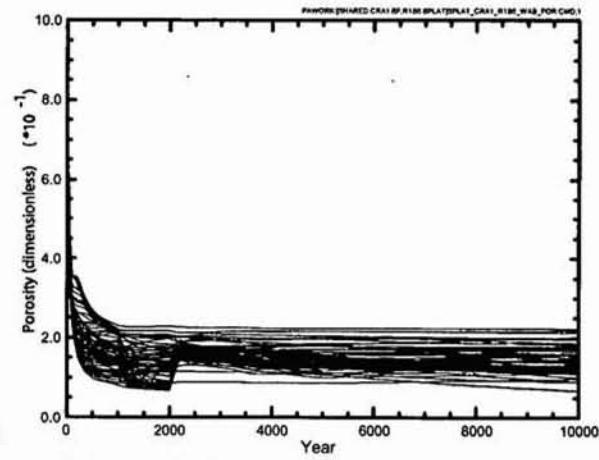
c) Scenario 3



d) Scenario 4



e) Scenario 5



f) Scenario 6

Figure 5.4.2: R1 – Horsetail Plots for Porosity in the Waste Panel in Six Scenarios

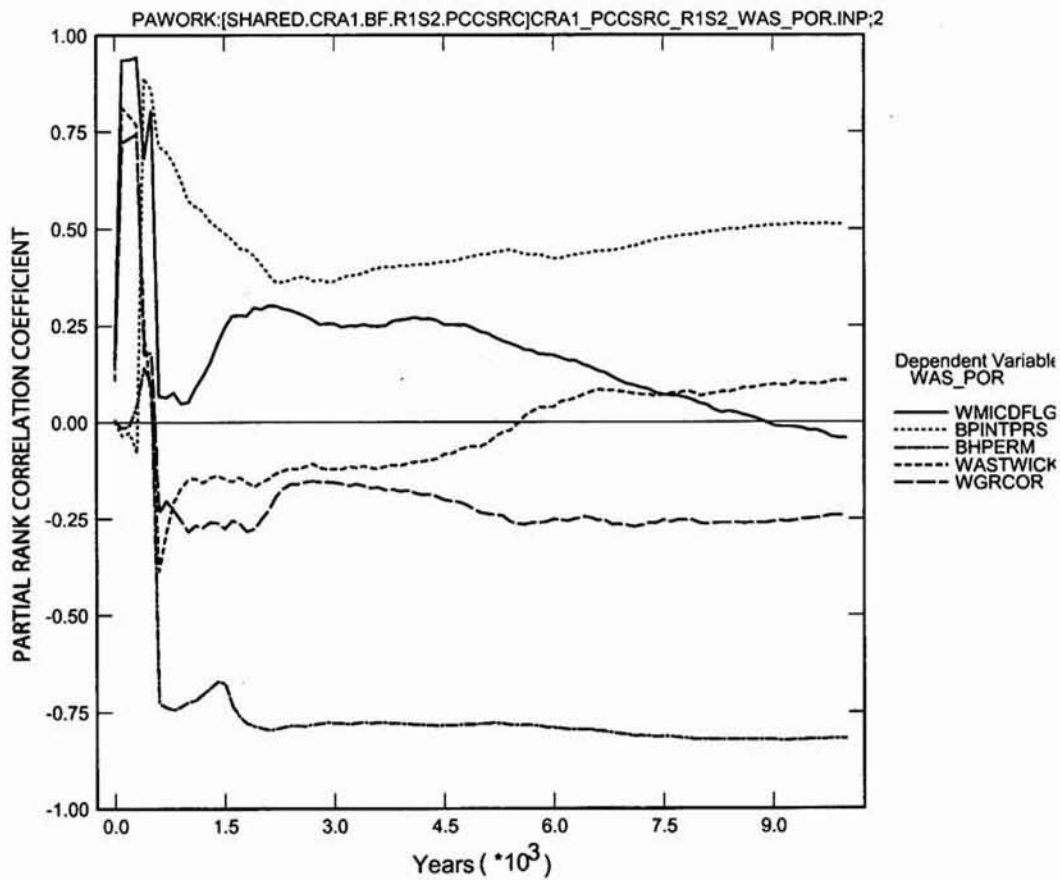


Figure 5.4.3: R1S2 - Primary Correlations for Porosity in the Waste Panel, WAS_POR, with Input Parameters

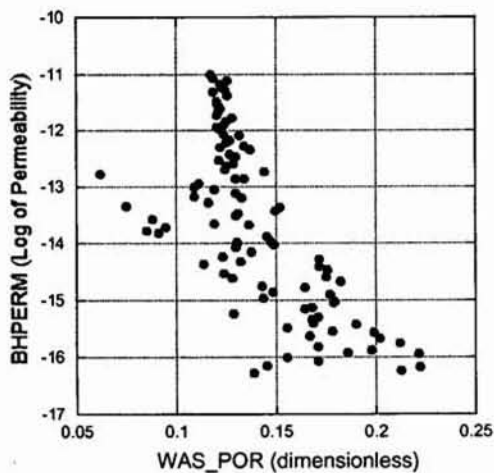


Figure 5.4.4: R1S2 - BHPERM versus WAS_POR

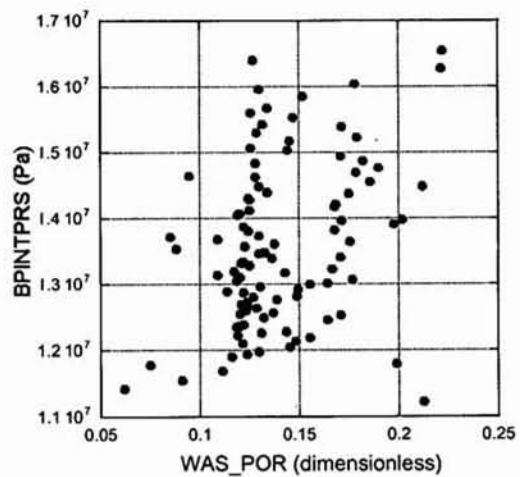


Figure 5.4.5: Brine Outflow at the Land Withdrawal Boundary

Information Only

5.4.3 Brine Inflow

Brine flow into the repository is important, because brine outflow cannot exceed inflow since the repository starts out without any brine present. It also is an important contributing factor determining brine saturation, which is an input to subsequent PA analyses.

A drilling intrusion results in increased brine flow into the repository (Figure 5.4.6). Table 5.4.1 summarizes selected statistics at 10,000 years in all six scenarios for the cumulative brine flow into the repository, BRNREPTC, and Figure 5.4.7 illustrates brine inflow trends over time. The undisturbed scenario, S1, has the lowest maximum, median, and average inflows, and the E1 intrusions have the highest brine inflow. The E1 intrusions permit the influx of brine up the borehole from the Castile, and the E2 intrusions permit the outward migration of fluids, primarily gas, resulting in decreased pressure within the repository. Since high pressure impedes inflow, the decrease allows increased brine inflow from the DRZ and the marker beds in the E2 scenarios.

TABLE 5.4.1: STATISTICS FOR CUMULATIVE BRINE FLOW INTO THE REPOSITORY at 10,000 Years

	Median (m ³)	Minimum (m ³)	Maximum (m ³)
Scenario 1 (undisturbed)	7,345	77	49,258
Scenario 2 (E1)	20,992	3,648	163,597
Scenario 3 (E1)	16,395	378	154,428
Scenario 4 (E2)	9,221	389	51,480
Scenario 5 (E2)	9,193	382	66,713
Scenario 6 (E2 then E1)	15,811	2,288	162,458

Brine inflow generally increases by more than 200 percent over the undisturbed scenario, S1, when there is a drilling intrusion through the repository and into a pressurized brine pocket in the Castile (E1 scenarios – S2, S3, And S6). The increase in brine inflow for low-flow vectors can be a much higher percentage (Table 5.4.1). The cumulative influx of brine reaches as much as 160,000 m³ in a few vectors, but the median values range from 16,000 to 21,000 m³, which is also 2 to 3 times the median value in the undisturbed scenario. Brine inflow is slightly higher in scenario S2, which has the earlier drilling event at 350 years. Pressure, which impedes brine inflow, is lower in the repository at early times because there has been less time for gas generation.

Vectors with the highest influx of brine show continuing inflow to the end of the 10,000-year modeling period, because brine continues to flow from the DRZ and the marker beds after the borehole connection to the Castile has been sealed by halite creep closure (Figure 5.4.7). However, brine inflow in most vectors declines and stops once this connection has been sealed due to increasing pressure from gas generation and to limited brine availability in the DRZ and marker beds, which is determined by sampled input parameters.

The E2 drilling intrusions result in smaller increases in brine inflow when compared with the undisturbed scenario, S1. The median values of brine inflow for the E2 intrusions (S4 and S5) are

about 20 percent higher than in the undisturbed scenario. The maximum brine inflows are even less of an increase from the S1 scenario.

Input parameter dependencies were evaluated for Scenario 2, which has the greatest brine inflows. The PRCC for total cumulative brine flow into the repository, BRNREPTC, with the permeability of the borehole, BHPERM increases rapidly to approximately 0.75 once the borehole plugs fail 200 years after the intrusion (Figure 5.4.8). There is a positive PRCC, because most of the brine influx comes up the borehole from a pressurized brine pocket in the Castile. The microbial gas generation control parameter, WMICDFLG, shows a strong negative PRCC, because microbial gas generation raises the pressure in the repository, which impedes brine inflow. The permeability of the DRZ, DRZPRM, shows a positive PRCC, because increasing DRZ permeability permits faster brine inflow from the DRZ and the marker beds.

A scatter plot of BHPERM versus BRNREPTC for Scenario 2 (Figure 5.4.9) illustrates that although BHPERM has the highest PRCC (Figure 5.4.8), the relationship between BHPERM and BRNREPTC is quite non-linear. There is little correlation between BRNREPTC and BHPERM at borehole permeabilities less than 10^{-12} m^2 , but increasing permeability, BHPERM, to 10^{-11} m^2 results in a dramatic increase in brine flow up the borehole into the repository.

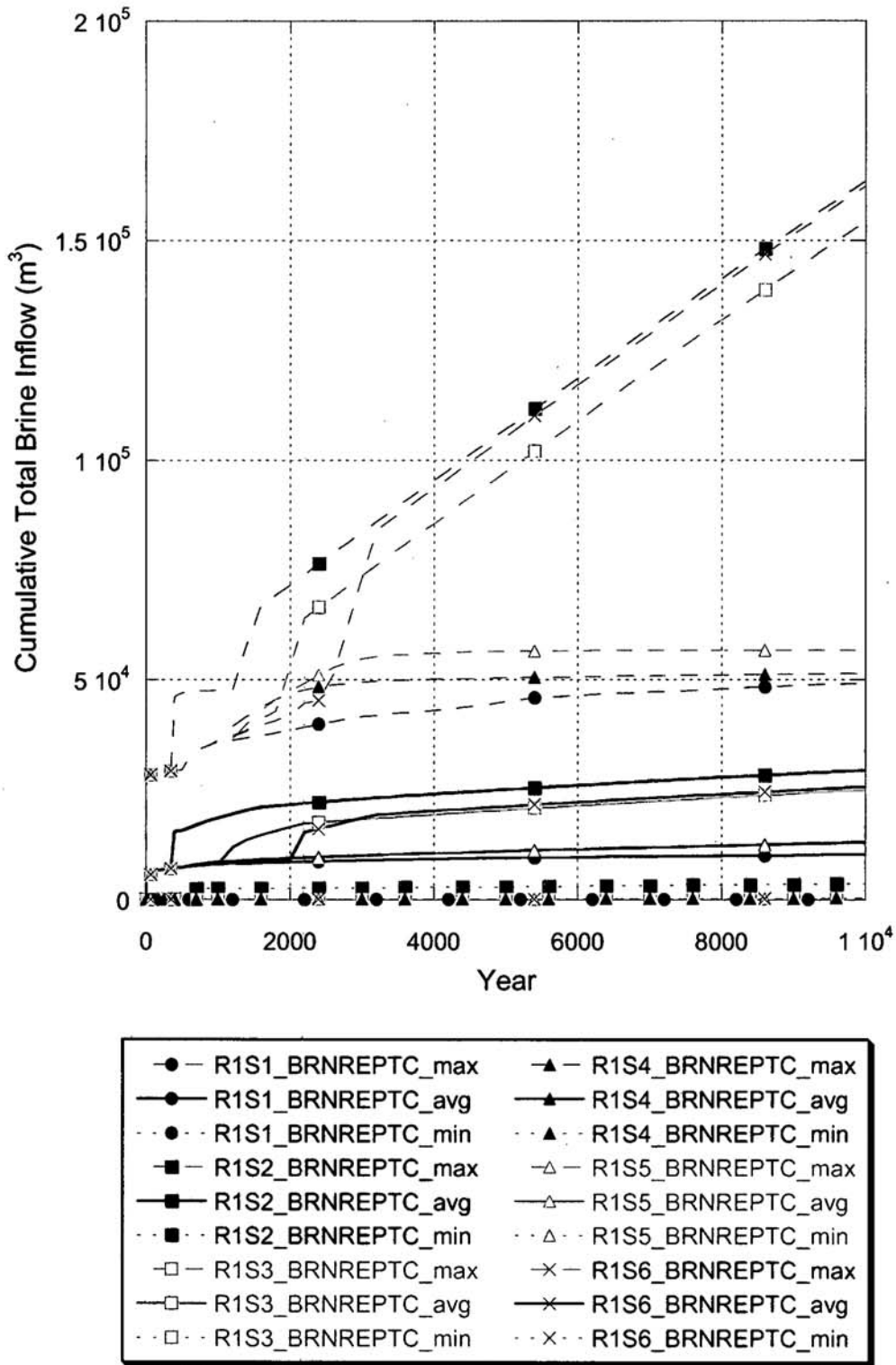
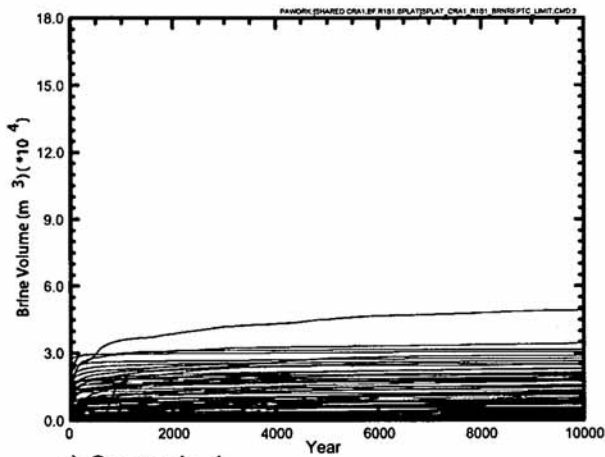
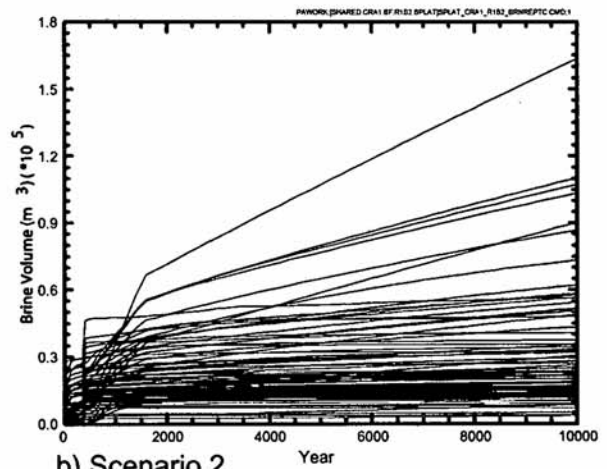


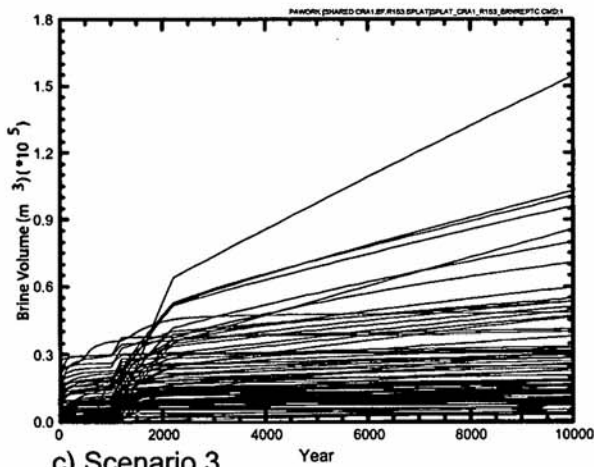
Figure 5.4.6: R1: Total Cumulative Brine Flow into the Repository in Six Scenarios



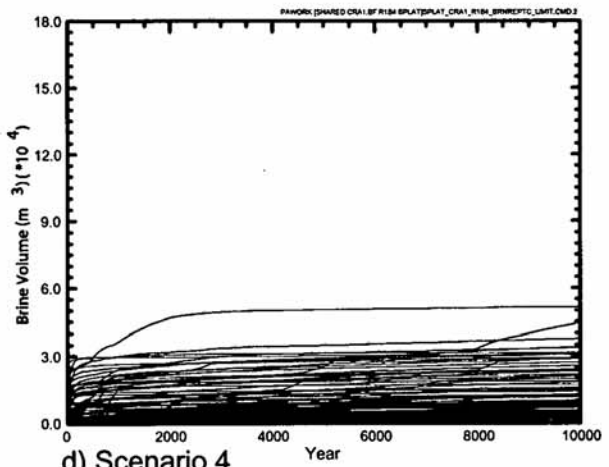
a) Scenario 1



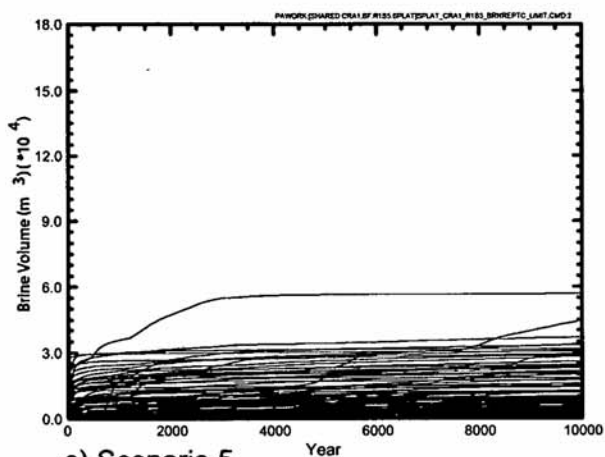
b) Scenario 2



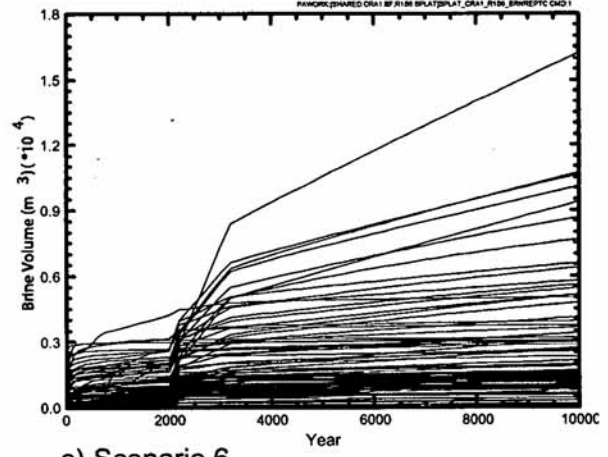
c) Scenario 3



d) Scenario 4



e) Scenario 5



e) Scenario 6

Figure 5.4.7: R1 – Horsetail Plots for Total Cumulative Brine Flow into the Repository in Six Scenarios

Information Only

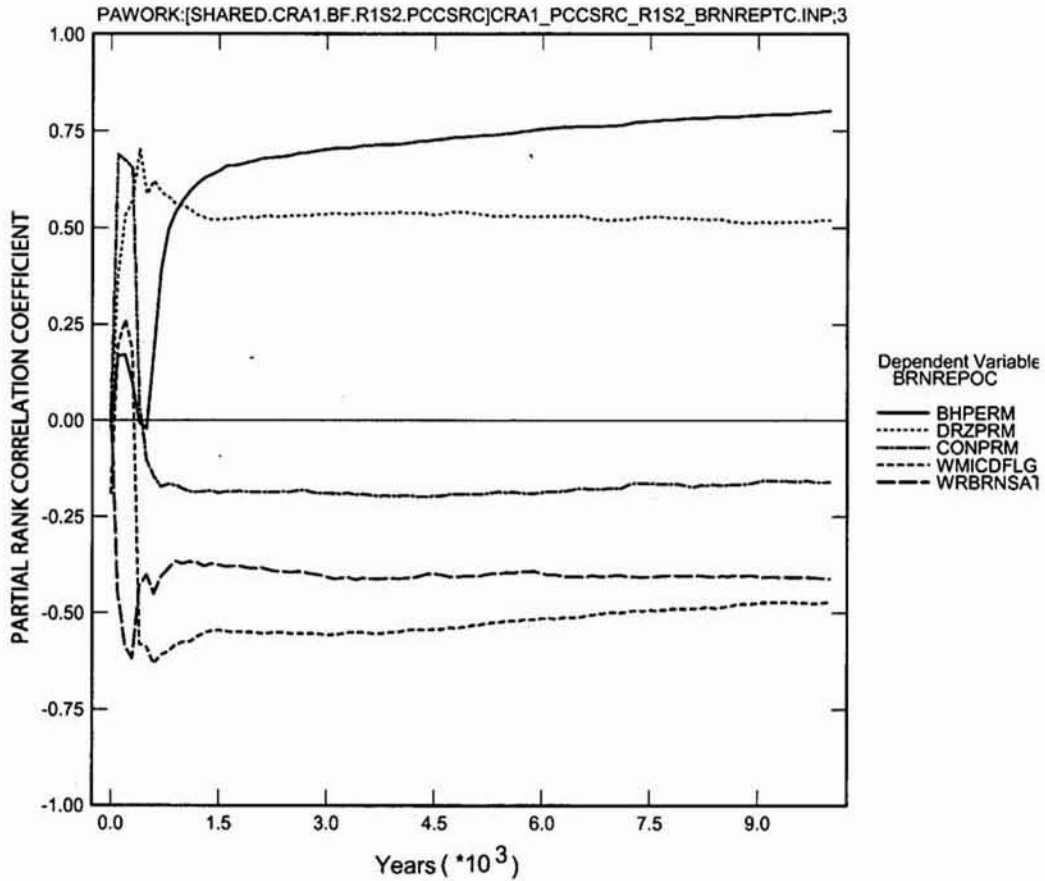


Figure 5.4.8: R1S2 - Primary Correlations for Brine Inflow, BRNREPTC, with Input Parameters

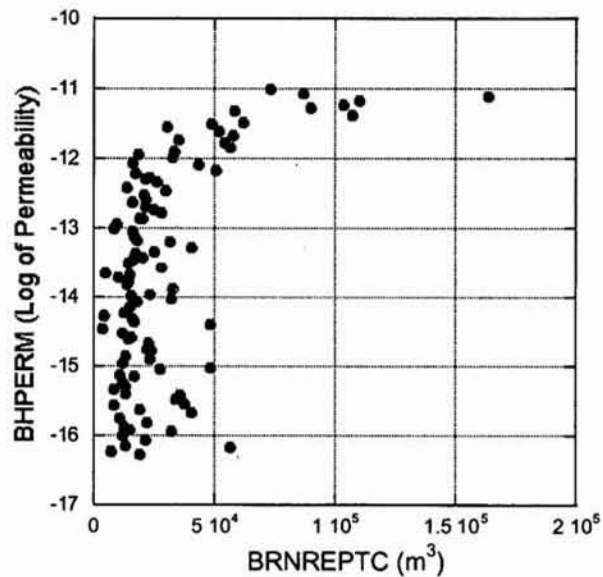


Figure 5.4.9: R1S2 - BHPERM versus BRNREPTC

5.4.4 Brine Saturation

One of the most direct consequences of greater brine inflow associated with a drilling intrusion is higher brine saturation in the Waste Panel. E1 intrusions usually permit an influx of brine from the Castile, and E2 drilling events usually reduce the pressure in the Waste Panel by releasing gas (and brine) up the borehole, thereby allowing increases brine inflow from the DRZ and the marker beds. Brine saturation is important to PA because the transport pathways of contaminated brine to the accessible environment (to the surface or through the Culebra) represent possible release mechanisms.

Brine saturation in the Waste Panel, WAS_SATB, is highest in the E2 scenarios (S2, S3, and S6) and lowest in the Undisturbed Scenario S1. Scenario S2 has the highest average value of WAS_SATB (~ 0.7) because the pressure difference between the repository and the brine reservoir is greater at 350 years than at 1,000 years. Consequently, earlier intrusions experience more brine flows from the Castile into the repository. In contrast, the average brine saturation for an E2 event, which does not encounter pressurized brine, does not exceed 0.35 over the 10,000-year regulatory period. The effect on maximum brine saturation plots is similar (Figure 5.4.10).

Brine saturation in the Waste Panel, WAS_SATB, exceeds 0.8 in most vectors of the E1 intrusion scenarios (S2, S3, and S6) whereas it is less than 0.20 in most vectors of the Undisturbed Scenario S1. It is also less than 0.20 in a majority of vectors in the E2 scenarios (S4 and S5), but unlike Scenario S1, there are a significant number of vectors with elevated brine saturation (Figure 5.4.11).

Plots of brine saturation in the Rest of Repository (SRR and NRR) and in the non-waste areas (NWA) are shown in figure 5.4.12 for the scenarios S2 and S5. These scenarios are representative of the conditions caused by E1 and E2 intrusions, respectively. The brine saturation effects of the intrusion are mostly dampened in the other excavated regions of the repository by the Option D panel closures (Figure 5.4.12). Brine saturation trends in the RoR-South (SRR), RoR-North (NRR), and the NWA are very similar between Scenarios S2 and S5. Figure 5.4.13 compares brine saturation statistics between the excavated areas for Scenario S2. Brine saturations in the Waste Panel and non-waste areas are highest, followed by the RoR-South and then the RoR-North. This pattern is consistent with the sources of brine inflow from the borehole and marker beds and the lack of corrosion and brine consumption in the non-waste areas.

The most significant PRCC for brine saturation in the Waste Panel, WAS_SATB, over the 10,000-year period is for the input parameters, WMICDFLG and BHPERM (Figure 5.4.14). The PRCC for WMICDFLG, drops below -0.75 after the plugs fail in the borehole and then stabilizes near -0.50. The amount of microbial gas generation effects pressure, which in turn influences the amount of brine that remains in the Waste Panel. The PRCC for BHPERM temporarily declines below 0.50, but then rises to stabilize near 0.65 becoming the dominant determinant of WAS_SATB after the borehole plugs fail at 550 years. However, scatter plots for WAS_SATB versus each of these input parameters, BHPERM (Figure 5.4.15) and WMICDFLG (Figure 5.4.16) show very little correlation. Brine saturation in the Waste Panel is the consequence of multiple processes and conditions. No single input parameter has a strong determining influence on WAS_SATB over the full range of input parameters represented in 100 vectors.

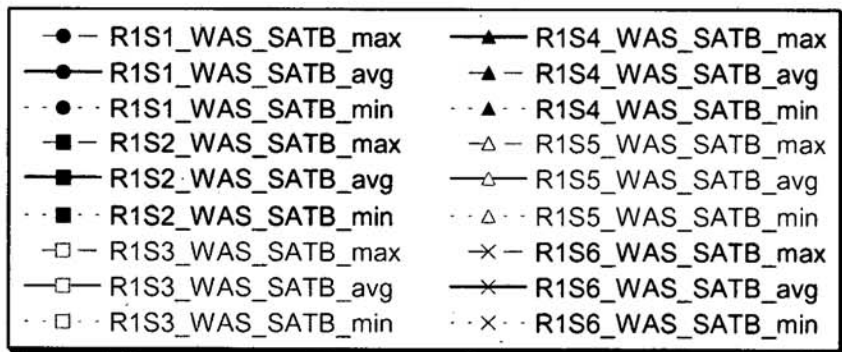
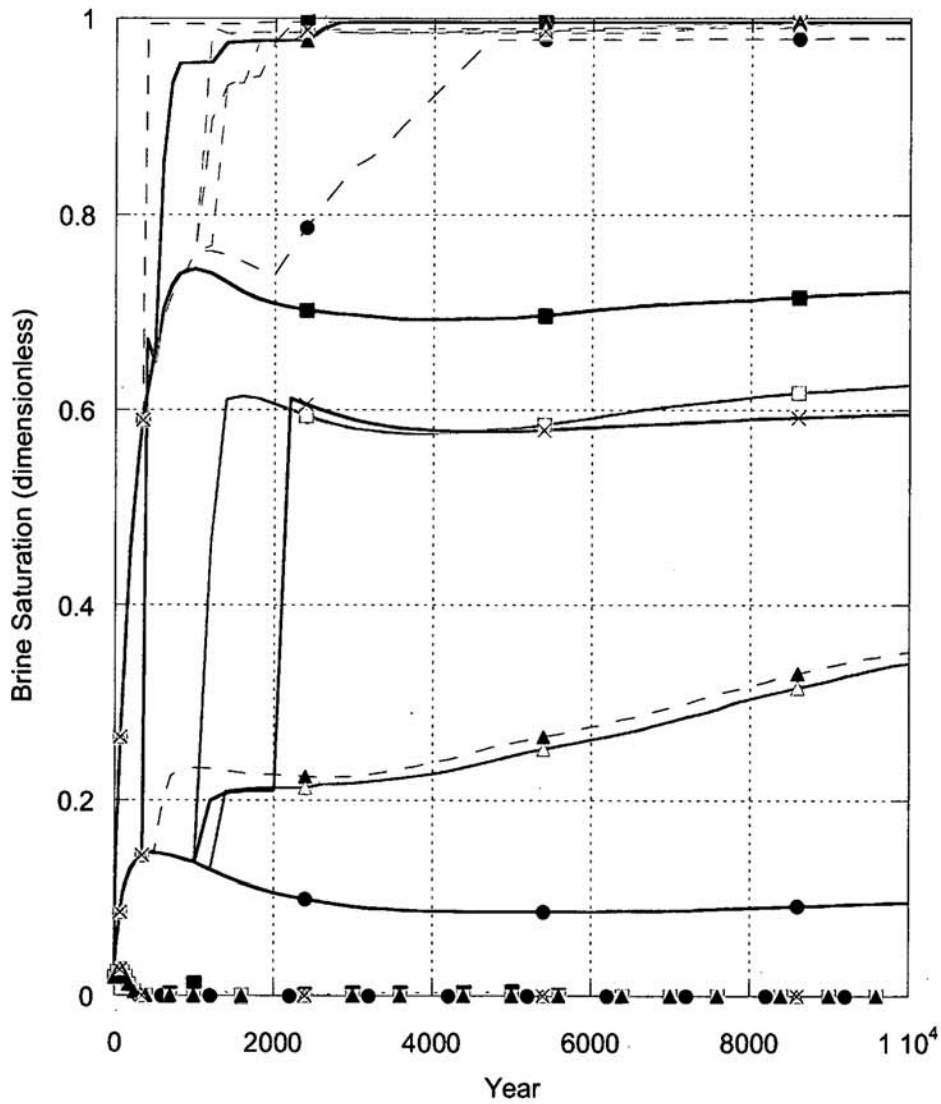


Figure 5.4.10: R1: Brine Saturation in the Waste Panel for Six Scenarios

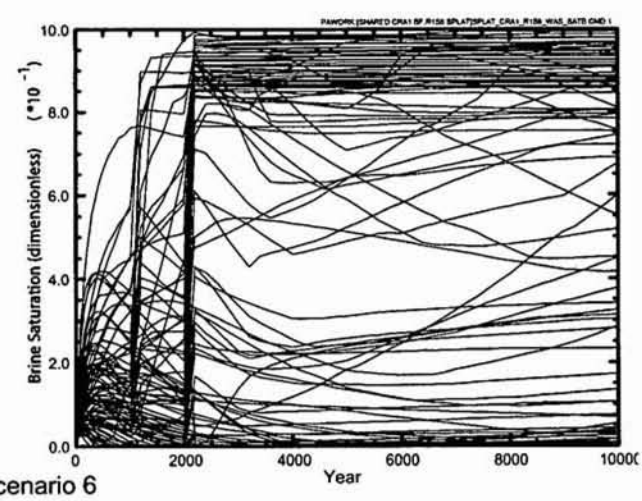
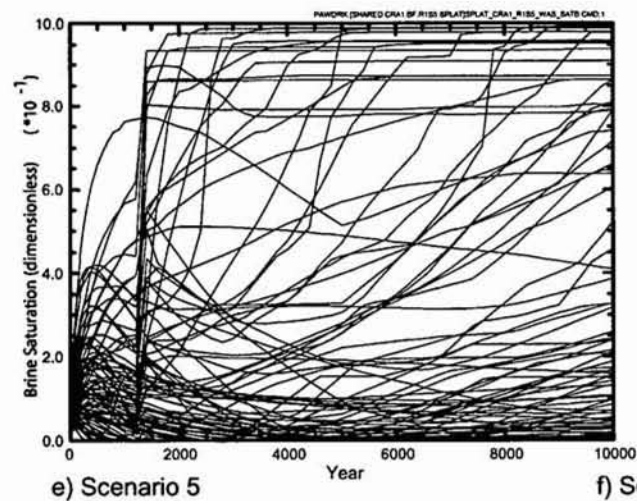
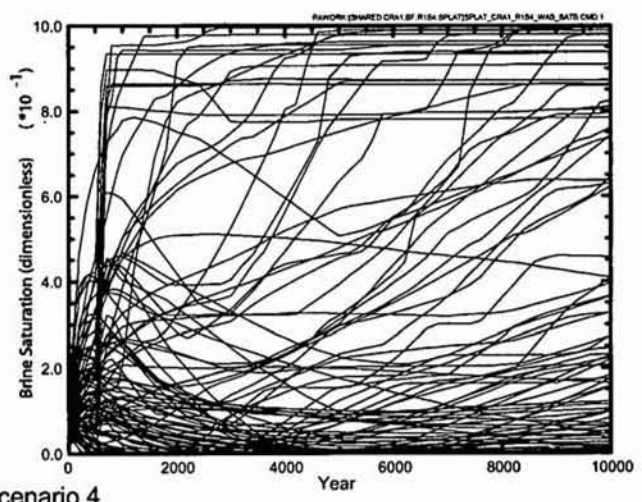
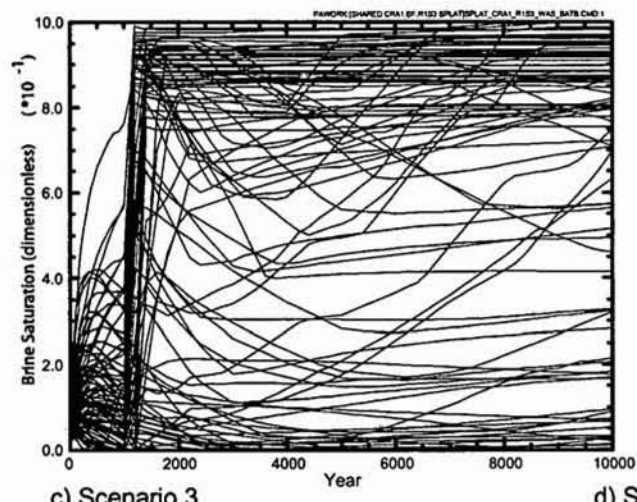
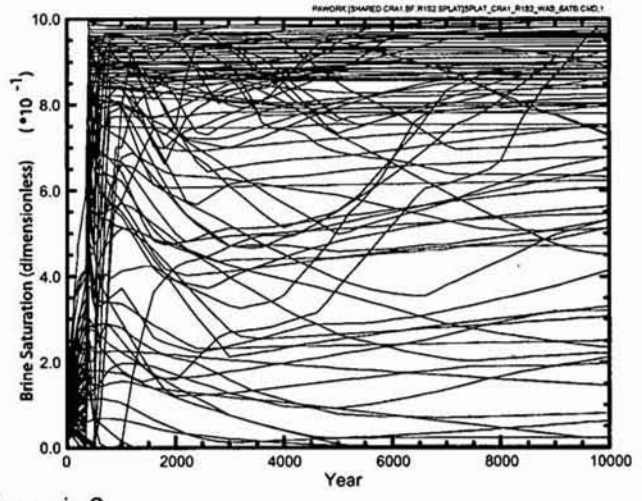
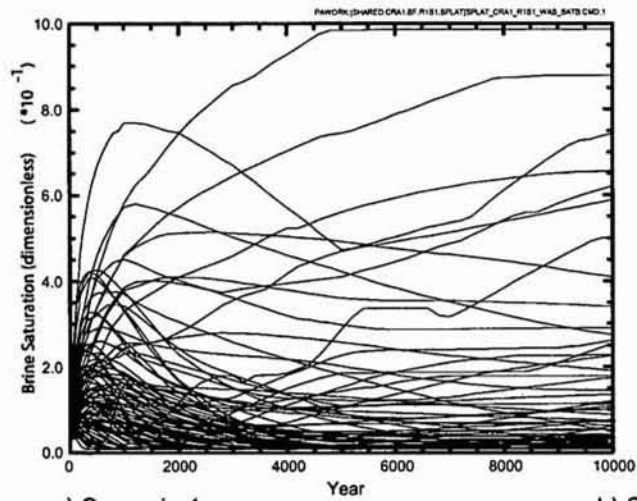
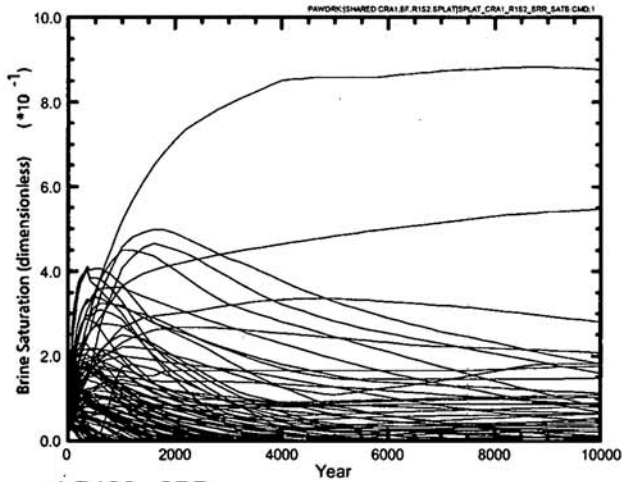
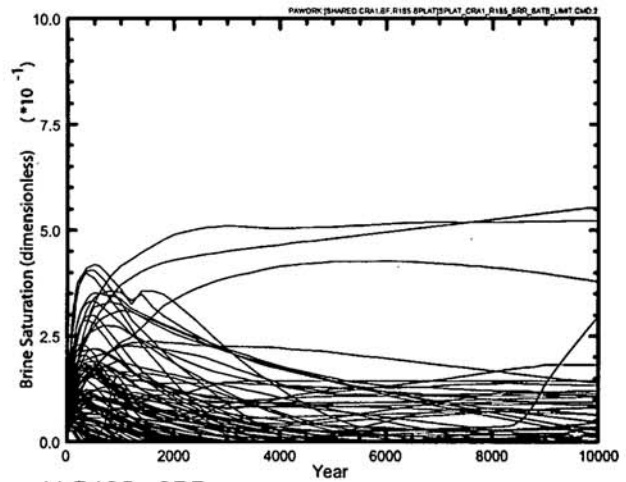


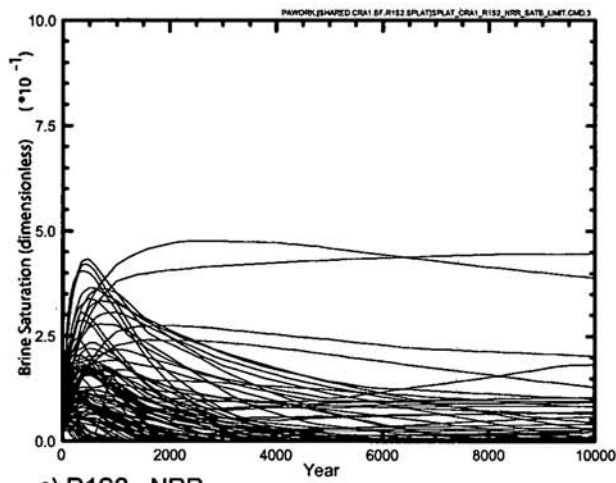
Figure 5.4.11: R1 – Horsetail Plots for Brine Saturation in the Waste Panel for Six Scenarios



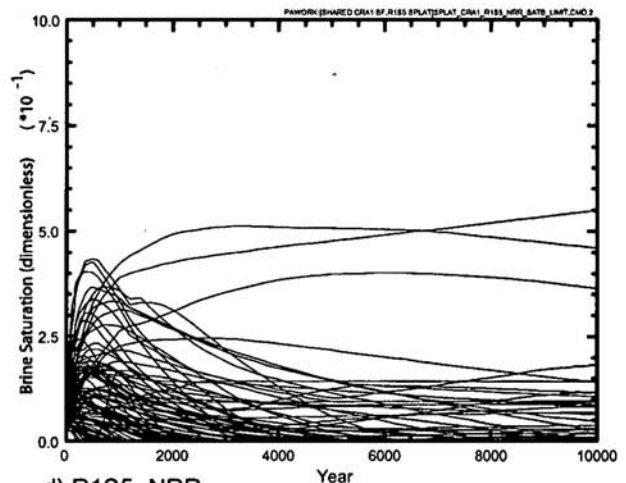
a) R1S2 - SRR



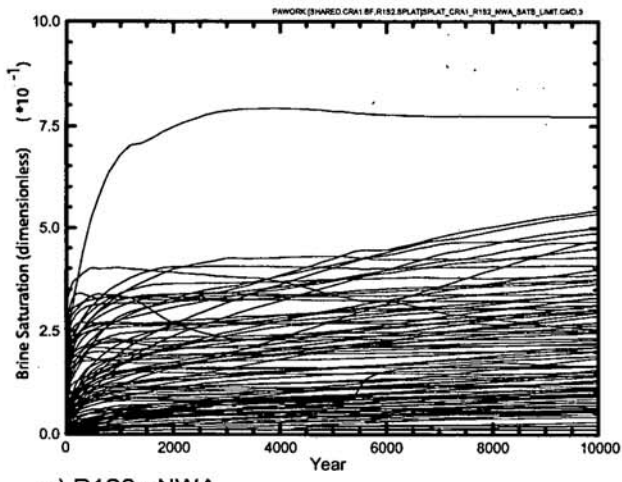
b) R1S5 - SRR



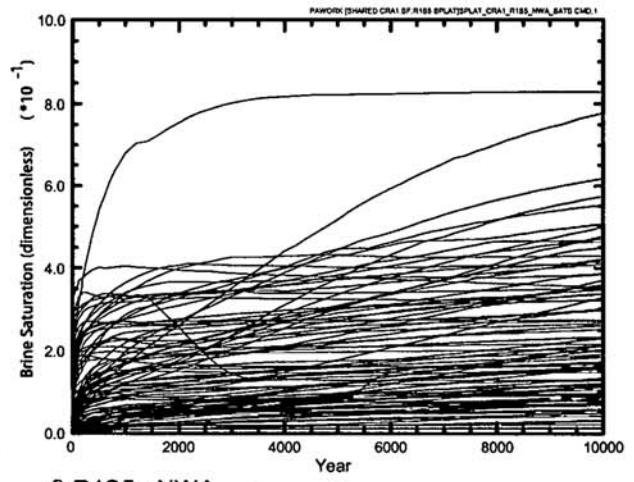
c) R1S2 - NRR



d) R1S5 - NRR



e) R1S2 - NWA



f) R1S5 - NWA

Figure 5.4.12: R1S2 and R1S5 – Horsetail Plots for Brine Saturation

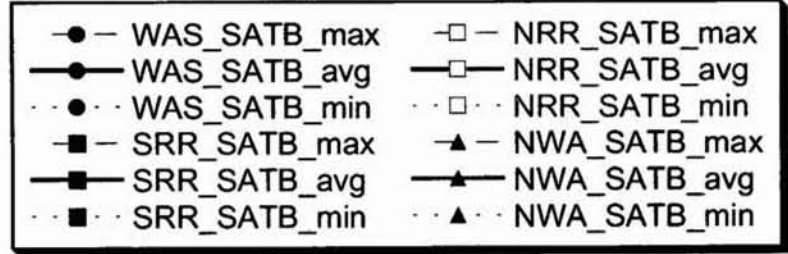
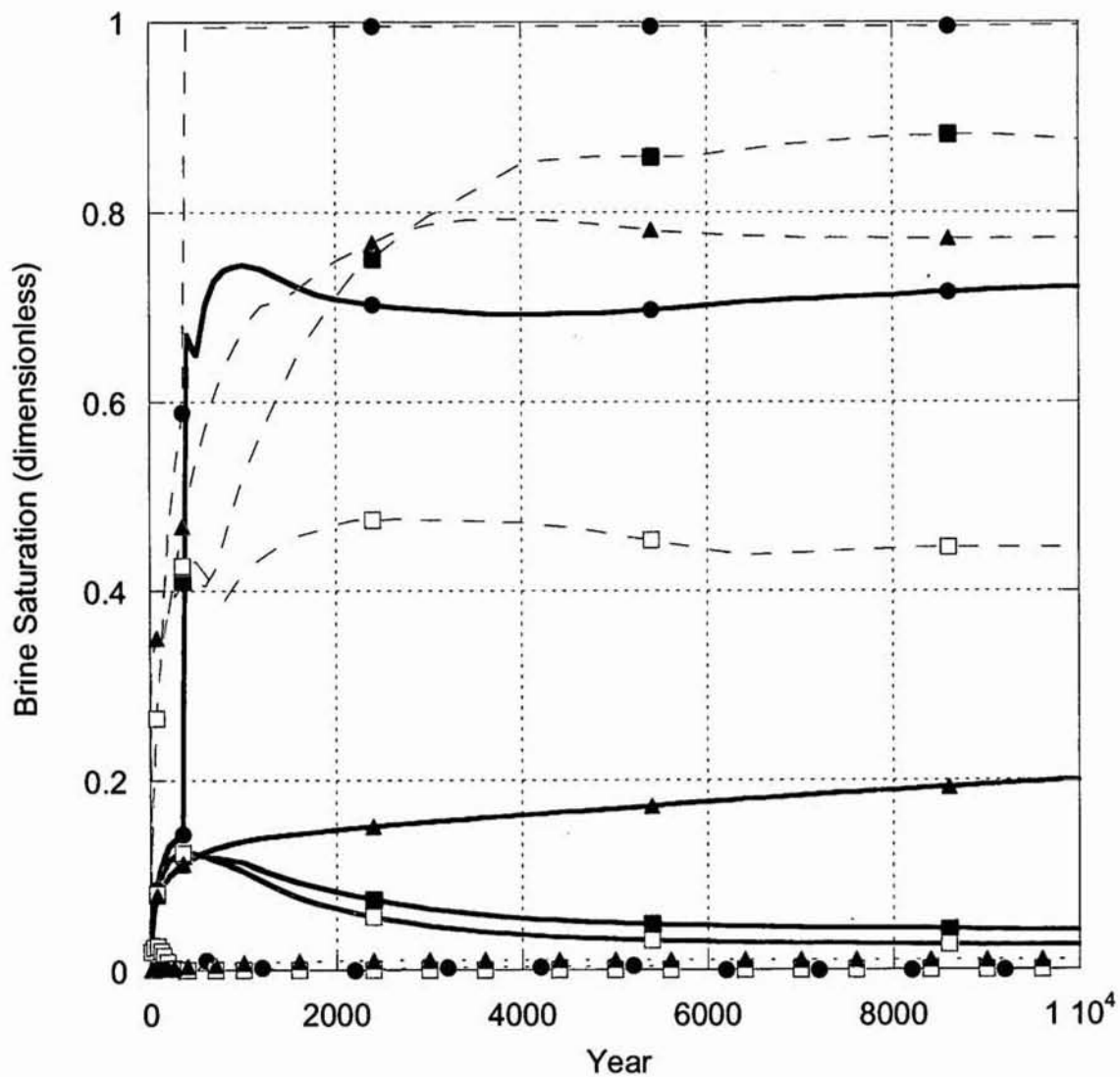


Figure 5.4.13: R1S2 - Brine Saturation in Excavated Areas

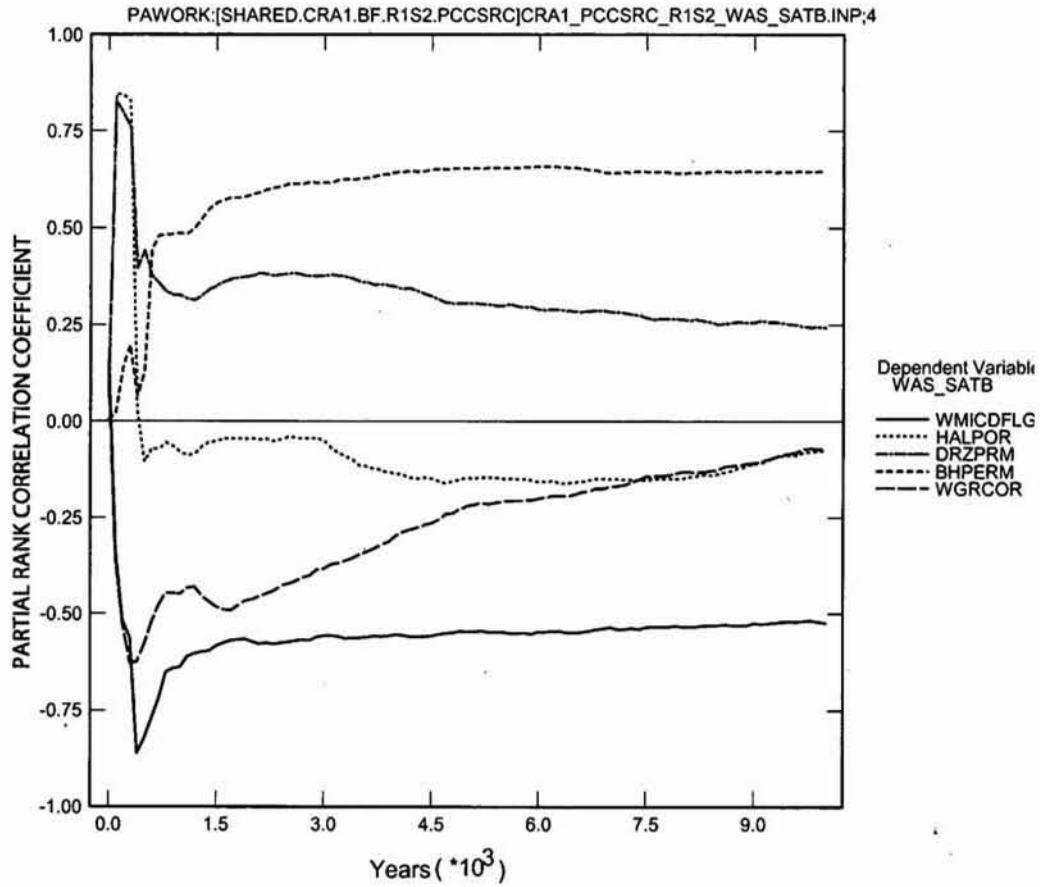


Figure 5.4.14: R1S2 - Primary Correlations for Brine Saturation in the Waste Panel, WAS_SATB, with Input Parameters

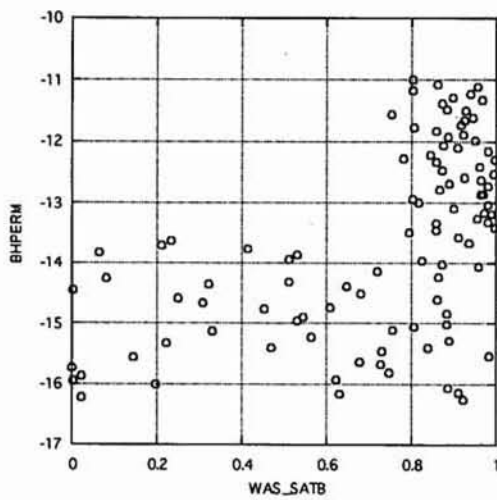


Figure 5.4.15: R1S2 - BHPERM versus WAS_SATB

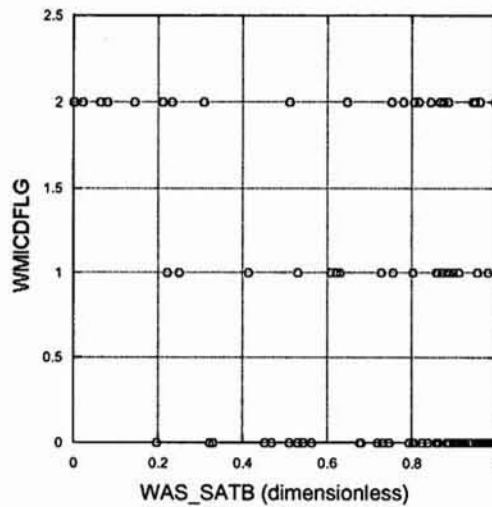


Figure 5.4.16: R1S2 - WMICDFLG versus WAS_SATB

5.4.5 Gas Generation

Table 5.4.2 summarizes average cumulative gas generation information at 10,000 years for the six scenarios. Drilling intrusions do not affect gas generation by microbial activity. Average cumulative microbial gas generation varies by less than 0.2% among all six scenarios. However, gas generation by corrosion is greater by 13% to 17% in E1 scenarios (S2, S3, & S6) and by about 9% in E2-only intrusions (Figure 5.4.17) than in the undisturbed scenario, S1. Brine is usually the limiting factor for corrosion, and increased corrosion is due to increased availability of brine in many vectors. At 10,000 years, the average brine saturation in the Waste Panel, WAS_SATB, increases from 0.075 in the undisturbed scenario (S1), to about 0.5 for an E2-only drilling intrusion (S4 & S5) and to 0.6 or more in the E1 intrusions (S2, S3, & S6) (Figure 5.4.10). However, horsetail plots of total gas generation are remarkably similar for all six scenarios (Figure 5.4.18).

TABLE 5.4.2: AVERAGE BRINE SATURATION AND CUMULATIVE GAS GENERATION RESULTS AT 10,000 YEARS

a) Average brine saturation and gas generation for 100 vectors

	S1	S2	S3	S4	S5	S6
WAS_SATB	0.096	0.721	0.626	0.352	0.341	0.596
GAS_MOLE	4.73E+08	5.25E+08	5.14E+08	5.00E+08	4.98E+08	5.12E+08
FE_MOLE	2.98E+08	3.50E+08	3.39E+08	3.26E+08	3.24E+08	3.37E+08
CELL_MOL	1.7414E+08	1.7439E+08	1.7442E+08	1.7413E+08	1.7426E+08	1.7431E+08

b) Percentage change versus the undisturbed scenario in the averages for 100 vectors

	S2	S3	S4	S5	S6
WAS_SATB	651%	552%	267%	255%	521%
GAS_MOLE	11%	9%	6%	5%	8%
FE_MOLE	17%	14%	9%	9%	13%
CELL_MOL	0%	0%	0%	0%	0%

The PRCC for moles of gas produced by corrosion, FE_MOLE, in the S2 scenario is shown in figure 5.4.19. The effects of the drilling intrusion on input dependencies is more gradual than for variables that are immediately dominated by the influx of brine from the Castile (e.g., brine inflow and brine saturation). The PRCC's for the corrosion rate, WGRCOR, and for WASTWICK are important early but begin to decline after the intrusion. WGRCOR continues to be the most important input parameter up to about 3,000 years, after which, the porosity of halite, HALPOR, becomes more important, because it controls the availability of brine in the DRZ. The PRCC's for DRZPRM and BHPERM are also positive, because increased brine flow from the DRZ and from the Castile favors increased corrosion due to the increase in the availability of brine.

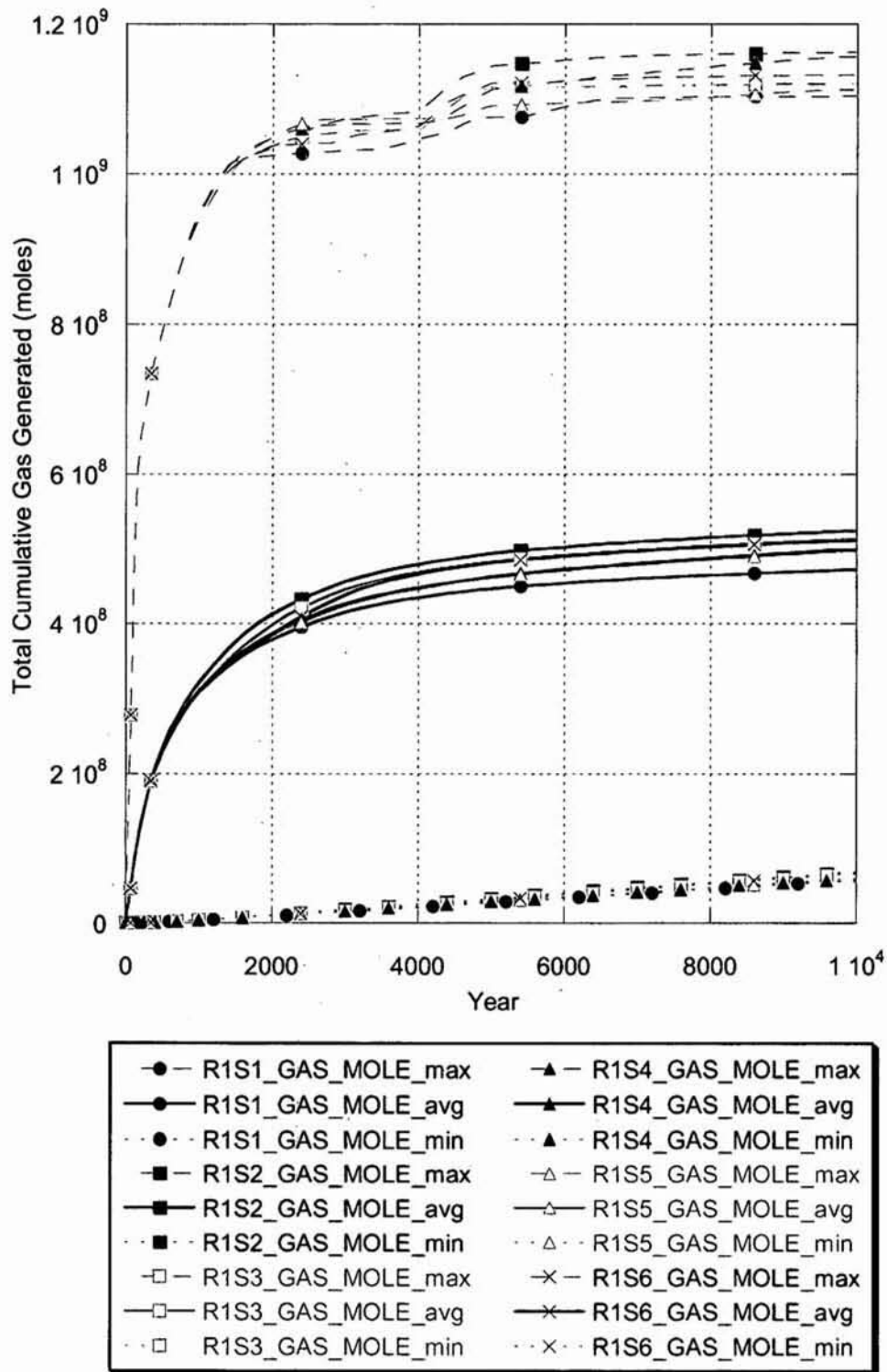


Figure 5.4.17: R1: Total Cumulative Gas Generation for Six Scenarios

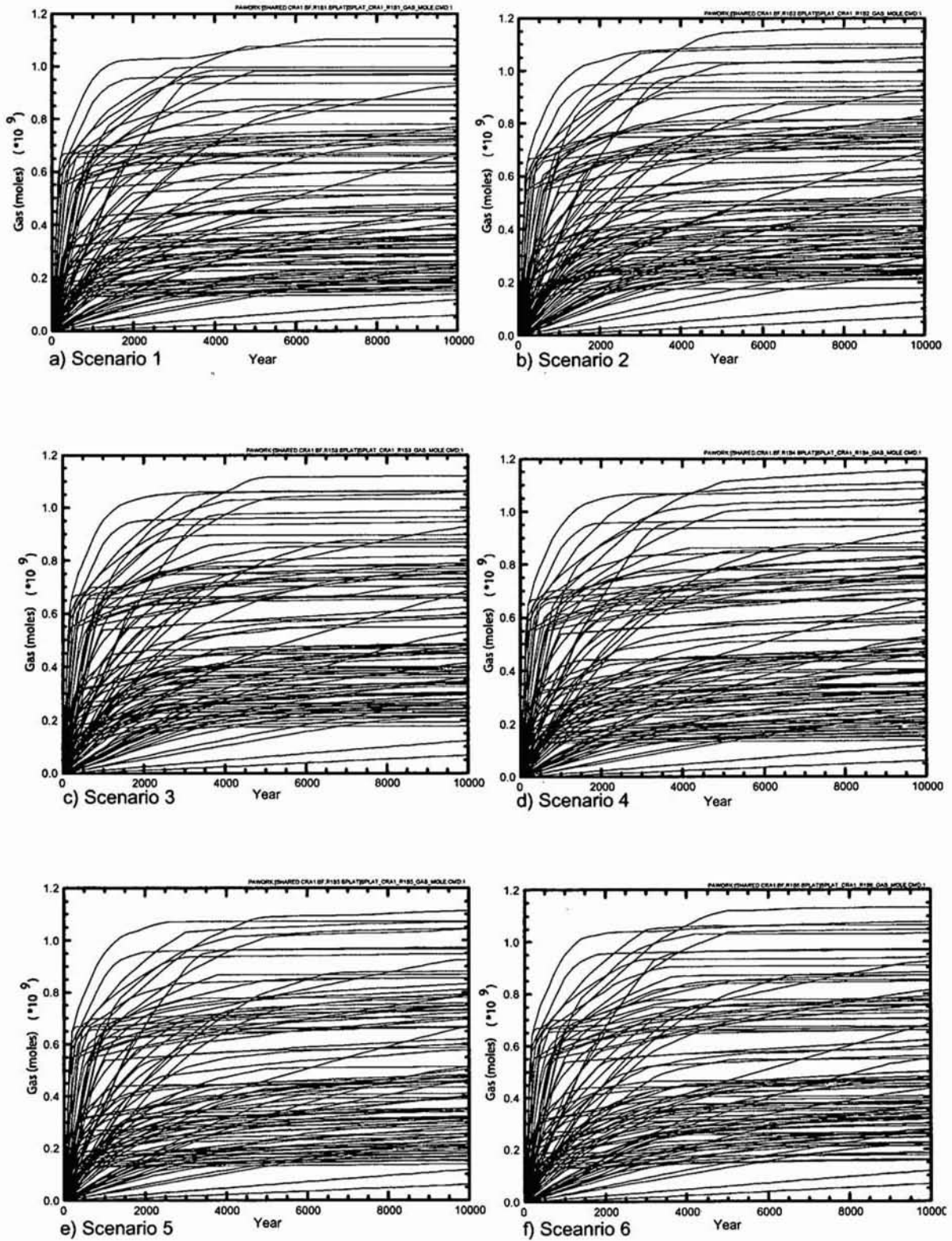


Figure 5.4.18: R1 – Horsetail Plots for Total Cumulative Gas Generation in the Waste Panel for Six Scenarios

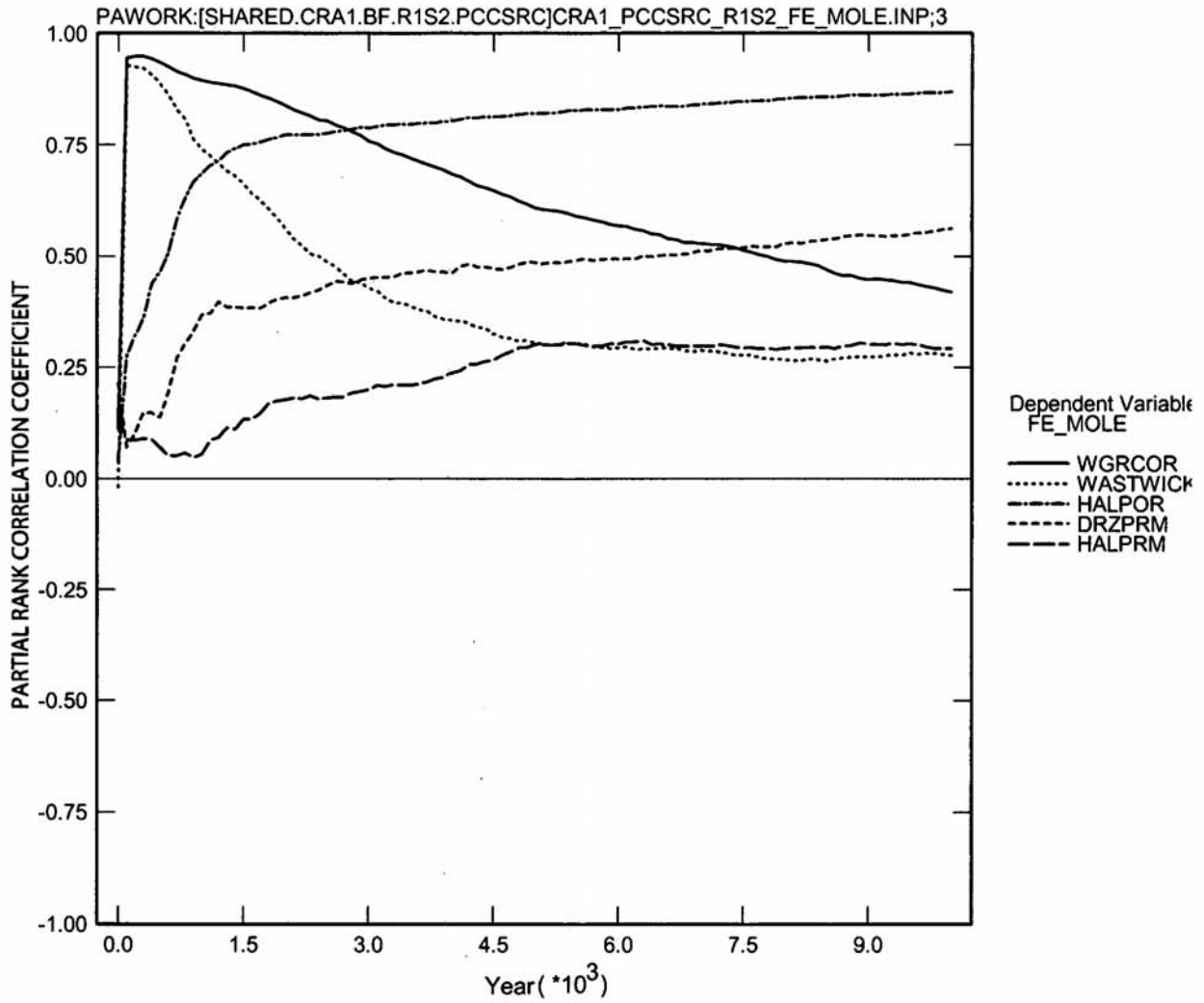


Figure 5.4.19: R1S2 - Primary Correlations for Gas Generation by Corrosion in the Waste Panel, FE_MOLE, with Input Parameters

5.4.6 Pressure

Pressure in the disturbed scenarios is identical to pressure in the undisturbed scenarios until the drilling intrusion occurs. Following the intrusion, pressure in the Waste Panel tends to change rapidly, especially once the borehole plugs fail 200 years after the intrusion. For the E1 intrusion scenarios (S2, S3, and S6), pressure in the Waste Panel can increase or decrease depending on whether the sampled brine pocket pressure in the Castile is greater or less than the pre-intrusion pressure in the Waste Panel. Once the borehole plugs fail, the pressure in the repository and the brine reservoir immediately begins to equalize, and for very high repository pressures, very little brine may flow to the repository from the brine pocket because the pressure gradient between the two areas is minimal.

Repository pressure in the disturbed scenarios stabilizes at lower values than the undisturbed Scenario 1 due to the borehole connection to the ground surface. The average pressure in the E1 scenarios (S2, S3, and S6) is about 80% of the pressure in Scenario S1 by 5,000 years, and the average pressure in E2 scenarios is 60% of the pressure in Scenario S1 by 1,200 years (Figure 5.4.20). The maximum pressures in each scenario are very similar, because gas is generated much faster than fluids can escape, usually because borehole permeability is relatively low.

The pressure in many vectors of the E1-only scenarios (S2 and S3) increases sharply at the time of the drilling intrusion and then declines sharply when the borehole plugs fail 200 years later (Figure 5.4.21b & c). Vectors with high repository pressure (a model output variable) at the time of the drilling event and lower pressure in the brine pocket (a sampled input parameter) can actually show a pressure decrease at the time of the drilling intrusion. However, only a few vectors show this combination of circumstances. The effect of borehole plug failure 200 years later varies depending upon gas generation and the sampled permeability of the degraded borehole material, BH_SAND, which represents the borehole from the repository to the surface to the end of the regulatory period. At the time of the intrusion, many vectors show a sharp drop in pressure due to the release of gas and brine up the borehole (Figure 5.4.21b & c). However, some vectors then show increasing pressure as gas generation exceeds the outward migration of gas and brine. Twelve hundred years after the drilling intrusion, the borehole connection to the Castile is sealed by creep closure. However, this material change does not appear to have a significant effect on pressure.

The E2 scenarios (S4 & S5) show the largest drop in pressure compared with the undisturbed Scenario S1. The borehole plugs, which have a relatively low permeability, are assumed to be emplaced immediately at the time of drilling, and therefore, there is no sharp change in pressure at the time of the drilling event (Figure 5.4.21d & e). When the plugs fail, 200 years after the borehole has been drilled, the pressures in the intruded panel tend to drop sharply as gas is allowed to escape up the borehole (Figure 5.4.21d & e). Pressure changes are largely dependent upon a variety of factors including the sampled borehole permeability and gas generation parameters.

Scenario S6 has two drilling intrusions. The first is an E2 event, and the resulting pressure drop is identical to Scenario S5. In most vectors, the pressure decreases so much that there is a sharp increase in WAS_PRES when the second drilling intrusion encounters pressurized brine. The

horsetail plots in Figure 5.4.21f show a low-pressure trough between the drilling events, and the pressure trend after the second event is very similar to the E1 scenarios (S2 and S3).

Pressure dependencies are very similar in E1 and E2 scenarios, because the permeability of borehole fill becomes the dominant determinant of pressure after the plugs fail in the borehole. The PRCC for pressure in the Waste Panel, WAS_PRES, stabilizes at about -0.8 for borehole permeability, BHPERM, after the connection to the Castile has been sealed by creep closure in Scenario 2 (Figure 5.4.22). The permeability of the borehole connection to the surface determines how high the pressure can rise due to gas generation. There are also positive PRCC's with the microbial gas generation parameter, WMICDFLG, and with the initial pressure in the Castile, BPINTPRS, because both can cause pressure to rise in the repository depending upon the permeability of the borehole. The PRCC for BHPERM in Scenario 5 also stabilizes near -0.8 after the borehole plugs fail (Figure 5.4.23).

The dominating importance of BHPERM to pressure in the Waste Panel is also illustrated by scatter plots of the three most significant input parameters, with the highest PRCC's, to WAS_PRES at 10,000 years. The plot of BHPERM versus WAS_PRES shows a negative correlation (Figure 5.4.24), but scatter plots for WMICDFLG (Figure 5.4.25) and BPINTPRS (Figure 5.4.26), which have the second and third most significant PRCCs, respectively, show no clear correlation.

The Option D panel closures delay equalization of pressure between excavated areas in many vectors. Figure 5.4.27 displays plots for the maximum, average, and minimum pressures within each excavated area in Scenario 2. Pressure within the Operations and Experimental non-waste areas are always very close because the concrete monolith that separates them in the model is relatively permeable.

At very high pressures the Option D panel closures allow rapid fluid exchange and pressure equalization to occur between the various excavated areas because the DRZ and marker beds are sufficiently fractured to permit equalization of pressure throughout the waste areas. However, even at high pressures there is a pressure difference of as much as 2 MPa between the waste and non-waste areas, which are separated in the model by a double-wide set of Option D panel closures. Under high pressure conditions the pressure in the waste and non-waste areas equalizes by about 3,000 years. At average pressures there is a longer delay in pressure equalization between different parts of the repository. It is about 1,500 years after the drilling intrusion when pressure equalizes between the Waste Panel and the RoR areas, and about 4,000 to 5,000 years when the non-waste areas reach pressures near the waste areas. At low pressures the delay in pressure equalization is greater than the 10,000 year modeling period and pressures do not equalize.

Pressure statistics are useful for evaluating potential repository performance, but analysis of individual vectors is a better approach for understanding the dynamics of pressure given a set of input parameters. Vector 52 has the highest pressure at 10,000 years (Figure 5.4.28). It shows almost no variability of pressure among the excavated areas because the DRZ is sufficiently fractured to allow the pressure to quickly equalize even with the non-waste areas. Vector 59 has a pressure value that is closest to the average at 10,000 years and pressures do not fully equalize

until about 7,000 years (Figure 5.4.29). Vector 2 has the minimum pressure at 10,000 years, but the pressure reaches 12 MPa immediately after the drilling intrusion when the borehole intersects the pressurized brine reservoir. Pressure in the RoR and non-waste areas are fairly close, but changes in pressure lag the Waste Panel by as much as 1,200 years (Figure 5.4.30).

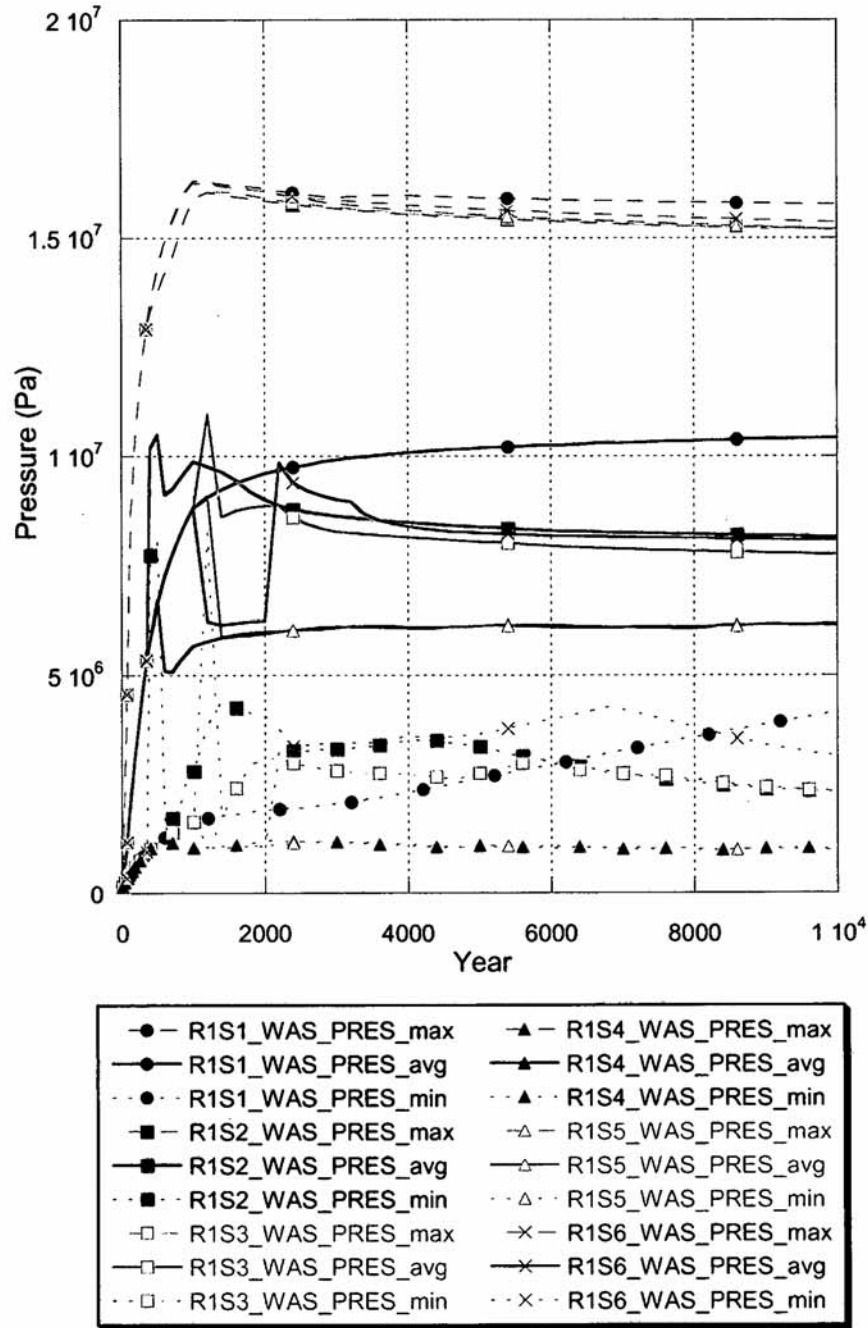


Figure 5.4.20: R1: Pressure in the Waste Panel for Six Scenarios

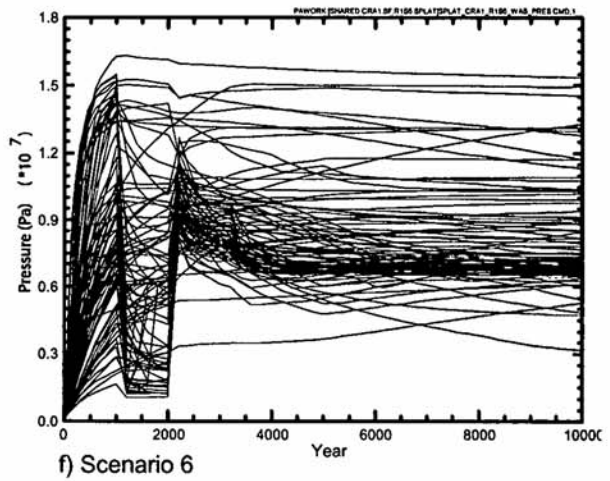
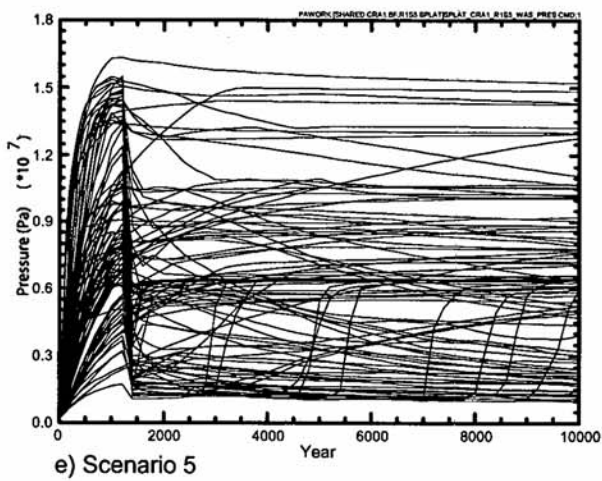
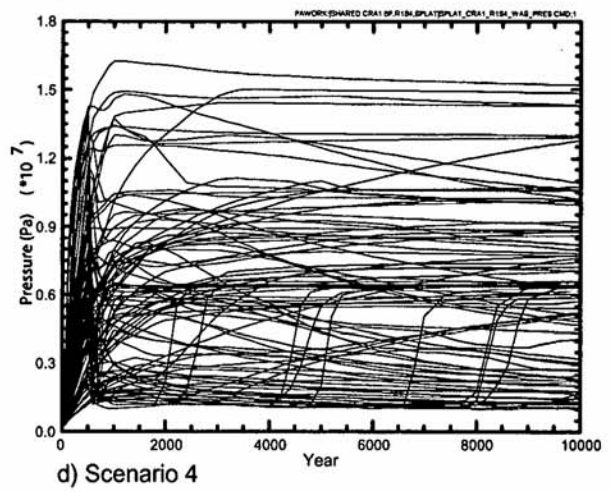
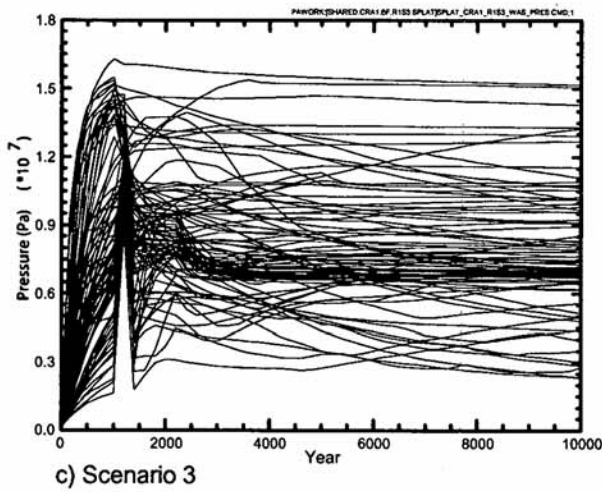
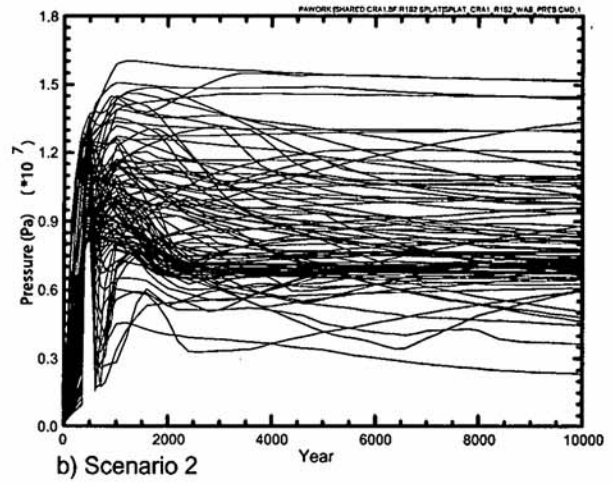
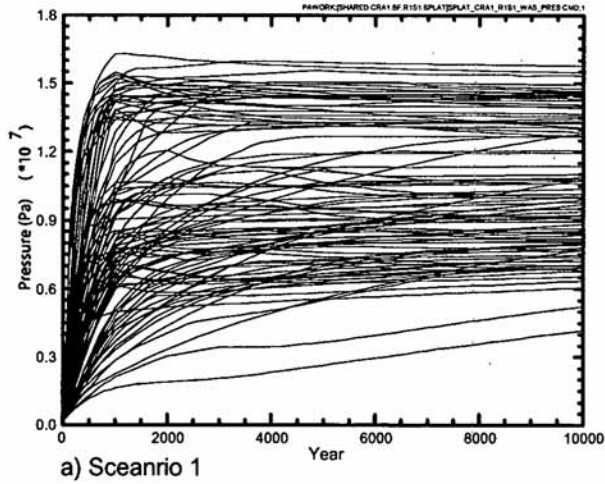


Figure 5.4.21: R1 – Horsetail Plots for Pressure in the Waste Panel for Six Scenarios

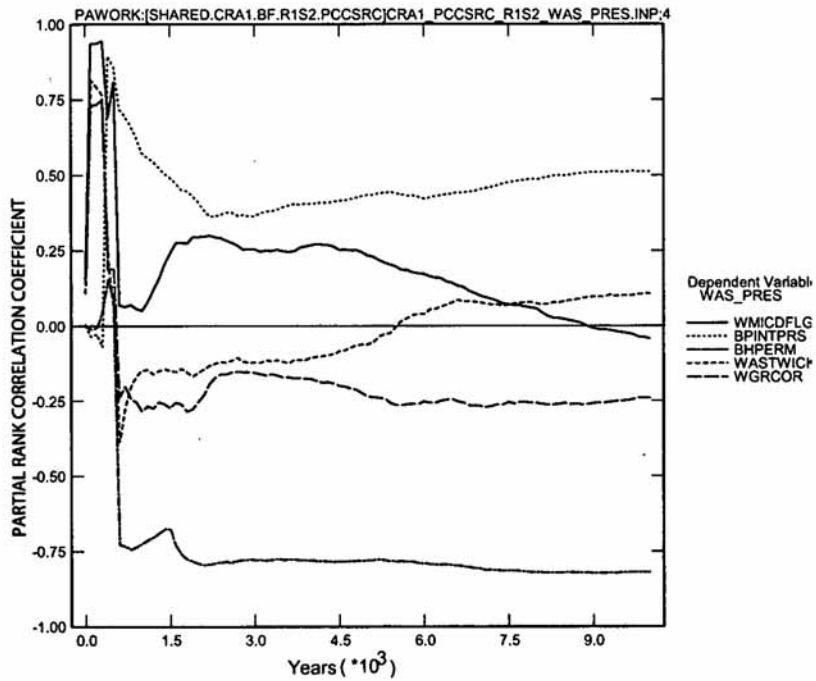


Figure 5.4.22: R1S2 - Primary Correlations for Pressure in the Waste Panel, WAS_PRES, with Input Parameters

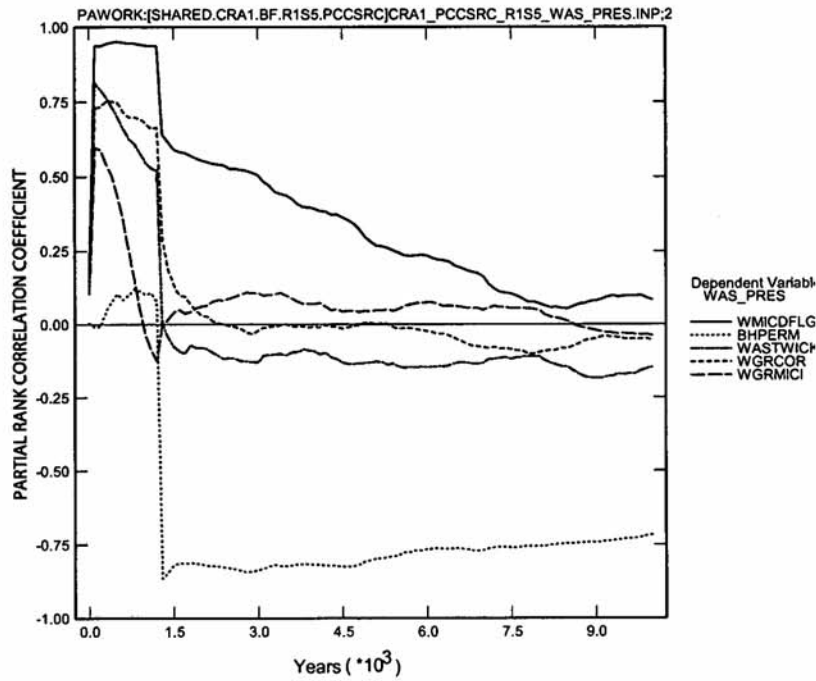


Figure 5.4.23: R1S5 - Primary Correlations for Pressure in the Waste Panel, WAS_PRES, with Input Parameters

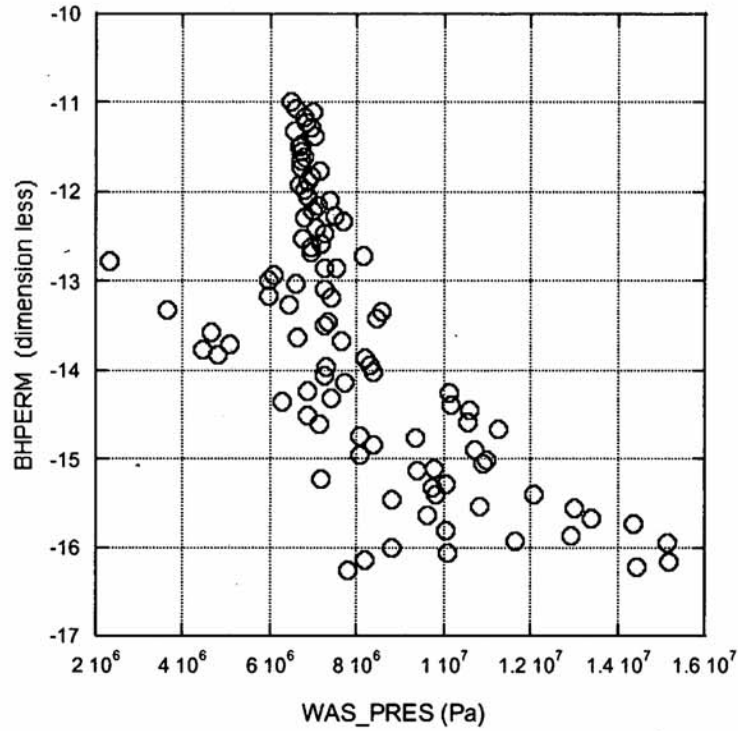


Figure 5.4.24: R1S2 – BHPERM versus WAS_SATB

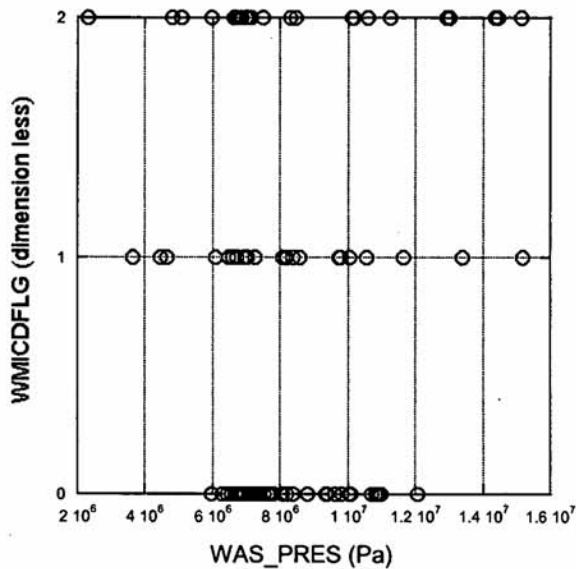


Figure 5.4.25: R1S2 – WMICDFLG versus WAS_PRE at 10,000 Years

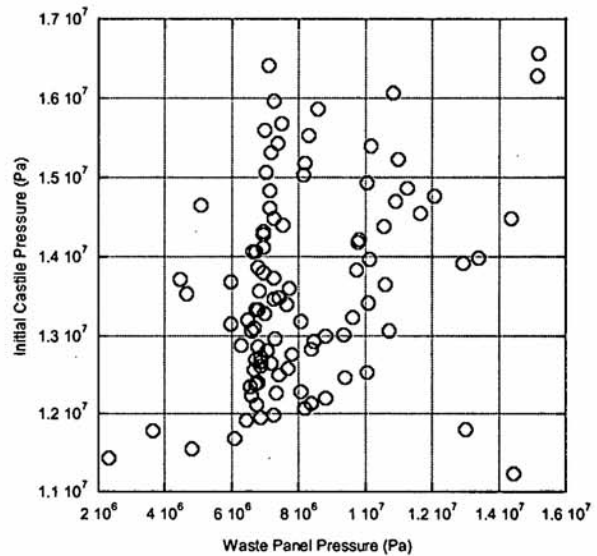


Figure 5.4.26: R1S2 – BPINTPRS versus WAS_PRE at 10,000 Years

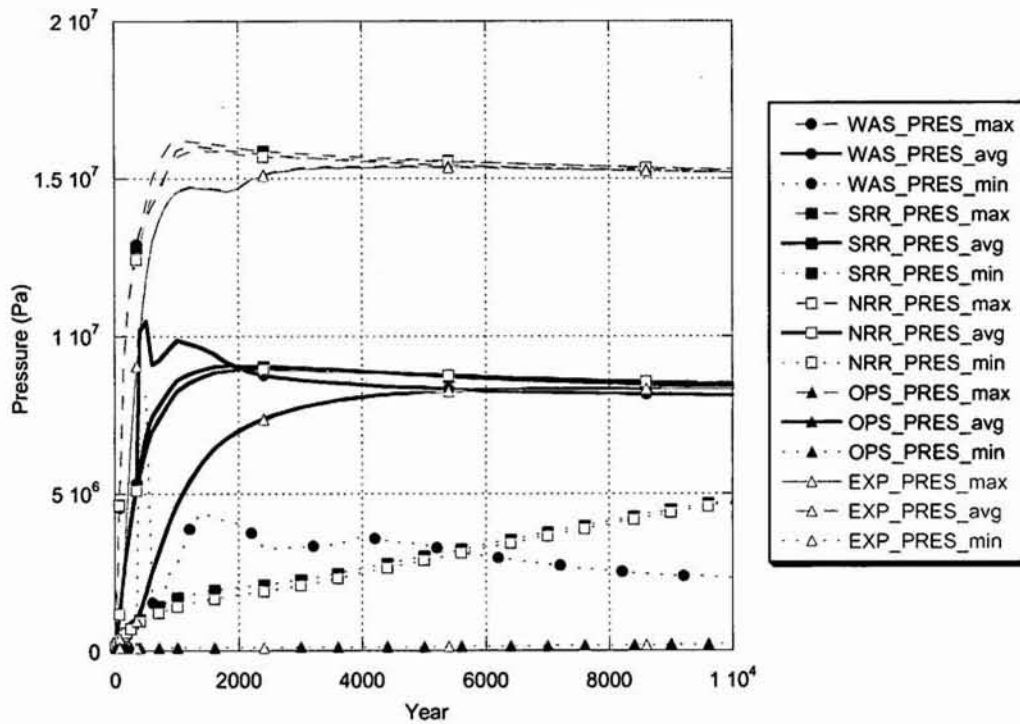


Figure 5.4.27: R1S2 - Pressure in Excavated Areas

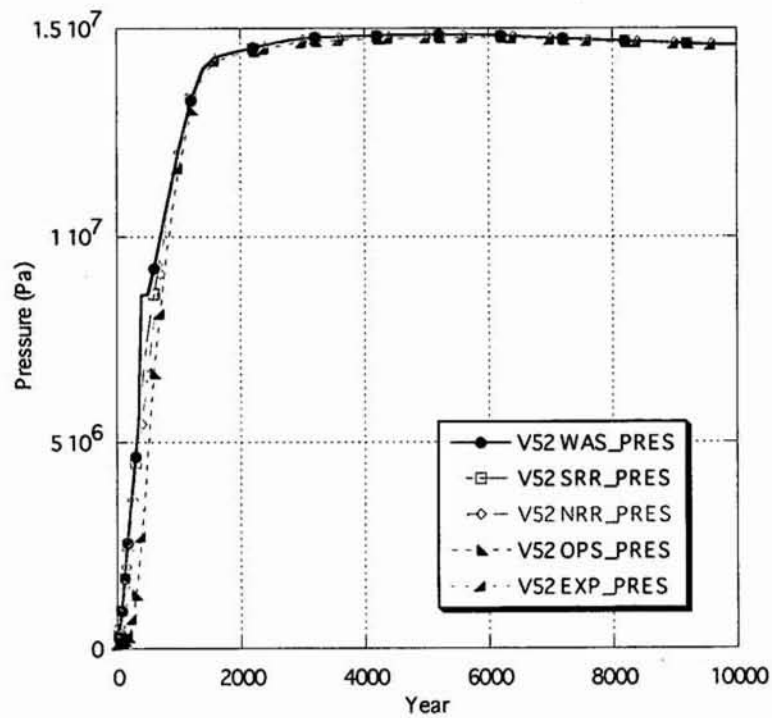


Figure 5.4.28: R1S2 V52 - Pressure in Excavated Areas

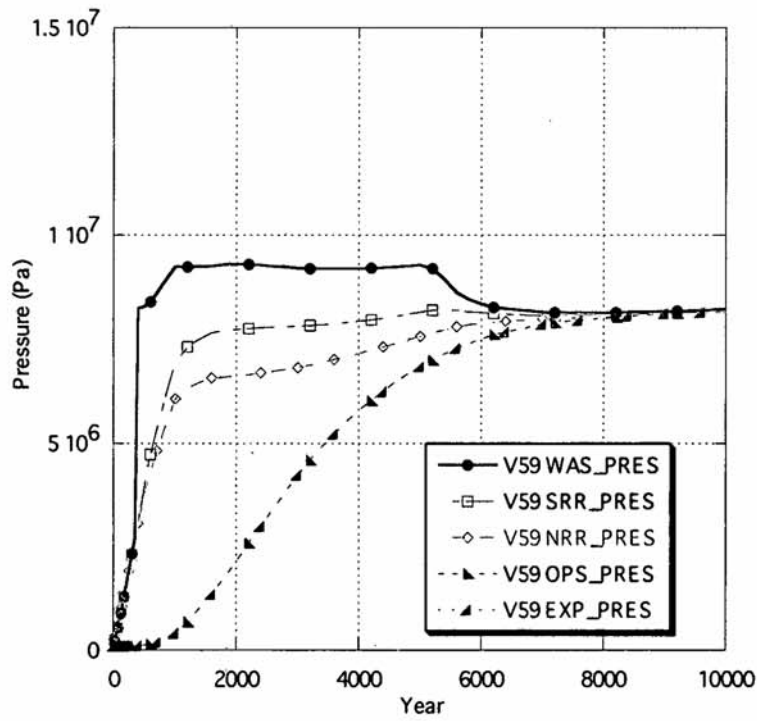


Figure 5.4.29: R1S2 V59 - Pressure in Excavated Areas

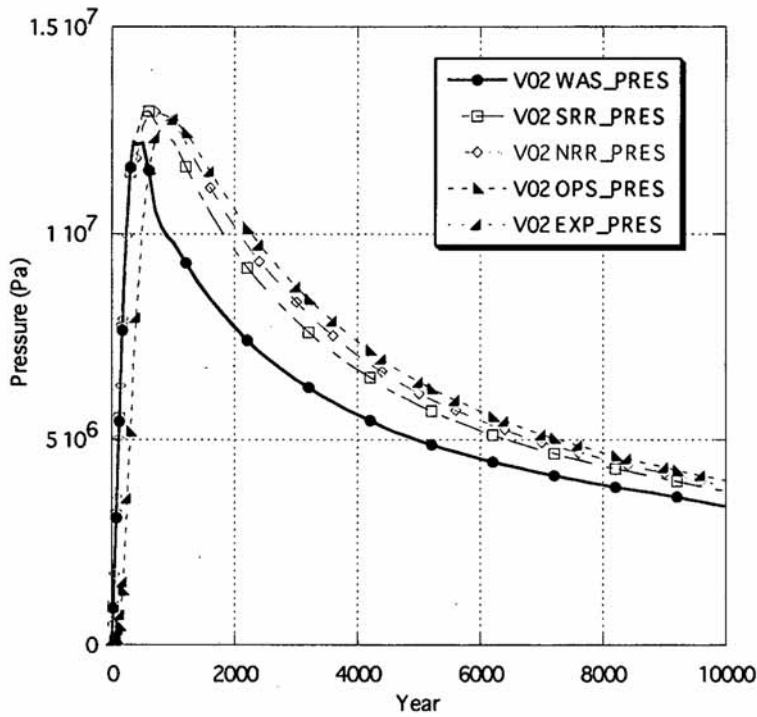


Figure 5.4.30: R1S2 V2 - Pressure in Excavated Areas

5.4.7 Rock Fracturing

Fracturing of the marker beds, which can enhance brine outflow, only occurs in a few vectors with high pressure. There are fewer vectors with marker bed fracturing in each of the disturbed scenarios than in the undisturbed Scenario S1, because the borehole connection to the ground surface results in reduced repository pressure in most vectors. Figure 5.4.31 shows the maximum, average, and minimum (always zero) fracture volumes in each of the six scenarios. The fracture trends are similar in the disturbed scenarios and the low average values indicate how few vectors are subject to marker bed fracturing.

Horsetail plots of marker bed fracturing (Figure 5.4.32) also show the reduced number of vectors in the disturbed scenarios that have any fracturing. Many vectors with fracturing also show a subsequent reduction in fracture volume as declining pressure in the repository permits permeability of the marker beds to be reduced.

Input dependencies for marker bed fracturing are complex and hard to identify. Fracturing requires high pressure, but a variety of input parameters influence pressure differently in different circumstances. Consequently no input parameter has a PRCC that exceeds 0.50. The PRCC for BHPERM stabilizes near -0.50 indicating that higher permeability of the borehole material results in lower repository pressure and less marker bed fracturing (Figure 5.4.33). The importance of repository pressure to marker bed fracturing is illustrated in a scatter plot of the average pressure in the waste regions, W_R_PRES, versus the total fracture volume, VFRAC_{TMB} (Figure 5.4.34). No fracturing occurs below 12 MPa, but vectors with fracturing that exceed this level generally (but not always) show fracturing in one or more marker beds.

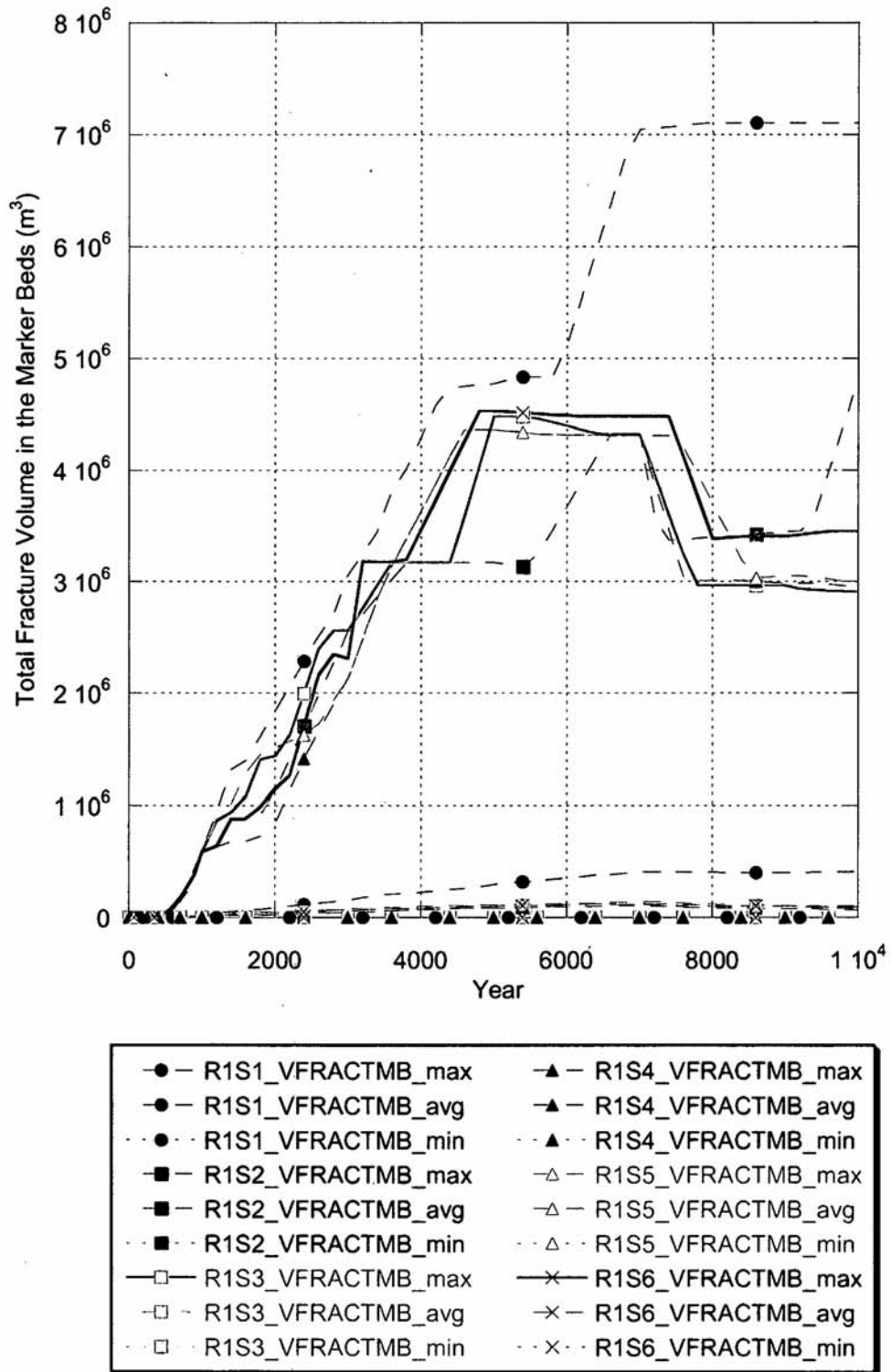


Figure 5.4.31: R1: Total Volume of Marker Bed Fracturing for Six Scenarios

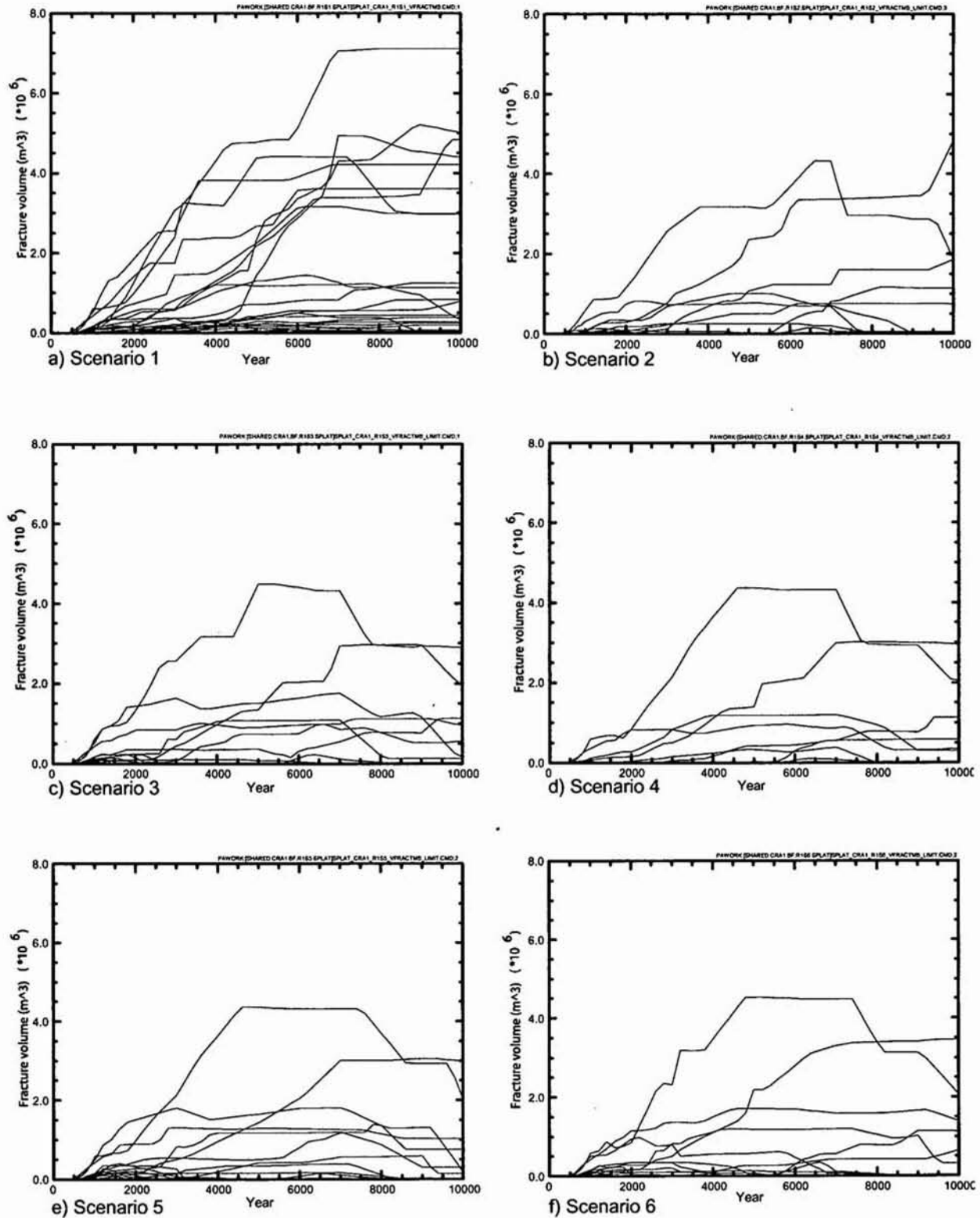


Figure 5.4.32: R1 – Horsetail Plots for Total Maker Bed Fracturing in Six Scenarios

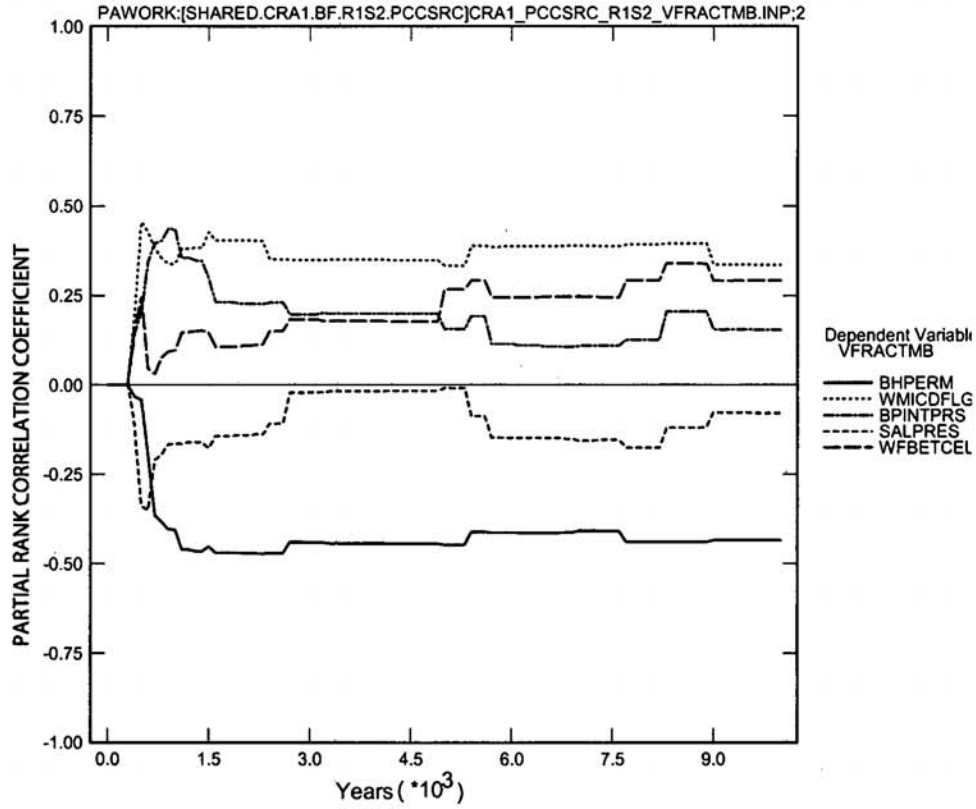


Figure 5.4.33: R1S2 - Primary Correlations for Total Marker Bed Fracture Volume, VFRACTMB, with Input Parameters

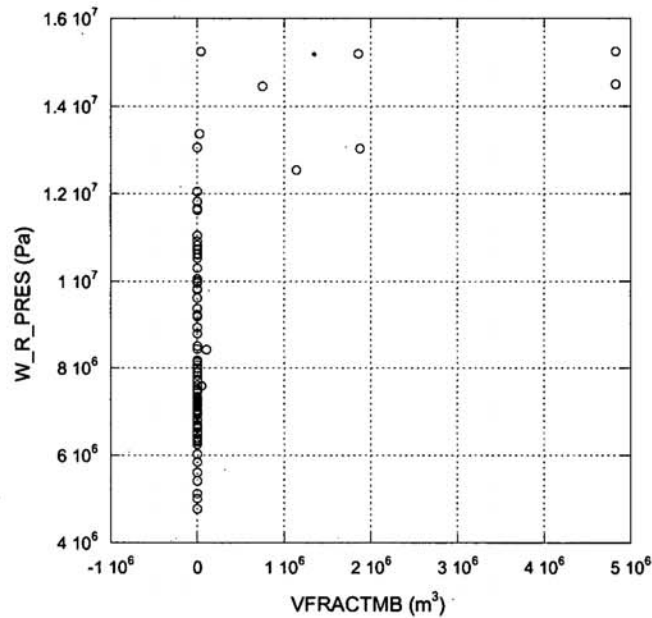


Figure 5.4.34: R1S2 - W_R_PRES versus VFRACTMB

5.4.8 Brine Flow Away From the Repository

There are two important brine outflow variables from the Salado Flow analysis. BRNREPOC is the total cumulative brine outflow from the repository, and BRNBHRCC is brine flow up the borehole at the base of the Culebra in the disturbed scenarios. The primary measuring point for borehole flow is at the base of the Culebra, because virtually all brine that enters into the borehole in the repository exits at the Culebra. Other potentially significant brine outflow output variables include 1) BRAALOC, the total cumulative brine outflow along the marker beds, 2) BRAALWC, the total cumulative brine outflow along the marker beds at the Land Withdrawal Boundaries, and 3) BRNSHRCC, the total cumulative brine flow up the shaft at the base of the Culebra. BRNREPOC does not equal the sum of the other outflow variables, because there can also be local brine exchange between the DRZ and the repository.

The E1 scenarios (S2, S3 and S6) have the highest maximum brine outflows (Figure 5.4.35). These scenarios provide the source of contaminants to the Culebra flow and transport calculations, which is the subject of a subsequent PA analysis. Statistics of total brine flow up the borehole to the Culebra are plotted in Figure 5.4.36. Statistics for cumulative brine outflows are also summarized in Table 5.4.3. These composite analyses of Salado Flow performance in the six scenarios are the basis for several observations:

- 1) The maximum brine outflow from the E1 scenarios is 154,000 m³ (S2), but the average and median outflows are more than an order of magnitude less.
- 2) The borehole accounts for virtually all brine outflow in high-flow vectors from the E1 scenarios.
- 3) The maximum brine outflow from the E1 scenarios continues at a steady rate to the end of 10,000 years.
- 4) Brine outflows from the E2 scenarios are similar to the undisturbed scenario.
- 5) Brine outflow in Scenario S6 has brine outflow that is very similar to an E1-only drilling intrusion.

Additional insight concerning brine outflow is provided by horsetail plots of BRNREPOC and BRNBHRCC for each scenario:

- 1) Only a few vectors from the E1 scenarios have brine outflows exceeding 30,000 m³ and most vectors have less than 10,000 m³ of cumulative brine outflow.
- 2) Brine outflow continues at a constant rate to 10,000 years in the high-flow vectors from the E1 scenarios.
- 3) The similarities in the horsetail plots for BRNREPOC and BRNBHRCC confirm that the borehole is the primary path for brine outflow from the E1 scenarios.

The borehole plugs prevent brine flow out of the repository up the borehole. When they fail 200 years after the intrusion, there is a sharp increase in brine outflow up the borehole to the Culebra, but this outflow does not rise above the Culebra. The differences at 10,000 years between total cumulative brine outflow and cumulative brine flow up the borehole is tabulated in Table 5.4.4. Brine flow up the borehole accounts for 92% to 99% of total cumulative brine flow out of the repository in these vectors.

**TABLE 5.4.3: STATISTICS FOR CUMULATIVE BRINE FLOW (m³) AWAY FROM THE REPOSITORY
at 10,000 Years**

	S1	S2	S3	S4	S5	S6
BRNREPOC						
Max	19,567	153,956	144,804	19,066	25,087	152,743
Min	1	13	10	4	3	4
Avg	646	13,344	10,418	1,274	1,303	11,157
Median	21	5,605	2,109	83	89	1,830
BRNBHRCC						
Max	N/A	152,301	144,456	5,667	5,362	152,208
Min	N/A	1	1	0	0	1
Avg	N/A	9,165	8,632	282	251	9,377
Median	N/A	67	36	2	2	92
BRAALOC						
Max	14,164	4,520	4,116	3,411	5,777	6,658
Min	0	0	0	0	0	0
Avg	465	170	160	113	183	186
Median	0	14	11	0	0	19
BRAALWC						
Max	433	374	387	407	411	423
Min	0	0	0	0	0	0
Avg	7	4	4	4	4	4
Median	0	0	0	0	0	0
BRNSHRCC						
Max	50	63	59	45	46	57
Min	0	0	0	0	0	0
Avg	2	2	2	2	2	2
Median	0	0	0	0	0	0

**TABLE 5.4.4: R1S2 – SEVEN VECTORS WITH THE HIGHEST CUMULATIVE BRINE OUTFLOW
(m³)**

Vector	BRNREPOC	BRNBHRCC	Difference	% Difference
46	153,956	152,301	1,655	1.1%
7	84,668	79,247	5,421	6.4%
17	79,882	81,580	-1,697	-2.1%
9	77,277	72,434	4,843	6.3%
31	77,194	71,385	5,809	7.5%
91	68,603	64,937	3,666	5.3%
23	61,627	60,496	1,131	1.8%

The small negative difference for vector 17 means that brine flow up the borehole at the base of the Culebra is slightly higher than total brine flow out of the repository. This means that there is additional brine flowing from the DRZ and the marker beds into the borehole above the repository. Vector 17 also has the lowest initial brine outflow into the repository from the DRZ indicating that the DRZ remains saturated.

Brine outflow occurs primarily up the borehole in all drilling disturbance scenarios (Figure 5.4.37). Horsetail plots for total cumulative brine outflow and for cumulative brine flow up the borehole at the base of the Culebra are very similar.

Brine inflow from the Castile into the repository stops 1,200 years after the drilling intrusion when the borehole connection to the pressurized brine reservoir becomes sealed by halite creep closure. This results in a corresponding drop in brine outflow, which is reflected in a decreased slope in the line for each vector (Figure 5.4.37b, c, d, e, j & k). The outflow rate, which is less variable among the vectors, is primarily dependent upon the permeability of borehole fill material. Cumulative brine outflow in the E2 drilling disturbance scenarios is comparatively small (Figure 5.4.37f, g, h & i).

Analyses of cumulative brine flows are important for regulatory performance, but consideration of annualized brine flow rates provides additional understanding about the processes and dynamics controlling the flow. Scenario S2 is used to evaluate brine outflow because it has the highest median, average, and maximum cumulative brine flows. Cumulative brine outflow, BRNREPOC, for most vectors is less than 10,000 m³ for the 10,000-year regulatory period, and only seven vectors, 7, 9, 17, 23, 31, 46, and 91, exceed 50,000 m³ (Table 5.4.4). The rates of brine flow vary sharply as modeling conditions change. Brine outflow in four of the seven high-flow vectors shows a spike at the time of the drilling intrusion (Figure 5.4.38) that does not occur in brine flow up the borehole out of the repository (Figure 5.4.39). This spike represents initial outflow into the DRZ and the marker beds. DRZ and Marker bed permeability is not sufficient in the other three high-flow vectors to permit much outflow into the surrounding rock.

The permeability of borehole fill, BHPERM, is the primary determinant of brine outflow up the borehole, which is the pathway for more than 90% of brine in the E1 scenarios. The influence of other input parameters is reduced from the undisturbed scenario (Figure 5.4.40).

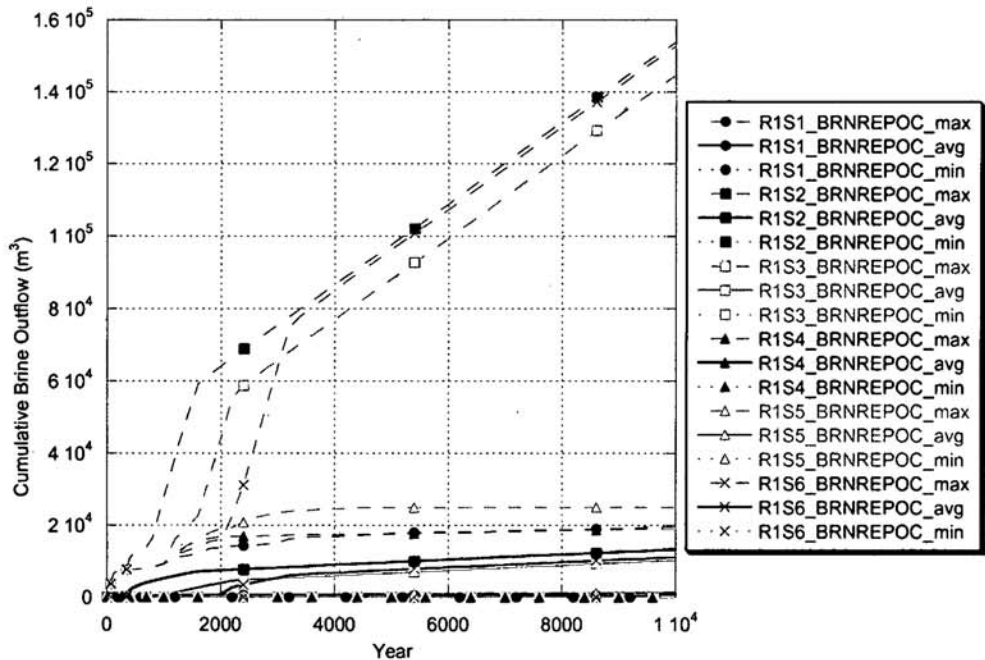


Figure 5.4.35: R1: Total Cumulative Brine Outflow from the Repository, BRNREPOC, for Six Scenarios

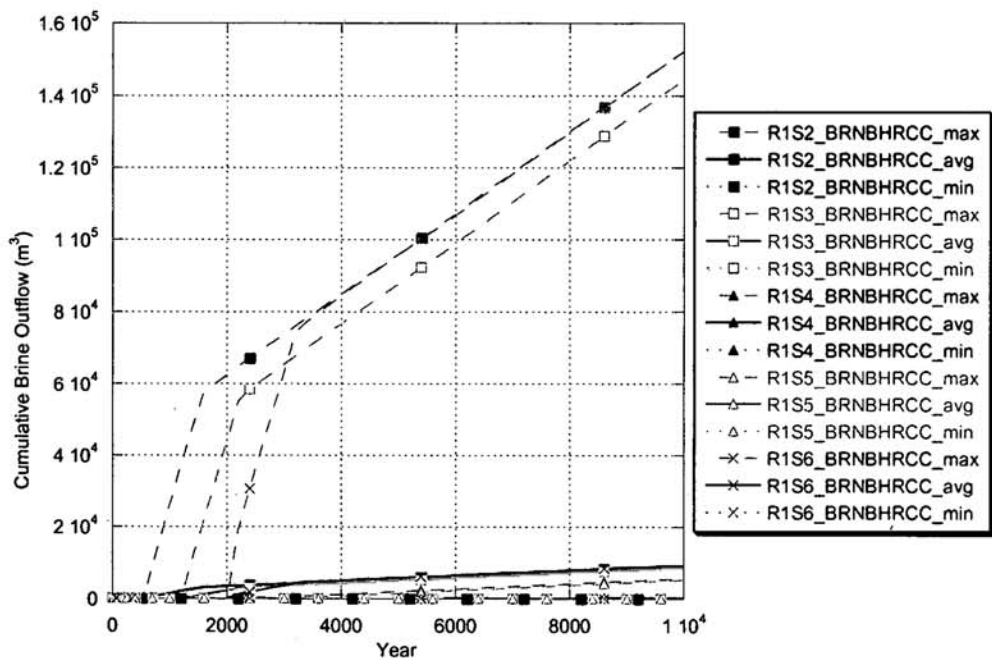
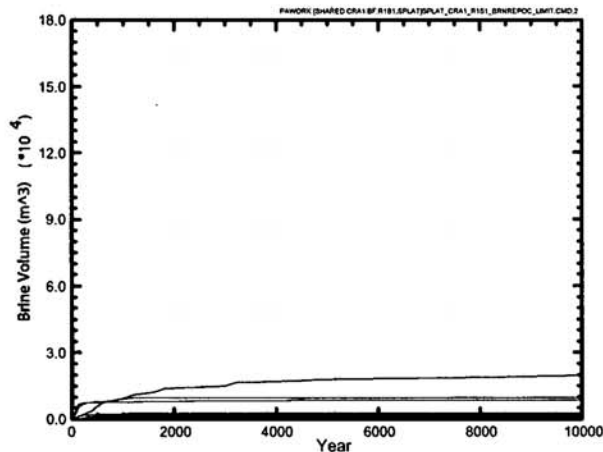
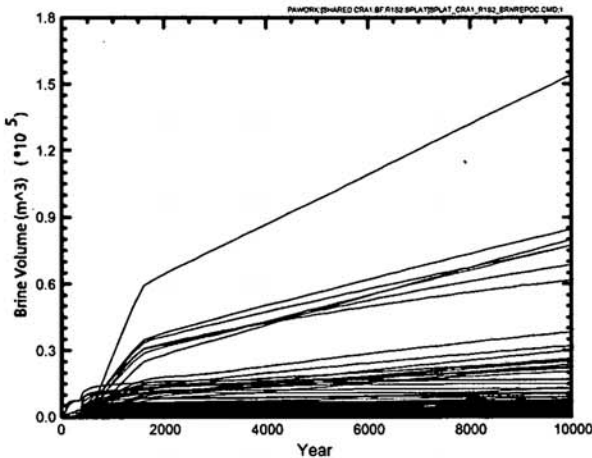


Figure 5.4.36: R1: Total Cumulative Brine Outflow Up the Borehole at the Base of the Culebra for Six Scenarios

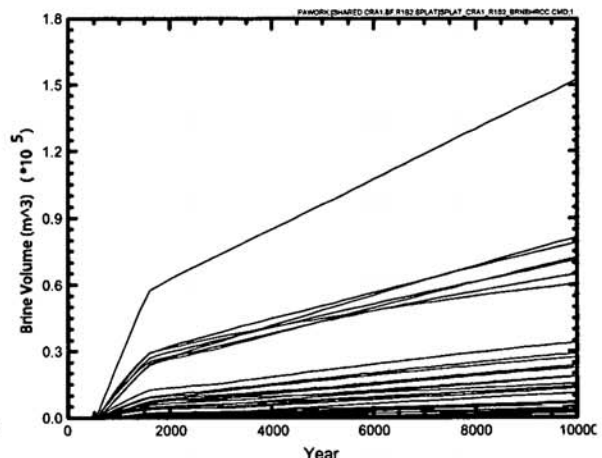


a: Scenario 1 - BRNREPOC

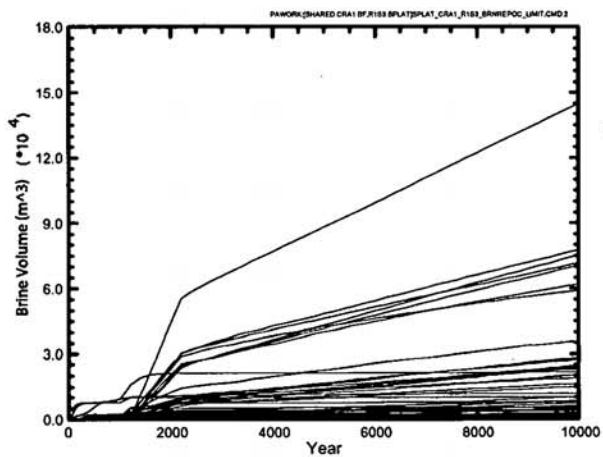
No borehole in Scenario 1



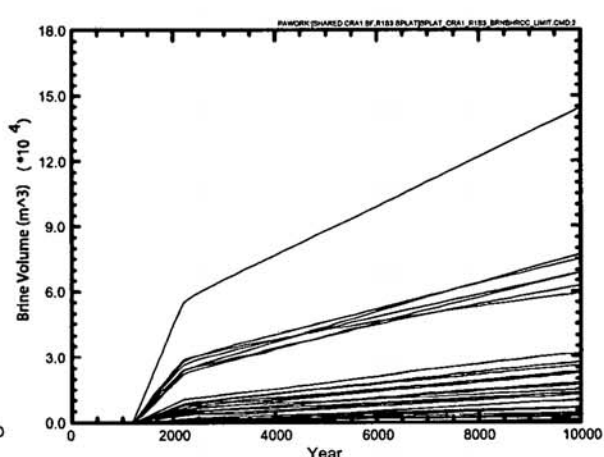
b: Scenario 2 - BRNREPOC



c: Scenario 2 - BRNBHRCC

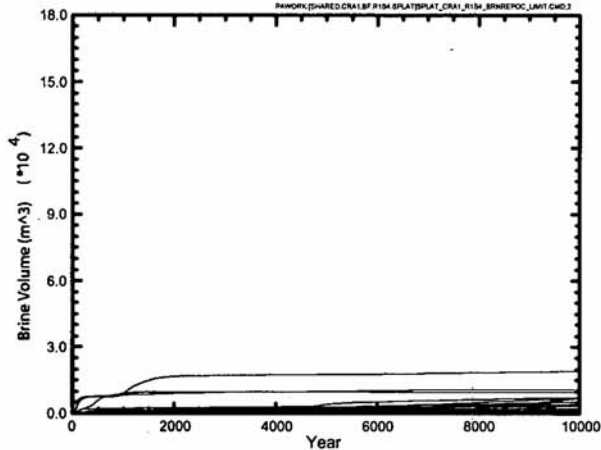


d: Scenario 3 - BRNREPOC

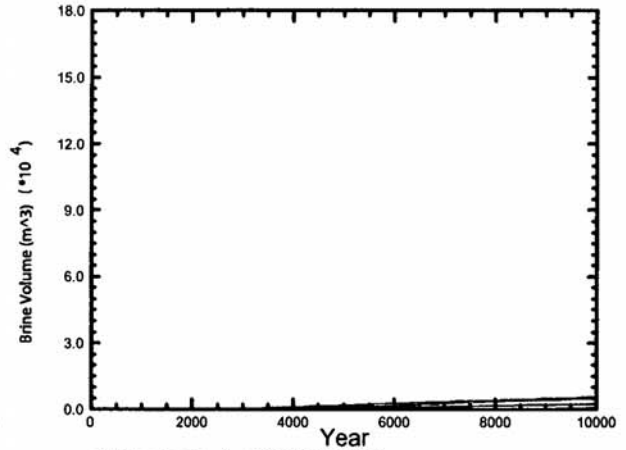


e: Scenario 3 - BRNBHRCC

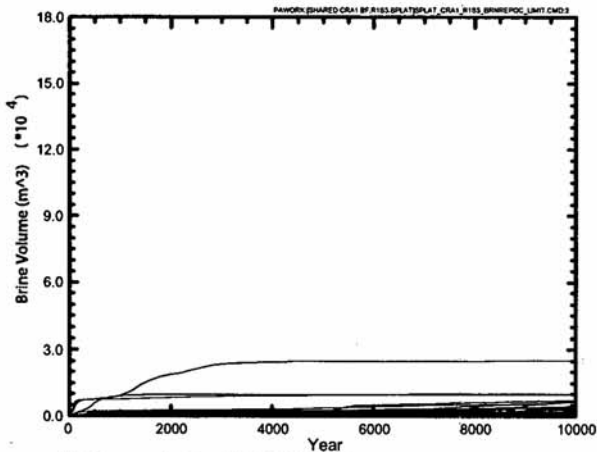
Figure 5.4.37: R1 – Horsetail Plots for Total Cumulative Brine Outflow and for Brine flow up the Borehole at the Base of the Culebra in Six Scenarios



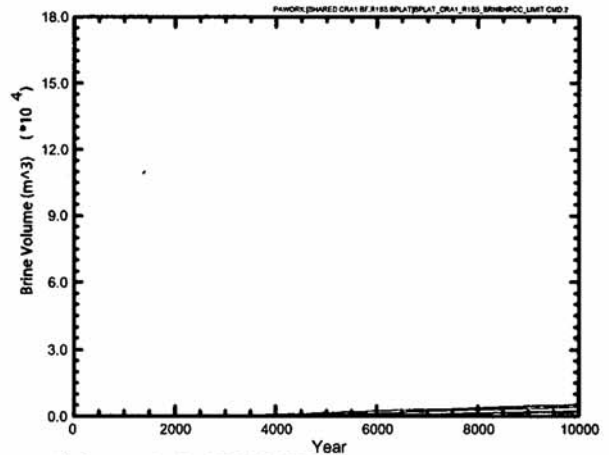
f) Scenario 4 - BRNREPOC



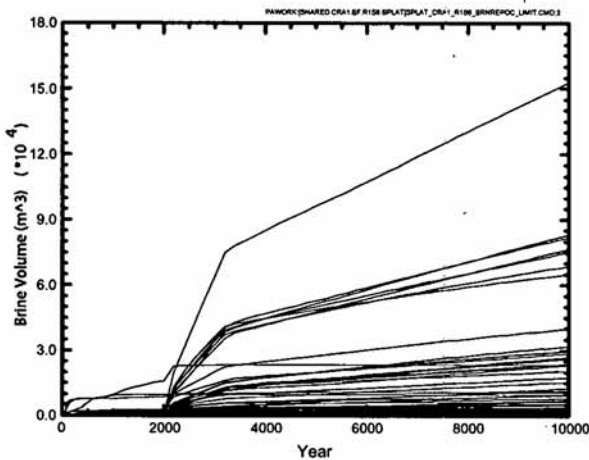
g) Scenario 4 - BRNBHRCC



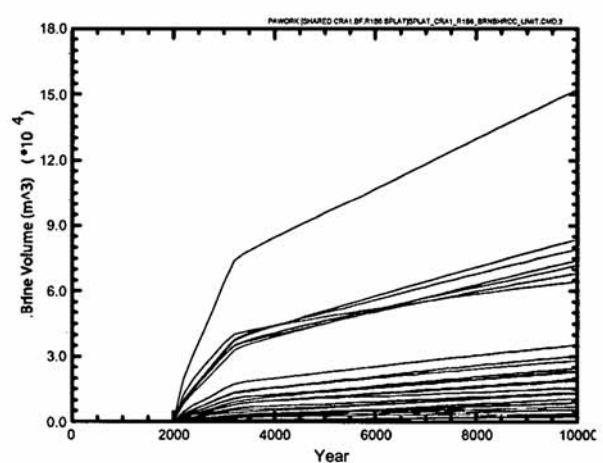
h) Scenario 5 - BRNREPOC



i) Scenario 5 - BRNBHRCC



j) Scenario 6 - BRNREPOC



k) Scenario 6 - BRNBHRCC

Figure 5.4.37: R1 – Horsetail Plots for Total Cumulative Brine Outflow and for Brine flow up the Borehole at the Base of the Culebra in Six Scenarios (continued)

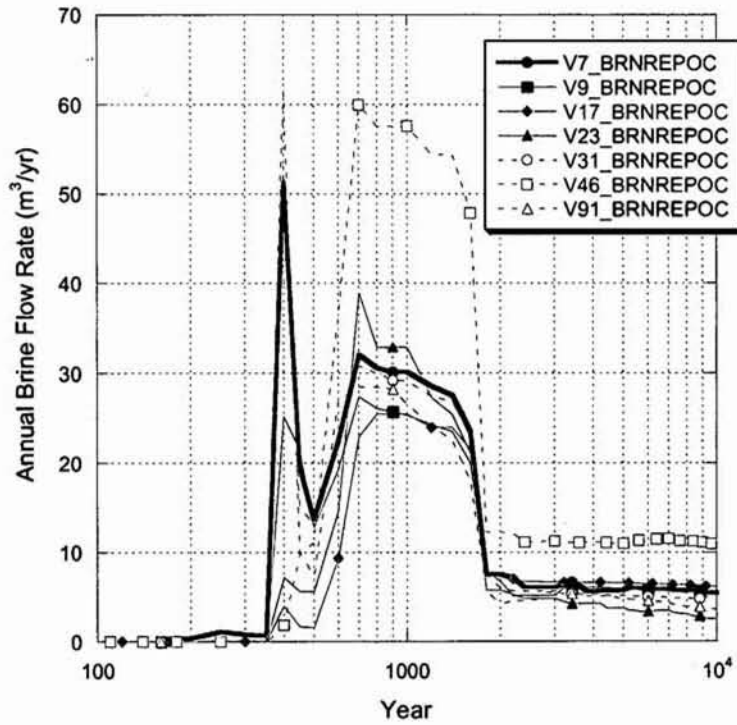


Figure 5.4.38: R1S2 – Annual Brine Outflow Rates in Seven Highest Flow Vectors

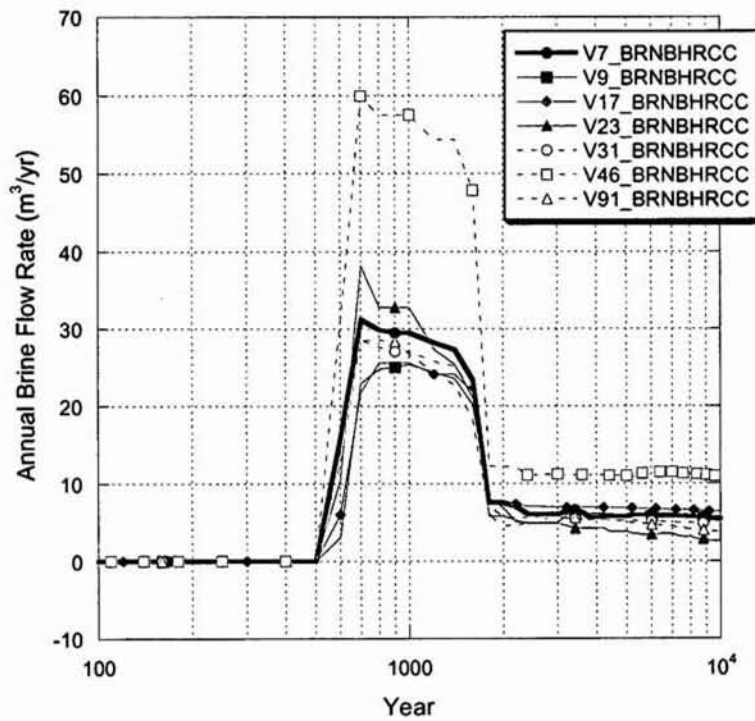


Figure 5.4.39: R1S2 – Annual Brine Flow Rates Up the Borehole in Seven Highest Flow Vectors

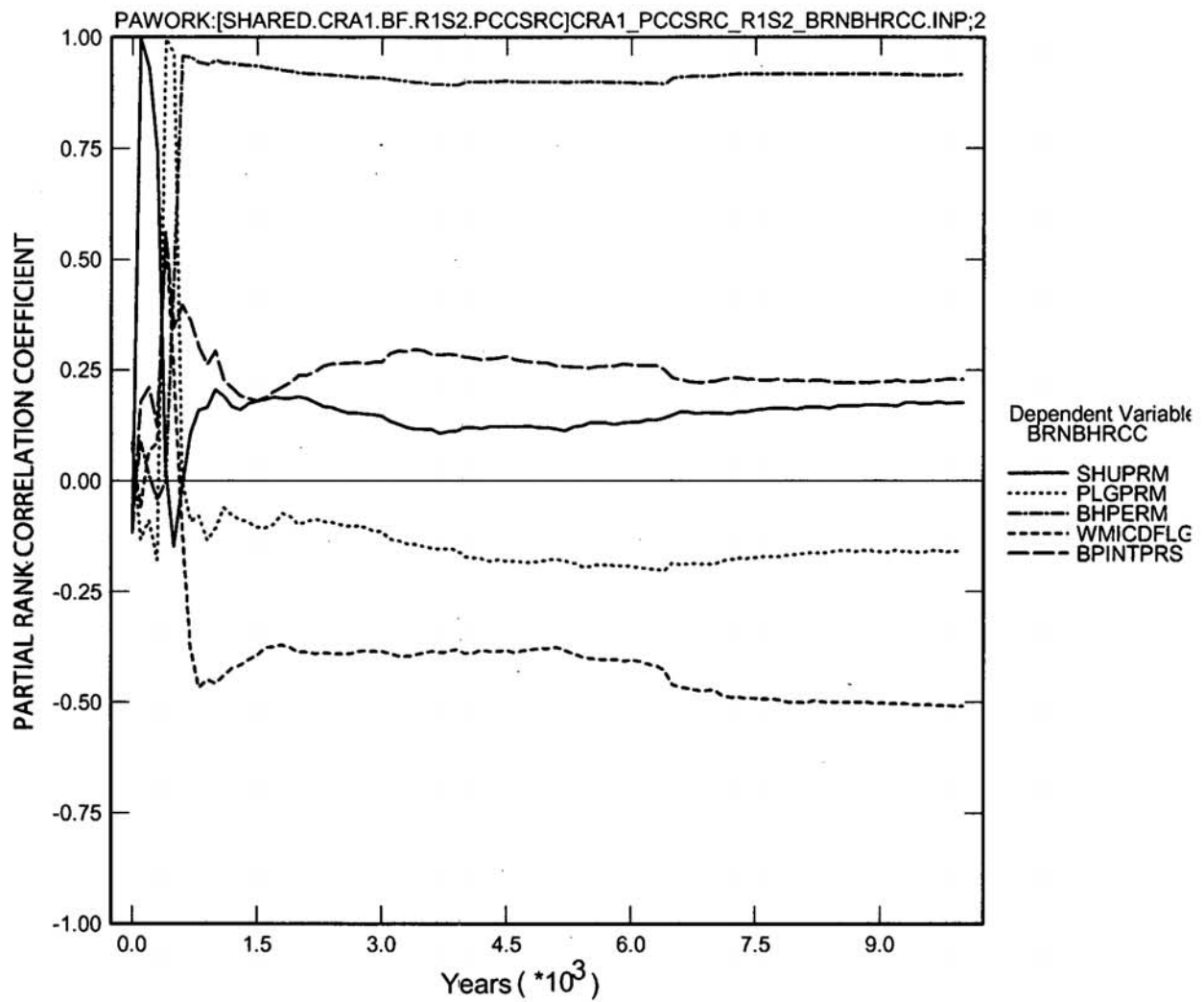


Figure 5.4.40: R1S2 - Primary Correlations for Cumulative Brine Flow up the Borehole at the Base of the Culebra, BRNBHRCC, with Input Parameters

5.5 COMPARISON OF REPLICATES

The Salado Flow Analysis employs three replicates to confirm the statistical reliability of the primary analysis of Replicate 1. Each is composed of the same six scenarios, but each replicate uses a different Latin Hypercube set of sampled input parameters.

Comparison of results from the three replicates is based upon three key output variables. These variables are chosen, because of their importance to other PA models, which calculate releases that are tallied in the final CCDF plots. Each of these variables are discussed in detail for replicate 1 in Sections 5.3 and 5.4:

- WAS_SATB - brine saturation in the waste panel
- WAS_PRES - pressure in the waste panel
- BRNREPOC - cumulative brine flow away from the repository

Plots of the maximum, 90th percentile, average, 10th percentile and minimum values for each variable are compared for the three replicates (Table 5.5.1). Scenario S2 is used to evaluate the statistical stability of results from the drilling-disturbance scenarios, because it yielded the most extreme output values.

TABLE 5.5.1: PLOTS VARIABLES IN THE THREE REPLICATES

Scenario	Variable	Figure
1	WAS_SATB	Figure 5.5.1
2	WAS_SATB	Figure 5.5.2
1	WAS_PRES	Figure 5.5.3
2	WAS_PRES	Figure 5.5.4
1	BRNREPOC	Figure 5.5.5
2	BRNREPOC	Figure 5.5.6

The analysis of these variables from the three replicates confirm that the results from Replicate 1 are statistically stable. Maximum and sometimes minimum values may vary significantly. This is expected, because combinations of input parameters with very low probabilities are unlikely to be duplicated in multiple replicates. However, the ranges for collective results for 100 vectors usually agree within a few percent, and the average values are particularly similar for the three replicates.

WAS_SATB: Brine Saturation in the Waste Panel: The maximum value for WAS_SATB in Replicate 3, Scenario 1 is about 40% less than the other two replicates at 10,000 years, but the plots for average values are close to 0.1 in all three replicates (Figure 5.5.1). The average for Replicate 3 is slightly lower reflecting the lower maximum value.

The greatest variability for WAS_SATB in Scenario 2 was for the 10th-percentile values, which ranged from near zero in Replicate 2 to about 0.2 in Replicate 1. The plots for

average values were within a few percent as they are for all the replicate analyses (Figure 5.5.2). The maximum and minimum values have little significance, because they are at their theoretical limits of 1.0 and 0.0 respectively.

WAS_PRES: Pressure in the Waste Panel: The plots of average pressure in both Scenario 1 (Figure 5.5.3) and Scenario 2 (Figure 5.5.4) are virtually coincident for the three replicates. The minimum pressure values show the greatest variability (about 15%) in Scenario 1, and the 90th percentile values have the greatest variability (about 15%) in Scenario 2.

BRNREPOC: Cumulative Brine Flow Away From the Repository: Average brine outflow values are very low in both Scenarios 1 (Figure 5.5.5) and Scenario 2 (Figure 5.5.6). The maximum values are about 15% lower in Replicate 2 than in the other replicates for both Scenarios 1 and 2.

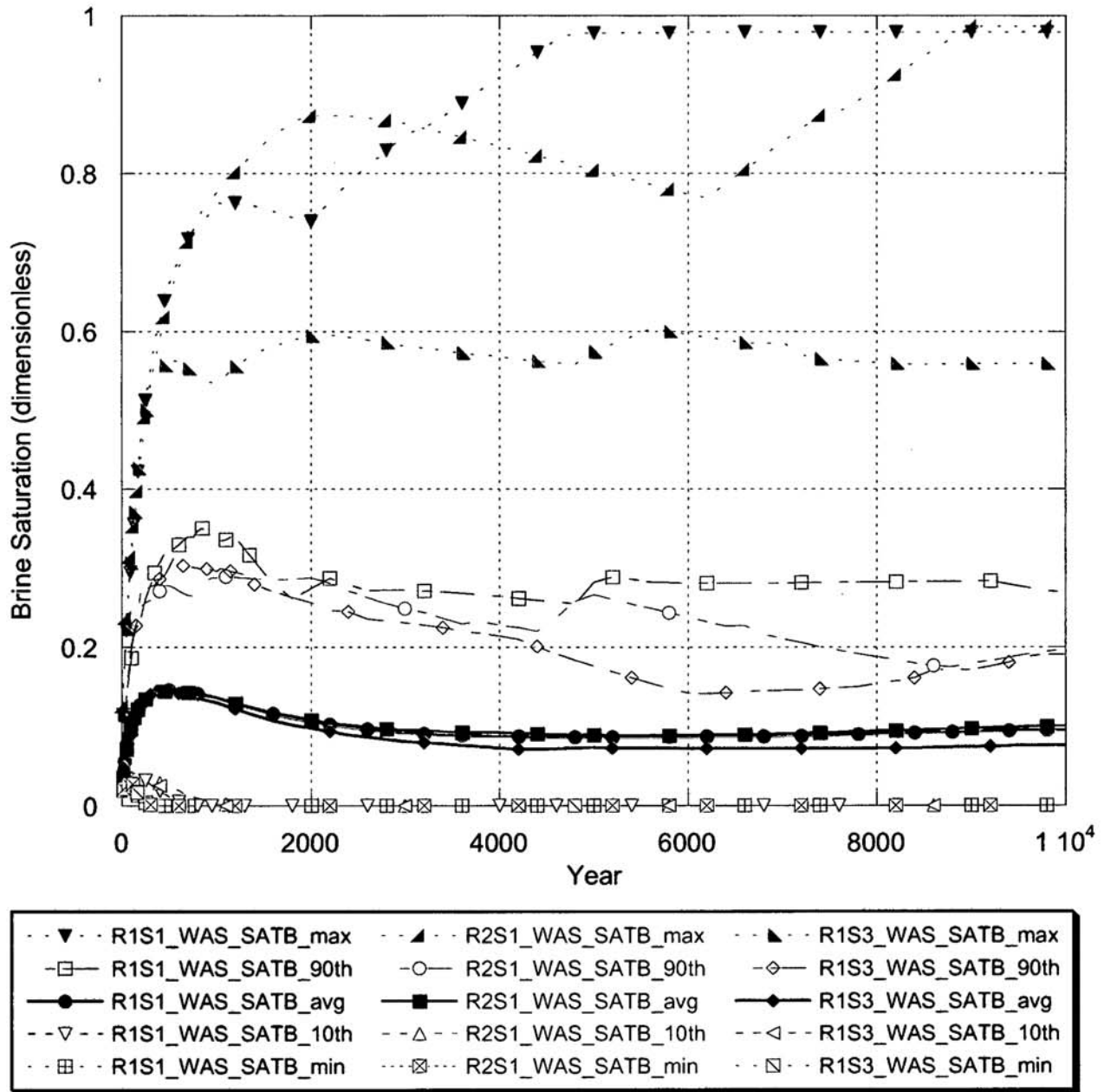


Figure 5.5.1: Scenario 1 – Comparison of Statistics for WAS_SATB in Three Replicates.

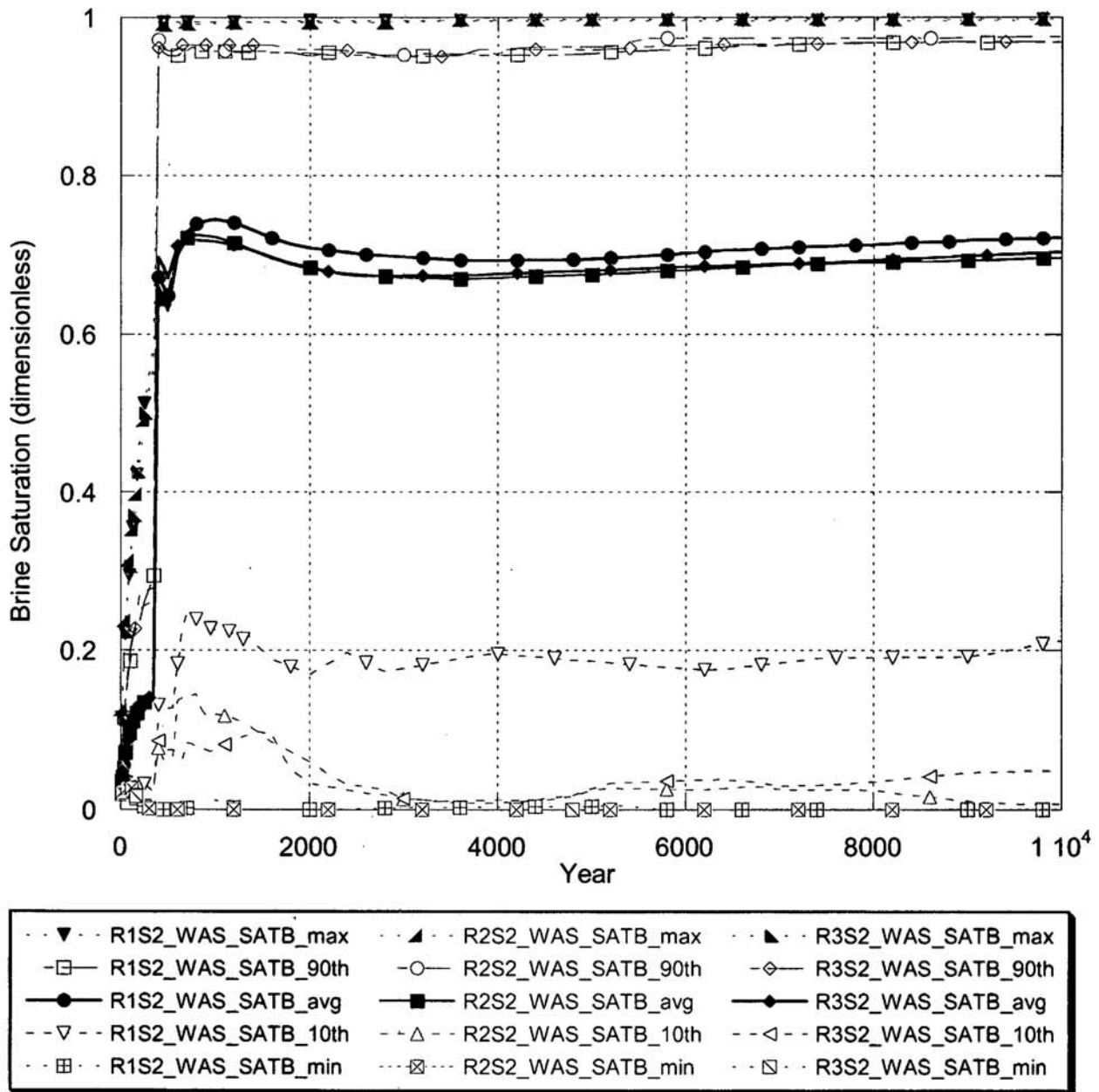


Figure 5.5.2: Scenario 2 – Comparison of Statistics for WAS_SATB in Three Replicates.

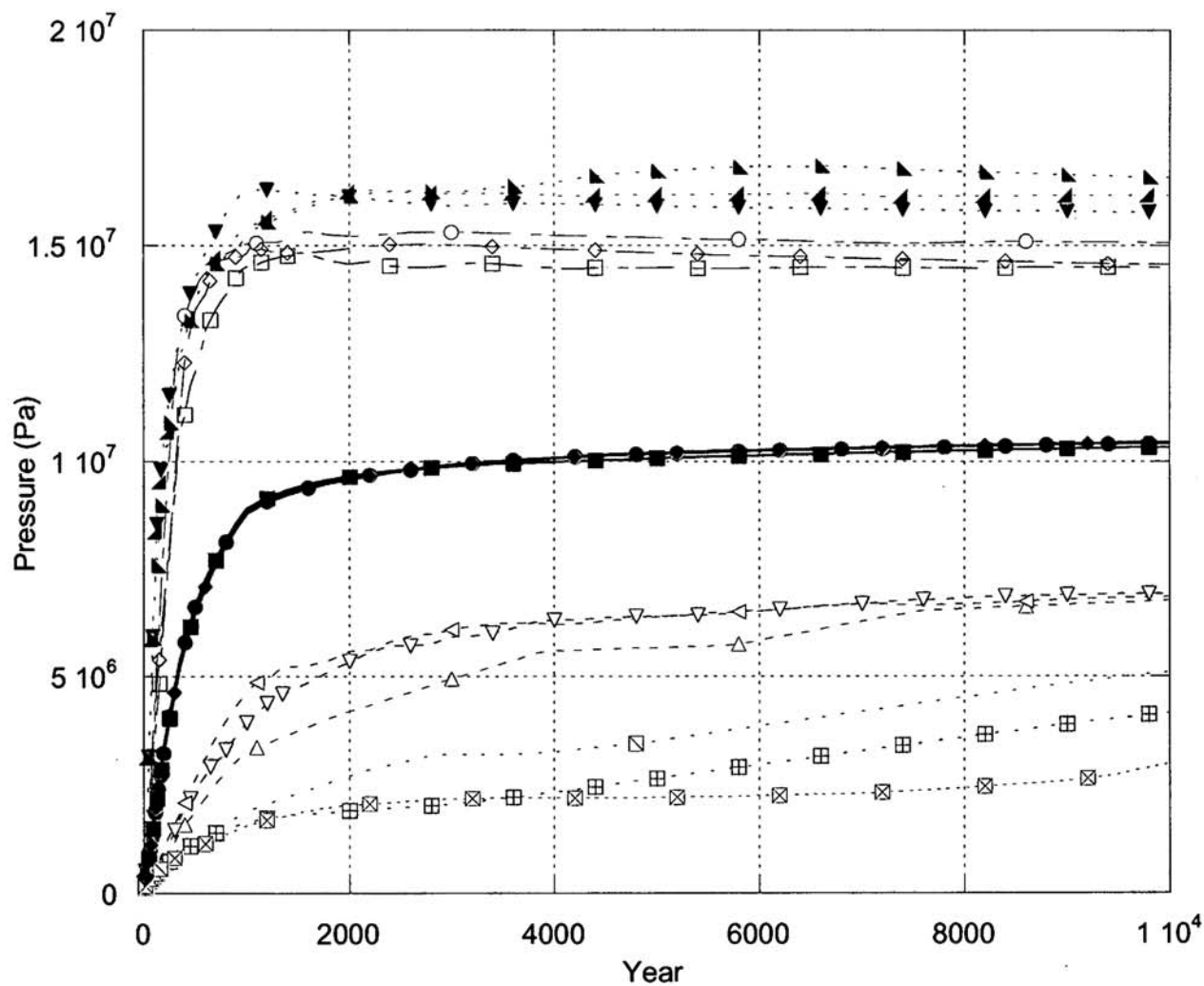


Figure 5.5.3: Scenario 1 – Comparison of Statistics for WAS_PRES in Three Replicates.

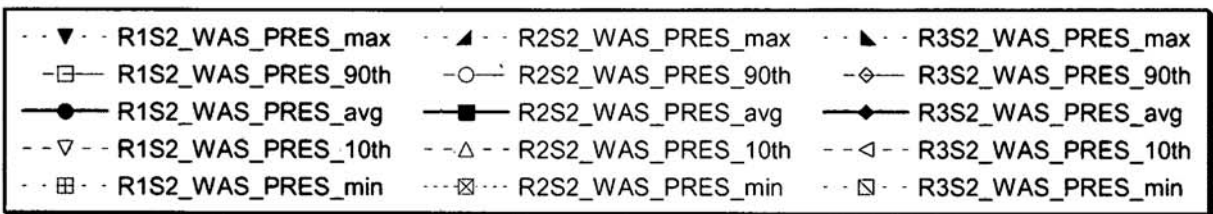
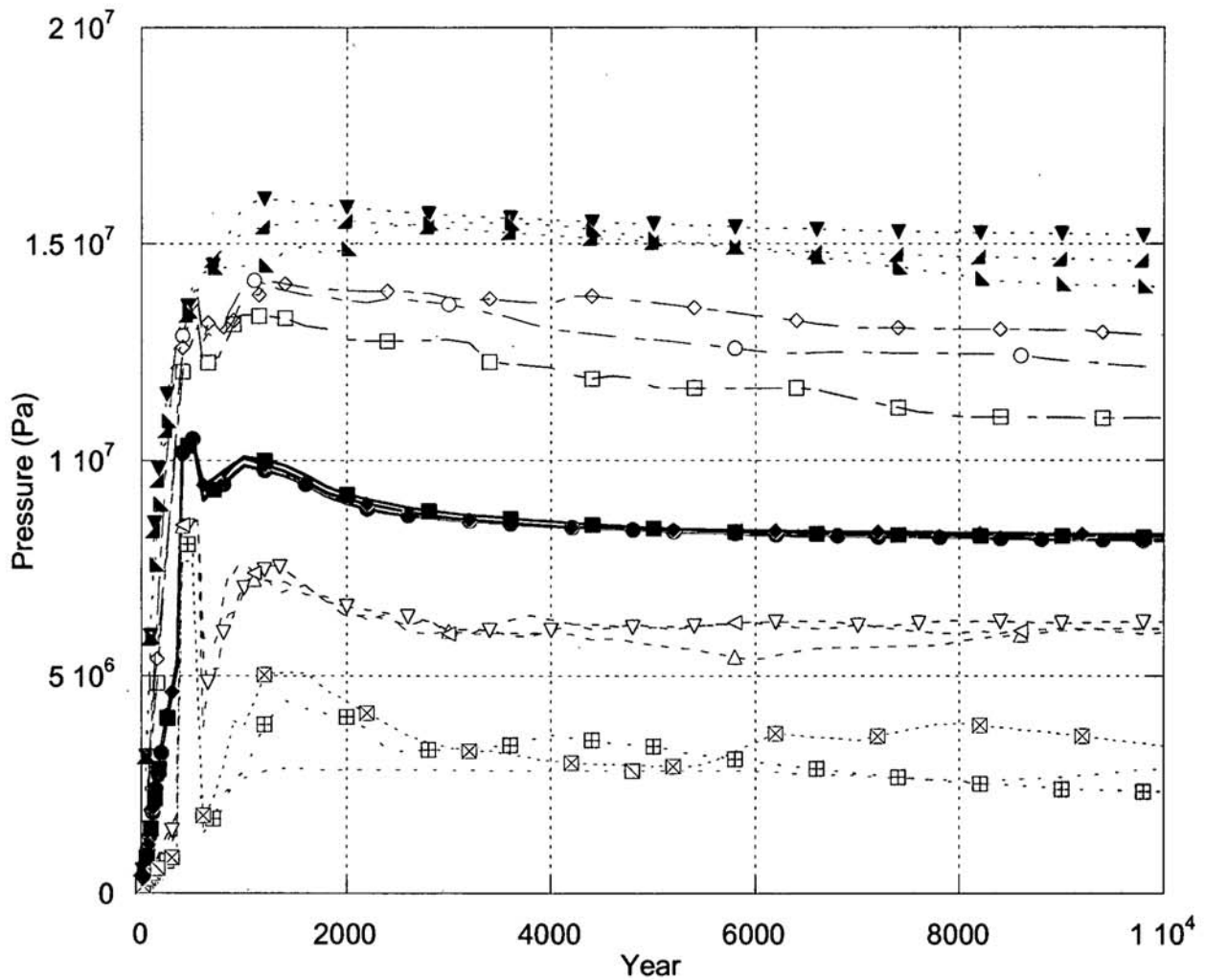


Figure 5.5.4: Scenario 2 – Comparison of Statistics for WAS_PRES in Three Replicates.

Information Only

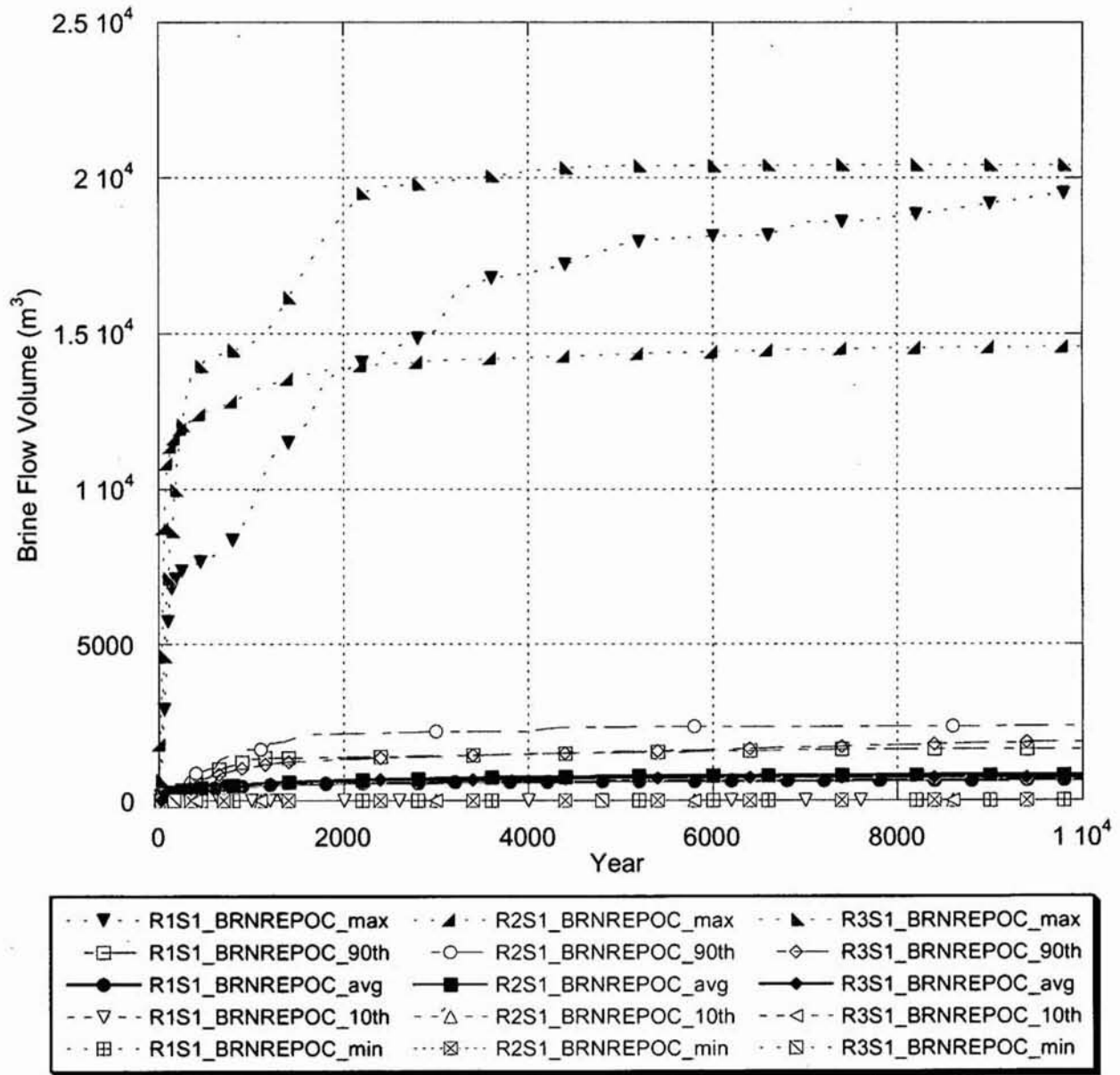


Figure 5.5.5: Scenario 1 – Comparison of Statistics for BRNREPOC in Three Replicates.

Information Only

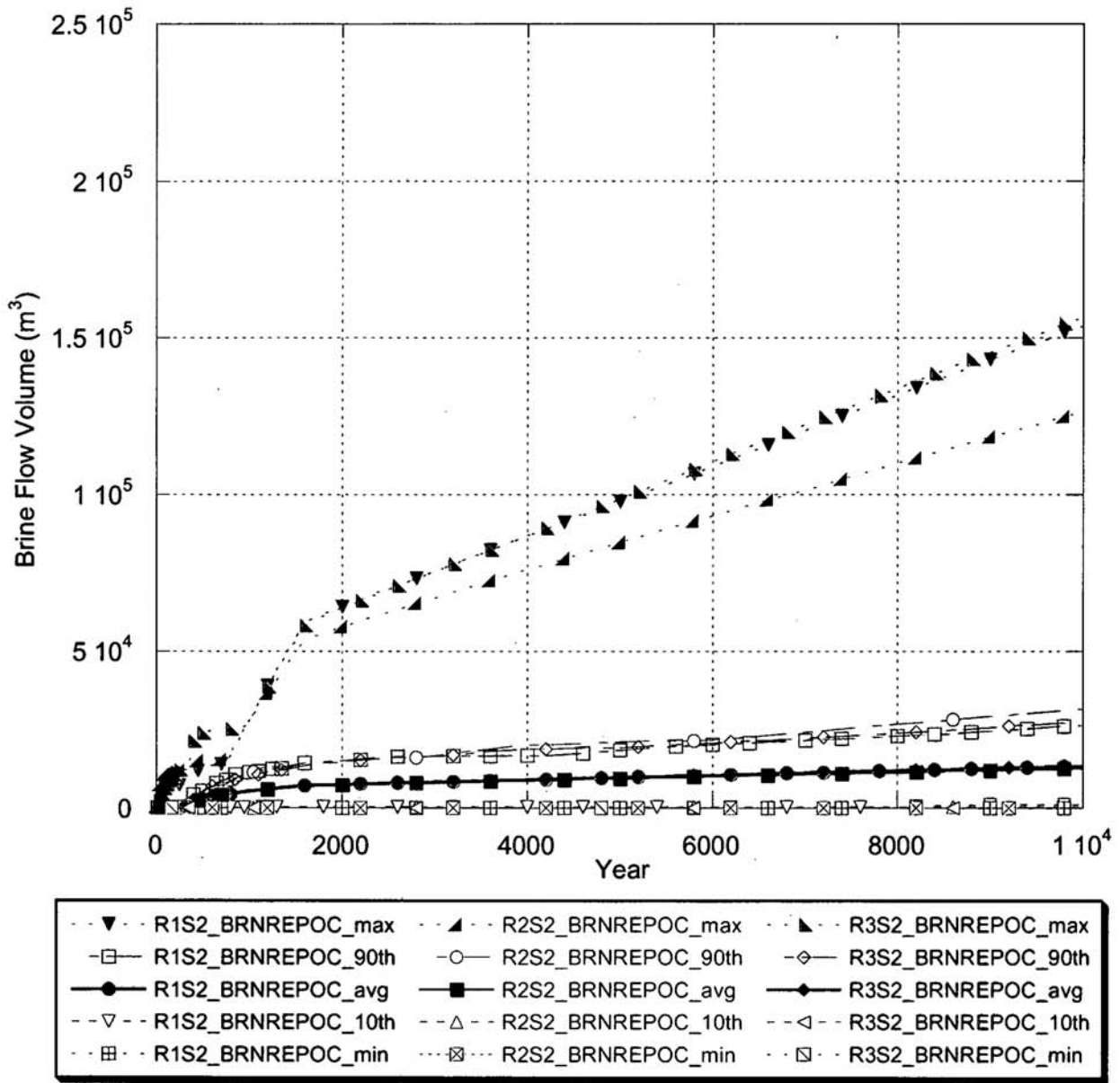


Figure 5.5.6: Scenario 2 – Comparison of Statistics for BRNREPOC in Three Replicates.

5.6 SUMMARY AND CONCLUSIONS

Three replicates of the Salado Flow model were run in support of the Performance Assessment for the Compliance Recertification Application. The model included undisturbed and disturbed scenarios. The results of these model runs provide information about the flow of brine from the repository and conditions in the repository (pressure and saturation) to other PA models that are used to calculate releases.

Results of the undisturbed scenario indicate that, in the absence of a drilling intrusion, pressures can rise to high levels, which may lead to fracturing in the surrounding marker beds. The consequences of such fracturing are examined in the Salado transport analysis (NUTS), which calculates radionuclide transport in the Salado Formation. The results of the Salado Flow (and Transport) calculations for the undisturbed scenario demonstrate that the undisturbed repository design is effective at containing radionuclides for 10,000 years. Option D panel closures have little effect on pressure within the waste-filled areas, because processes (e.g., gas generation) are proceeding at similar rates, but pressure equalization between waste-filled and non-waste areas is delayed by as much as 2,000 years in the undisturbed scenario.

Results of the disturbed scenarios indicate that possible future drilling intrusion events into the repository can result in significant brine flow up the borehole to the Culebra, but there is no brine flow across the Land Withdrawal Boundary (LWB) from any other pathway, including the anhydrite marker beds or through the shaft seal. Direct brine release to the surface is modeled separately, but brine entering the Culebra via the borehole provides a model input for the code CCDFGF, which scales the transport results in the Culebra.

Another important result of drilling intrusions is that they tend to result in decreased pressure in the repository due to the borehole connection to the surface. Option D panel closures are effective at most pressures in delaying pressure equalization among the waste regions, resulting in non-intruded panels remaining pressurized for thousands of years following the depressurization of an intruded panel. However, at very high pressures, fracturing of the DRZ and marker beds can create alternate fluid pathways that can result in significant fluid movement between panels and pressure equalization.

Working files (e.g. Excel spreadsheets) used in this analysis that are not preserved in CMS libraries are archived on CD's in Appendix C of this report.

6.0 REFERENCES

- Anderson, R.Y., dean, W.E., Jr., Kirkland, D.W., and Snider, H.I. 1972. "Permian Castile Varved Evaporite Sequence, West Texas and new Mexico." *Geological Society of America Bulletin*, Vol. 83, No. 1, pp. 59-85
- Anderson, M.P., and Woessner, W.W. 1992. *Applied Groundwater Modeling: Simulation of Flow and Advective Transport*. San Diego: Academic Press.
- Butcher, B.M., S.W. Webb, and J.W. Berglund. 1995. System Prioritization Method of Iteration 2. Baseline Position Paper: Disposal Room and Cuttings Models, Volume 2, Appendix F. March 28, 1995. Albuquerque, NM: Sandia National Laboratories
- Caporuscio, F., Gibbons, J., and Oswald, E. 2002. *Waste Isolation Pilot Plant: Salado Flow Conceptual Models Peer Review Report*. Report prepared for the U.S. Department of Energy, Carlsbad Area Office, Office of Regulatory Compliance. ERMS# 523783.
- Caporuscio, F., Gibbons, J., and Oswald, E. 2003. *Waste Isolation Pilot Plant: Salado Flow Conceptual Models Final Peer Review Report*. Report prepared for the U.S. Department of Energy, Carlsbad Area Office, Office of Regulatory Compliance. ERMS# 526879.
- Christian-Frear, T.L., and S.W. Webb, 1996. *Effect of Explicit Representation of Detailed Stratigraphy on Brine and gas Flow at the waste isolation Pilot Plant*. SAND94-3173. Albuquerque, NM: Sandia National Laboratories. Sandia WIPP Central Files WPO # 37240.
- Freeze, G., and K. Larson. 1996. "Initial Pressure in the Castile Brine Reservoir." Memo to M. Tierney, March 20, 1996. Albuquerque, NM: Sandia National Laboratories. Sandia WIPP Central Files WPO # 37148.
- Hansen, C., Leigh, C., Lord, D., and Stein, J. 2002. "BRAGFLO Results for the Technical Baseline Migration." Carlsbad, NM: Sandia National Laboratories. ERMS# 523209.
- Helton, J.C., Bean, J.E., Berglund, J.W., Davis, F.J., Garner, J.W., Johnson, J.D., MacKinnon, R.J., Miller, J., O'Brien, D.G., Ramsey, J.L., Schreiber, J.D., Shinta, A., Smith, L.N., Stoelzel, D.M., Stockman, C., and Vaughn, P. 1998. *Uncertainty and Sensitivity Analysis Results Obtained in the 1996 Performance Assessment for the Waste Isolation Pilot Plant*. SAND98-0365. Albuquerque, NM: Sandia National Laboratories.
- Hurtado, L.D., Knowles, M.K., Kelley, V.A., Jones, T.L., Ogintz, J.B., and Pfeifle, T.W. 1997. *WIPP Shaft Seal System Parameters Recommended to Support Compliance Calculations*. SAND97-1287. Albuquerque, NM: Sandia National Laboratories.
- Iman, R. L. and M. J. Shortencarrier. (1984). "A FORTRAN 77 Program and User's Guide for the Generation of Latin Hypercube and Random Samples for Use with Computer Models," NUREG/CR-3624. SAND83-2365. Sandia National Laboratories, Albuquerque, NM.

Information Only

- James, S.J., and Stein, J. 2002. "Analysis Plan for the Development of a Simplified Shaft Seal Model for the WIPP Performance Assessment." AP-094. Carlsbad, NM: Sandia National Laboratories. ERMS# 524958.
- James, S.J., and Stein, J. 2003. "Analysis Report for the Development of a Simplified Shaft Seal Model for the WIPP Performance Assessment Rev. 1." Carlsbad, NM: Sandia National Laboratories. ERMS# 525203.
- Jones, C.L., Bowles, C.G., and Bell, K.G., 1960, *Experimental Drill Hole Logging in Potash Deposits of the Carlsbad district, New Mexico*. USGS Open-File Rpt 60-84.
- Long, J. 2003. "Execution of the Performance Assessment for the Compliance Recertification Application (CRA1)." Carlsbad, NM: Sandia National Laboratories. ERMS# 530150.
- Lucas, S.G., and Anderson, O.J., 1993. "Triassic Stratigraphy of Southeastern New Mexico and southwestern Texas." In *Geology of the Carlsbad Region New Mexico and West Texas*, D.W. Loved et al., eds., Forty-Fourth Annual Field Conference Guidebook. New Mexico Geological society, Socorro, NM.
- Mercer, J.W., 1987, *Compilation of Hydrological Data From Drilling the Salado and Castile formation Near the Waste Isolation Pilot Plant (WIPP) site in Southeastern New Mexico*. SAND86-0954. Albuquerque, NM: Sandia National Laboratories.
- PAVT, 1997, Supplemental Summary of EPA-Mandated Performance Assessment Verification Test (All Replicates) and Comparison with the Compliance Certification Application Calculations, WPO# 46702, Report # 414879.
- Popielak, R.S., R.L. Beauheim, S.R. Black, W.E. Coons, C.T. Ellingson, and R.L. Olsen. 1983. *Brine Reservoirs in the Castile Formation, Waste Isolation Pilot Plant (WIPP) Project, Southeastern New Mexico*. TME-3153. Albuquerque, NM: U.S. Department of Energy, Waste Isolation Pilot Plant. (Available from the NTIS as DE86004341/XAB).
- Powers, D.W., and Holt, R.M. 1999. "The Los Medaños Member of the Permian Rustler Formation," *New Mexico Geology*. Vol. 21, no. 4, 97-103.]
- Powers, D.W., J.M. Sigda, and R.M. Holt. 1996. "Probability of Intercepting a Pressurized Brine Reservoir Under the WIPP." Albuquerque, NM: Sandia National Laboratories. Sandia WIPP Central Files WPO # 40199.
- SNL. 1996. Waste Isolation Pilot Plant Shaft Sealing System compliance submittal design report. SAND96-1326. Albuquerque, NM: Sandia National Laboratories.
- Stein, J.S. 2002a. "Methodology behind the TBM BRAGFLO grid." Memorandum to M.K. Knowles, May 13, 2002. Carlsbad, NM: Sandia National Laboratories. ERMS# 522373.]

Information Only

- Stein, J. 2002b. "Parameter values for new materials CONC_PCS and DRZ_PCS." Memorandum to M.K. Knowles, Feb 13, 2002. Carlsbad, NM: Sandia National Laboratories. ERMS# 520524.
- Stein, J. 2003. "Analysis Plan for Calculations of Salado Flow and Transport: Compliance Recertification Application." AP-99. Carlsbad, NM: Sandia National Laboratories. ERMS# 526891
- Stein, J.S., and Zelinski, W.P. 2003. " Analysis Report for: Testing of a Proposed BRAGFLO Grid to be used for the Compliance Recertification Application Performance Assessment Calculations" Carlsbad, NM: Sandia National Laboratories. ERMS# 526868.
- Stone, C.M. 1995, "Transfer of Porosity and Gas Curves From SANTOS for the Final Porosity Surface," Memorandum to B.M. Butcher, Sandia National Laboratories, Albuquerque, NM. December 19, 1995.
- U.S. DOE (U.S. Department of Energy). 1980. *Final Environmental Impact Statement: Waste Isolation Pilot Plant*. DOE/EIS-0026. Washington, DC: U.S. Department of Energy, Assistant Secretary for Defense Programs. Vols. 1-2.
- U.S. DOE (U.S. Department of Energy). 1990. *Final Supplement: Environmental Impact Statement, Waste Isolation Pilot Plant*. DOE/EIS-0026-FS. Washington, DC: U.S. Department of Energy, Office of Environmental Restoration and Waste Management. Vols. 1-13.
- U.S. DOE (U.S. Department of Energy). 1993. *Waste Isolation Pilot Plant Strategic Plan*. DOE/EM-48063. Washington, DC: U.S. Department of Energy.
- U.S. DOE (U.S. Department of Energy). 1996. *Title 40 CFR Part 191 Compliance Certification Application for the Waste Isolation Pilot Plant*. DOE/CAO-1996-2184. Carlsbad, NM: U.S. Department of Energy, Waste Isolation Pilot Plant, Carlsbad Area Office.
- U.S. EPA (U.S. Environmental Protection Agency). 1985. "40 CFR 191: Environmental Standards for the Management and Disposal of Spent Nuclear Fuel, High-Level and Transuranic Radioactive Wastes; Final Rule," *Federal Register*. Vol. 50, no. 182, 38066-38089.
- U.S. EPA (U.S. Environmental Protection Agency). 1993. "40 CFR 191: Environmental Radiation Protection Standards for the Management and Disposal of Spent Nuclear Fuel, High-Level and Transuranic Radioactive Wastes; Final Rule," *Federal Register*. Vol. 58, no. 242, 66398-66416.
- U.S. EPA (U.S. Environmental Protection Agency). 1996. "40 CFR Part 194: Criteria for the Certification and Re-Certification of the Waste Isolation Pilot Plant's Compliance With the 40 CFR Part 191 Disposal Regulations; Final Rule," *Federal Register*. Vol. 61, no. 28, 5224-5245.

Information Only

Wang, H.F., and Anderson, M.P. 1982. *Introduction to Groundwater Modeling*. San Diego: Academic Press.

Webb, S.W., and Larsen, K.W., 1996. *The Effect of Stratigraphic Dip on Brine and Gas Migration at the Waste Isolation Pilot Plant*. SAND94-0932. Albuquerque, NM: Sandia National Laboratories. Sandia WIPP Central Files WPO # 28005.

WIPP PA (Performance Assessment) Department, 1995a. *User's Manual for GENMESH, Version 6.07*, Document Version 1.00, WPO # 23291. Sandia National Laboratories, Albuquerque, NM

WIPP PA (Performance Assessment) Department, 1995b. *User's Manual for PCCSRC, Version 2.21*, Document Version 1.00, WPO # 27773. Sandia National Laboratories, Albuquerque, NM

WIPP PA (Performance Assessment) Department, 1996a. *User's Manual for LHS, Version 2.41*, Document Version 1.00, WPO # 30732. Sandia National Laboratories, Albuquerque, NM

WIPP PA (Performance Assessment) Department, 1996b., 1996b. "Verification of 2-D Radial Flaring Using 3-D Geometry", WPO # 30840. Sandia National Laboratories, Albuquerque, NM

WIPP PA (Performance Assessment) Department, 1996c. *User's Manual for ICSET, Version 2.22*, Document Version 1.00, WPO # 30694. Sandia National Laboratories, Albuquerque, NM

WIPP PA (Performance Assessment) Department, 1996d. *User's Manual for ALGEBRACDB, Version 2.35*, Document Version 1.01, WPO# 41864. Sandia National Laboratories, Albuquerque, NM

WIPP PA (Performance Assessment) Department, 2000. *User's Manual for MATSET Version 9.04*, Document Version 9.04, ERMS# 513616. Sandia National Laboratories, Albuquerque, NM

WIPP PA (Performance Assessment) Department, 2003a. *User's Manual for BRAGFLO Version 5.00*, Document Version 5.00, ERMS# 525702. Sandia National Laboratories, Albuquerque, NM.

WIPP PA (Performance Assessment) Department, 2003b. *User's Manual for PREBRAG Version 7.00*, Document Version 7.00, ERMS# 526643. Sandia National Laboratories, Albuquerque, NM

Information Only

APPENDIX A: OUTPUT VARIABLES

Name	Type/Units	Description
FE_KG	Steel (kg)	Remaining Mass Of Steel
CELL_KG	Cellulose (kg)	Remaining Mass Of Cellulose
FE_REM	Fraction of Initial Steel	Remaining Fraction Of Steel
CELL_REM	Fraction of Initial Cellulose	Remaining Fraction Of Cellulose
FE_MOLE	Gas (moles)	Cumulative Gas Generation By Corrosion
CELL_MOL	Gas (moles)	Cumulative Gas Generation By Total Microbial Activity
GAS_MOLE	Gas (moles)	Cumulative Total Gas Generation
CELL_M_H	Gas (moles)	Cumulative Gas Generation By Microbial Activity In A Humid Environment
CELL_M_I	Gas (moles)	Cumulative Gas Generation By Microbial Activity In An Inundated Environment
C_M_HI_T	Gas (moles)	Cumulative Gas Generation By Total Microbial Activity
FE_MOL_D	Gas (moles/drum)	Cumulative Gas Generation By Corrosion
CEL_MH_D	Gas (moles/drum)	Cumulative Gas Generation By Microbial Activity In A Humid Environment
CEL_MI_D	Gas (moles/drum)	Cumulative Gas Generation By Microbial Activity In An Inundated Environment
CELMOL_D	Gas (moles/drum)	Cumulative Gas Generation By Total Microbial Activity (CELL_MOL/DRUMTOT)
C_MHIT_D	Gas (moles/drum)	Cumulative Gas Generation By Total Microbial Activity (C_M_HI_T/DRUMTOT)
GASMOL_D	Gas (moles/drum)	Cumulative Total Gas Generation
GAS_FE_V	Gas Volume (m ³)	Cumulative Gas Generation By Corrosion
GAS_CMH	Gas Volume (m ³)	Cumulative Gas Generation By Humid Microbial Activity
GAS_CMI	Gas Volume (m ³)	Cumulative Gas Generation By Inundated Microbial Activity
GAS_C_V	Gas Volume (m ³)	Cumulative Gas Generation By Total Microbial Activity (CELL_MOL)
C_MHIT_V	Gas Volume (m ³)	Cumulative Gas Generation By Total Microbial Activity (C_M_HI_T)
GAS_VOL	Gas Volume (m ³)	Cumulative Total Gas Generation
WAS_PRES	Pressure (Pa)	Volume-Averaged Pressure: Waste Panel
SRR_PRES	Pressure (Pa)	Volume-Averaged Pressure: RoR South

Information Only

Name	Type/Units	Description
NRR_PRES	Pressure (Pa)	Volume-Averaged Pressure: RoR North
REP_PRES	Pressure (Pa)	Volume-Averaged Pressure: RoR (North + South)
OPS_PRES	Pressure (Pa)	Volume-Averaged Pressure: Ops Region
EXP_PRES	Pressure (Pa)	Volume-Averaged Pressure: Exp Region
W_R_PRES	Pressure (Pa)	Volume-Averaged Pressure: All Waste Regions
B_P_PRES	Pressure (Pa)	Volume-Averaged Pressure: Castile Brine Pocket
PORVOL_T	Pore Volume (m ³)	Total Pore Volume In The Repository
BRNVOL_W	Brine Volume (m ³)	Brine Volume: Waste Panel
BRNVOL_S	Brine Volume (m ³)	Brine Volume: RoR South
BRNVOL_N	Brine Volume (m ³)	Brine Volume: RoR North
BRNVOL_R	Brine Volume (m ³)	Brine Volume: RoR (North + South)
BRNVOL_T	Brine Volume (m ³)	Brine Volume: All Waste Regions
BRNVOL_O	Brine Volume (m ³)	Brine Volume: Ops Region
BRNVOL_E	Brine Volume (m ³)	Brine Volume: Exp Region
BRNVOL_A	Brine Volume (m ³)	Brine Volume: All Excavated Areas
WAS_SATG	Gas Saturation (dimensionless)	Volume-Averaged Gas Saturation: Waste Panel
SRR_SATG	Gas Saturation (dimensionless)	Volume-Averaged Gas Saturation: RoR South
NRR_SATG	Gas Saturation (dimensionless)	Volume-Averaged Gas Saturation: RoR North
REP_SATG	Gas Saturation (dimensionless)	Volume-Averaged Gas Saturation: RoR (North + South)
OPS_SATG	Gas Saturation (dimensionless)	Volume-Averaged Gas Saturation: Ops Region
EXP_SATG	Gas Saturation (dimensionless)	Volume-Averaged Gas Saturation: Exp Region
W_R_SATG	Gas Saturation (dimensionless)	Volume-Averaged Gas Saturation: All Waste Regions
B_P_SATG	Gas Saturation (dimensionless)	Volume-Averaged Gas Saturation: Castile Brine Pocket
WAS_SATB	Brine Saturation (dimensionless)	Volume-Averaged Brine Saturation: Waste Panel
SRR_SATB	Brine Saturation (dimensionless)	Volume-Averaged Brine Saturation: RoR South
NRR_SATB	Brine Saturation (dimensionless)	Volume-Averaged Brine Saturation: RoR North
REP_SATB	Brine Saturation (dimensionless)	Volume-Averaged Brine Saturation: RoR (North + South)
OPS_SATB	Brine Saturation (dimensionless)	Volume-Averaged Brine Saturation: Ops Region
EXP_SATB	Brine Saturation (dimensionless)	Volume-Averaged Brine Saturation: Exp Region
W_R_SATB	Brine Saturation (dimensionless)	Volume-Averaged Brine Saturation: All Waste Regions

Information Only

Name	Type/Units	Description
B_P_SATB	Brine Saturation (dimensionless)	Volume-Averaged Brine Saturation: Castile Brine Pocket
WAS_POR	Porosity (dimensionless)	Volume-Averaged Porosity: Waste Panel
SRR_POR	Porosity (dimensionless)	Volume-Averaged Porosity: ROR South
NRR_POR	Porosity (dimensionless)	Volume-Averaged Porosity: ROR North
REP_POR	Porosity (dimensionless)	Volume-Averaged Porosity: ROR (North + South)
OPS_POR	Porosity (dimensionless)	Volume-Averaged Porosity: Ops Region
EXP_POR	Porosity (dimensionless)	Volume-Averaged Porosity: Exp Region
W_R_POR	Porosity (dimensionless)	Volume-Averaged Porosity: All Waste Regions
BRN_RMV	Brine Volume (m ³)	Brine Consumed
BRNREPTC	Brine Volume (m ³)	Total Brine Flow Into Repository
BRNWPIC	Brine Volume (m ³)	Total Brine Flow Into Waste Panel
BRNSRRIC	Brine Volume (m ³)	Total Brine Flow Into ROR South
BRNNRRIC	Brine Volume (m ³)	Total Brine Flow Into ROR North
BRNRRIC	Brine Volume (m ³)	Total Brine Flow Into ROR (North + South)
BRNORIC	Brine Volume (m ³)	Total Brine Flow Into Ops Region
BRNEAIC	Brine Volume (m ³)	Total Brine Flow Into Exp Region
BRNREPOC	Brine Volume (m ³)	Total Brine Flow Out Of Repository
BRNREPMC	Brine Volume (m ³)	Net Brine Flow Into Repository
BRNWPOC	Brine Volume (m ³)	Total Brine Flow Out Of Waste Panel
BRNWPNC	Brine Volume (m ³)	Net Brine Flow Into Waste Panel
BRNSRROC	Brine Volume (m ³)	Total Brine Flow Out Of ROR South
BRNSRRNC	Brine Volume (m ³)	Net Brine Flow Into ROR South
BRNNRROC	Brine Volume (m ³)	Total Brine Flow Out Of ROR North
BRNNRRNC	Brine Volume (m ³)	Net Brine Flow Into ROR North
BRNRROC	Brine Volume (m ³)	Total Brine Flow Out Of ROR (North + South)
BRNRANC	Brine Volume (m ³)	Net Brine Flow Into ROR (North + South)
BRNOROC	Brine Volume (m ³)	Total Brine Flow Out Of Ops Region
BRNOANC	Brine Volume (m ³)	Net Brine Flow Into Ops Region
BRNEAOC	Brine Volume (m ³)	Total Brine Flow Out Of Exp Region
BRNEANC	Brine Volume (m ³)	Net Brine Flow Into Exp Region

Information Only

Name	Type/Units	Description
BRNBHUPP	Brine Volume (m ³)	Brine Flow Up Borehole: Bottom Of Waste Panel (@Element 1410)
BRNBHUPC	Brine Volume (m ³)	Brine Flow Up Borehole: Bottom Of Upper DRZ (@Element 1168)
BRNBHRCC	Brine Volume (m ³)	Brine Flow Up Borehole: Culebra/Unnamed Contact (@Element 1845)
BRNBHRUC	Brine Volume (m ³)	Brine Flow Up Borehole: Dewey Lake/49er Contact (@Element 1979)
BRNBHRSC	Brine Volume (m ³)	Brine Flow Up Borehole: Santa Rosa (@Element 2155)
BNBHLDRZ	Brine Volume (m ³)	Brine Flow Up Borehole: Bottom Of Lower DRZ (@Element 1111)
BNBHURZ	Brine Volume (m ³)	Brine Flow Up Borehole: Top Of Upper DRZ (@Element 1493)
BRNSHRSC	Brine Volume (m ³)	Brine Flow up shaft: Santa Rosa (@element 1364)
BNSHDSCZ	Brine Volume (m ³)	Brine Flow down shaft: Santa Rosa (@element 1496)
BRNSHRUC	Brine Volume (m ³)	Brine Flow up shaft: Dewey Lake/49er Contact (@element 1493)
BNSHDRUZ	Brine Volume (m ³)	Brine Flow Down Shaft: Dewey Lake/49er Contact (@Element 1493)
BRNSHRCC	Brine Volume (m ³)	Brine Flow up Shaft: Culebra/unnamed Contact (@element 1489)
BNSHDRCC	Brine Volume (m ³)	Brine Flow down Shaft: Culebra/unnamed Contact (@element 1489)
BNSHURZ	Brine Volume (m ³)	Brine Flow up Shaft: MB138/U_DRZ Contact (@element 1381)
BNSHDDRZ	Brine Volume (m ³)	Brine Flow down Shaft: MB138/U_DRZ Contact (@element 1381)
BRNSHABC	Brine Volume (m ³)	Brine Flow Up Shaft: Anhy AB/CONC_MON Contact (@element 1315)
BNSHDABC	Brine Volume (m ³)	Brine Flow down Shaft: Anhy AB/CONC_MON Contact (@element 1315)
BRM38NIC	Brine Volume (m ³)	Total Lateral Brine Flow Out Of MB Toward Repository: MB 138, North
BRAABNIC	Brine Volume (m ³)	Total Lateral Brine Flow Out Of MB Toward Repository: Anhydrite A & B, North
BRM39NIC	Brine Volume (m ³)	Total Lateral Brine Flow Out Of MB Toward Repository: MB 139, North
BRM38SIC	Brine Volume (m ³)	Total Lateral Brine Flow Out Of MB Toward Repository: MB 138, South
BRAABSIC	Brine Volume (m ³)	Total Lateral Brine Flow Out Of MB Toward Repository: Anhydrite A & B, South
BRM39SIC	Brine Volume (m ³)	Total Lateral Brine Flow Out Of MB Toward Repository: MB 139, South
BRAALIC	Brine Volume (m ³)	Total Lateral Brine Flow Out Of MB Toward Repository: All Marker Beds
BRM38NOC	Brine Volume (m ³)	Total Lateral Brine Flow Into MB Away From Repository: MB 138, North
BRAABNOC	Brine Volume (m ³)	Total Lateral Brine Flow Into MB Away From Repository: Anhydrite A & B, North
BRM39NOC	Brine Volume (m ³)	Total Lateral Brine Flow Into MB Away From Repository: MB 139, North
BRM38SOC	Brine Volume (m ³)	Total Lateral Brine Flow Into MB Away From Repository: MB 138, South
BRAABSOC	Brine Volume (m ³)	Total Lateral Brine Flow Into MB Away From Repository: Anhydrite A & B, South

Information Only

Name	Type/Units	Description
BRM39SOC	Brine Volume (m ³)	Total Lateral Brine Flow Into MB Away From Repository: MB 139, South
BRAALOC	Brine Volume (m ³)	Total Lateral Brine Flow Into MB Away From Repository: All Marker Beds
BRM38NNC	Brine Volume (m ³)	Net Lateral Brine Flow Through MB: MB 138, North
BRAABNNC	Brine Volume (m ³)	Net Lateral Brine Flow Through MB: Anhydrite A & B, North
BRM39NNC	Brine Volume (m ³)	Net Lateral Brine Flow Through MB: MB 139, North
BRM38SNC	Brine Volume (m ³)	Net Lateral Brine Flow Through MB: MB 138, South
BRAABSNC	Brine Volume (m ³)	Net Lateral Brine Flow Through MB: Anhydrite A & B, South
BRM39SNC	Brine Volume (m ³)	Net Lateral Brine Flow Through MB: MB 139, South
BRAALNC	Brine Volume (m ³)	Net Lateral Brine Flow Into DRZ Through All Anhydrite Layers
GASBHUPC	Gas Volume (m ³)	Cumulative Gas Flow Up Borehole: Top Of Waste Panel
GASBHUDZ	Gas Volume (m ³)	Cumulative Gas Flow Up Borehole: Top Of Upper DRZ
GSSHUSCC	Gas Volume at Reference Conditions (m ³)	Gas flow up shaft (@element 1496 Santa Rosa)
GSSHRRUC	Gas Volume at Reference Conditions (m ³)	Gas Flow Up Shaft (@Element 1493 49er/Dewey Lake)
GSSHUCUC	Gas Volume at Reference Conditions (m ³)	Gas flow up shaft (@element 1489 unnamed/Culebra)
GSSHUDRZ	Gas Volume at Reference Conditions (m ³)	Gas flow up shaft (@element 1381 U_DRZ/Upper 138)
GASSHABC	Gas Volume at Reference Conditions (m ³)	Gas flow up shaft (@element 1315 Anhy AB/CONC_MON)
GSM38NOC	Gas Volume at Reference Conditions (m ³)	Total Gas Flow Through MB Away From Repository: MB 138, North
GSAABNOC	Gas Volume at Reference Conditions (m ³)	Total Gas Flow Through MB Away From Repository: Anhydrite A & B, North
GSM39NOC	Gas Volume at Reference Conditions (m ³)	Total Gas Flow Through MB Away From Repository: MB 139, North
GSM38SOC	Gas Volume at Reference Conditions (m ³)	Total Gas Flow Through MB Away From Repository: MB 138, South
GSAABSOC	Gas Volume at Reference Conditions (m ³)	Total Gas Flow Through MB Away From Repository: Anhydrite A & B, South
GSM39SOC	Gas Volume at Reference Conditions (m ³)	Total Gas Flow Through MB Away From Repository: MB 139, South
GSAALOC	Gas Volume at Reference Conditions (m ³)	Total Gas Flow Through MB Away From Repository: All Marker Beds
FRACX38N	Fracture Length (m)	Interbed Fracturing: Length Of Fracture Zone: MB 138, North

Information Only

Name	Type/Units	Description
FRACXABN	Fracture Length (m)	Interbed Fracturing: Length Of Fracture Zone: Anhydrite A & B, North
FRACX39N	Fracture Length (m)	Interbed Fracturing: Length Of Fracture Zone: MB 139, North
FRACX38S	Fracture Length (m)	Interbed Fracturing: Length Of Fracture Zone: MB 138, South
FRACXABS	Fracture Length (m)	Interbed Fracturing: Length Of Fracture Zone: Anhydrite A & B, South
FRACX39S	Fracture Length (m)	Interbed Fracturing: Length Of Fracture Zone: MB 139, South
VFRAC38N	Fracture volume (m ³)	Interbed Fracturing: Vol Of Fracturing Zone: MB 138, North
VFRACABN	Fracture volume (m ³)	Interbed Fracturing: Vol Of Fracturing Zone: Anhydrite A & B, North
VFRAC39N	Fracture volume (m ³)	Interbed Fracturing: Vol Of Fracturing Zone: MB 139, North
VFRAC38S	Fracture volume (m ³)	Interbed Fracturing: Vol Of Fracturing Zone: MB 138, South
VFRACABS	Fracture volume (m ³)	Interbed Fracturing: Vol Of Fracturing Zone: Anhydrite A & B, South
VFRAC39S	Fracture volume (m ³)	Interbed Fracturing: Vol Of Fracturing Zone: MB 139, South
VFRAC38TMB	Fracture volume (m ³)	Total MB Fracture Vol: All Marker Beds
APERM38N	Permeability (m ²)	Vol-Averaged Permeability In Fracture Zone: MB 138, North
APERMABN	Permeability (m ²)	Vol-Averaged Permeability In Fracture Zone: Anhydrite A & B, North
APERM39N	Permeability (m ²)	Vol-Averaged Permeability In Fracture Zone: MB 139, North
APERM38S	Permeability (m ²)	Vol-Averaged Permeability In Fracture Zone: MB 138, South
APERMABS	Permeability (m ²)	Vol-Averaged Permeability In Fracture Zone: Anhydrite A & B, South
APERM39S	Permeability (m ²)	Vol-Averaged Permeability In Fracture Zone: MB 139, South
PVOLI38N	Permeability (m ²)	Increase In Pore Vol In Fracture Zone: MB 138, North
PVOLIABN	Permeability (m ²)	Increase In Pore Vol In Fracture Zone: Anhydrite A & B, North
PVOLI39N	Permeability (m ²)	Increase In Pore Vol In Fracture Zone: MB 139, North
PVOLI38S	Permeability (m ²)	Increase In Pore Vol In Fracture Zone: MB 138, South
PVOLIABS	Permeability (m ²)	Increase In Pore Vol In Fracture Zone: Anhydrite A & B, South
PVOLI39S	Permeability (m ²)	Increase In Pore Vol In Fracture Zone: MB 139, South
PVOLI_T	Permeability (m ²)	Total Frac Zone Pore Vol Increase: All Marker Beds
BRNVOL_B	Brine Volume (m ³)	Brine Vol: Castile Brine Pocket
BNBHDNUZ	Brine Volume (m ³)	Downward Brine Flow: Borehole At Top Of MB 138
BRNBHDNC	Brine Volume (m ³)	Downward Brine Flow: Borehole At Top Of Waste Panel
FEKG_W	Steel (kg)	Steel Mass Remaining: Waste Panel
CELLKG_W	Cellulose (kg)	Cellulose Mass Remaining: Waste Panel

Information Only

Name	Type/Units	Description
FEREM_W	Fraction of Initial Iron & Steel	Fraction Steel Remaining: Waste Panel
CELREM_W	Fraction of Initial Cellulose	Fraction Cellulose Remaining: Waste Panel
GASMOL_W	Gas (moles)	Total Number Of Moles Of Gas Generated: Waste Panel
GASVOL_W	Gas at Reference Conditions (m ³) Total	Gas Volume Generated: Waste Panel
PORVOL_W	Pore volume (m ³)	Total Pore Volume: Waste Panel
BRNM38I	Brine Volume (m ³)	Total Brine Flow Out Of MB, Towards Repository: MB 138
BRNAABI	Brine Volume (m ³)	Total Brine Flow Out Of MB, Towards Repository: Anhydrite A & B
BRNM39I	Brine Volume (m ³)	Total Brine Flow Out Of MB, Towards Repository: MB 139
BRNM38O	Brine Volume (m ³)	Total Brine Flow Into MB, Away From Repository: MB 138
BRNAABO	Brine Volume (m ³)	Total Brine Flow Into MB, Away From Repository: Anhydrite A & B
BRNM39O	Brine Volume (m ³)	Total Brine Flow Into MB, Away From Repository: MB 139
BRN_RMVW	Brine Volume (m ³)	Brine Consumed: Waste Panel
BRN_RMSR	Brine Volume (m ³)	Brine Consumed: ROR South
BRN_RMNR	Brine Volume (m ³)	Brine Consumed: ROR North
BRN_RMVR	Brine Volume (m ³)	Brine Consumed: ROR (North + South)
FEREM_SR	Fraction of Initial Iron & Steel	Fraction Of Steel Remaining: ROR South
CELREM_S	Fraction of Initial Cellulose	Fraction Of Cellulose Remaining: ROR South
FEREM_NR	Fraction of Initial Iron & Steel	Fraction Of Steel Remaining: ROR North
CELREM_N	Fraction of Initial Cellulose	Fraction Of Cellulose Remaining: ROR North
FEREM_R	Fraction of Initial Iron & Steel	Fraction Of Steel Remaining: ROR (North + South)
CELREM_R	Fraction of Initial Cellulose	Fraction Of Cellulose Remaining: ROR (North + South)
GASMOL_S	Gas (moles)	Total Number Of Moles Of Gas Generated: ROR South
GASMOL_N	Gas (moles)	Total Number Of Moles Of Gas Generated: ROR North
GASMOL_R	Gas (moles)	Total Number Of Moles Of Gas Generated: ROR (North + South)
BRWI_XBH	Brine Volume (m ³)	Cumulative Brine Flow Into Waste Panel, Excluding Borehole
SAL_BR_T	Fraction of Total Brine Inflow	(Salado Brine Inflow)/(Total Brine Inflow): DRZ
SAL_BR_U	Fraction of Unconsumed Brine Inflow	(Salado Brine Inflow)/(Unconsumed Brine Inflow): DRZ
SB_TB_WP	Fraction of Total Brine Inflow	(Salado Brine Inflow)/(Total Brine Inflow): Waste Panel
SB_UB_WP	Fraction of Unconsumed	Brine Inflow: (Salado Brine Inflow)/(Unconsumed Brine Inflow): Waste Panel

Information Only

Name	Type/Units	Description
BRNBHUMC	Brine Volume (m ³)	Brine Flow Up: Borehole At Magenta Dolomite
BRNSHUMC	Brine Volume (m ³)	Brine Flow Up: Shaft At Magenta Dolomite
BRM38NLMW	Brine Volume (m ³)	Total Outward Brine Flow In MB's Across LWB: MB 138, North
BRAABNLMW	Brine Volume (m ³)	Total Outward Brine Flow In MB's Across LWB: Anhydrite A & B, North
BRM39NLMW	Brine Volume (m ³)	Total Outward Brine Flow In MB's Across LWB: MB 139, North
BRM38SLW	Brine Volume (m ³)	Total Outward Brine Flow In MB's Across LWB: MB 138, South
BRAABSLW	Brine Volume (m ³)	Total Outward Brine Flow In MB's Across LWB: Anhydrite A & B, South
BRM39SLW	Brine Volume (m ³)	Total Outward Brine Flow In MB's Across LWB: MB 139, South
BRAALLMC	Brine Volume (m ³)	Total Outward Brine Flow In MB's Across LWB: All Marker Beds
FR_TG_C	Fraction of Total Gas	Fraction Of Total Gas Due To Steel Corrosion: All Waste Regions
FR_TG_M	Fraction of Total Gas	Fraction Of Total Gas Due To Total Microbial Activity: All Waste Regions
FR_TG_H	Fraction of Total Gas	Fraction Of Total Gas Due To Humid Microbial Activity: All Waste Regions
FR_TG_I	Fraction of Total Gas	Fraction Of Total Gas Due To Inundated Microbial Activity: All Waste Regions
FR_MG_H	Fraction of Total Gas	Fraction Of Microbial Activity Gas From Humid Conditions: All Waste Regions
FR_MG_I	Fraction of Total Gas	Fraction Of Microbial Activity Gas From Inundated Conditions: All Waste Regions
PORVOL_S	Pore volume (m ³)	Total Pore Vol: ROR South
PORVOL_N	Pore volume (m ³)	Total Pore Vol: ROR North
PORVOL_R	Pore volume (m ³)	Total Pore Vol: ROR (North + South)

Information Only

APPENDIX B: CREEP CLOSURE, MINIMUM POROSITIES

Vector	Year	Minimum Porosity (temporary)	Porosity at 10,000 Years
1	700	0.15	0.18
1	6800	0.17	0.18
3	1200	0.09	0.13
3	9200	0.12	0.13
4	150	0.35	0.22
4	7200	0.22	0.22
5	1400	0.18	0.18
6	1200	0.20	0.21
7	1000	0.11	0.17
8	1200	0.15	0.15
8	4400	0.14	0.15
9	1200	0.19	0.20
10	2400	0.22	0.23
11	9200	0.12	0.13
12	1200	0.18	0.21
13	5800	0.14	0.14
14	700	0.22	0.22
14	2000	0.21	0.22
15	1400	0.21	0.22
15	8000	0.22	0.22
16	1400	0.18	0.18
16	3200	0.18	0.18
17	1600	0.17	0.17
18	1400	0.21	0.21
19	1200	0.14	0.16
19	6400	0.15	0.16
20	1200	0.17	0.18
20	2800	0.18	0.18
21	2800	0.07	0.08
22	160	0.35	0.22
22	1600	0.22	0.22
22	7600	0.22	0.22
23	3000	0.17	0.17
25	1800	0.08	0.10
26	1400	0.22	0.22
26	9000	0.22	0.22
27	600	0.22	0.22
27	1400	0.21	0.22
27	5600	0.22	0.22
28	6800	0.14	0.14
29	1600	0.23	0.23

29	6400	0.23	0.23
30	1400	0.22	0.22
30	8400	0.22	0.22
31	1200	0.10	0.18
32	1200	0.11	0.12
32	9400	0.12	0.12
33	1200	0.13	0.15
33	5400	0.14	0.15
34	700	0.17	0.22
34	5800	0.22	0.22
36	1200	0.14	0.16
37	700	0.13	0.18
39	2400	0.16	0.17
39	7200	0.17	0.17
40	180	0.35	0.20
41	1400	0.22	0.25
41	8200	0.24	0.25
42	700	0.14	0.17
43	1800	0.15	0.17
44	3200	0.12	0.12
45	600	0.22	0.25
45	1200	0.22	0.25
45	7200	0.24	0.25
46	1200	0.17	0.17
47	700	0.14	0.20
48	900	0.13	0.18
48	8400	0.18	0.18
49	1200	0.13	0.17
50	1200	0.12	0.15
50	5200	0.13	0.15
52	1200	0.18	0.17
52	7000	0.17	0.17
53	1800	0.17	0.17
54	1200	0.13	0.15
54	4200	0.15	0.15
55	8200	0.14	0.15
57	1200	0.10	0.14
57	8400	0.13	0.14
58	800	0.13	0.13
58	1200	0.13	0.13
59	2000	0.13	0.16
60	1200	0.12	0.14
60	7200	0.13	0.14
61	700	0.14	0.15
61	4800	0.15	0.15
62	1400	0.13	0.13
62	8000	0.13	0.13

129
Information Only

63	700	0.13	0.20
64	600	0.22	0.22
64	1400	0.22	0.22
64	7400	0.22	0.22
65	1200	0.12	0.14
66	1200	0.14	0.16
67	700	0.18	0.22
67	5800	0.22	0.22
68	1200	0.22	0.23
69	700	0.16	0.18
69	1200	0.16	0.18
70	1200	0.16	0.17
71	1200	0.12	0.12
72	1400	0.22	0.22
72	5400	0.22	0.22
73	1200	0.16	0.18
74	2600	0.14	0.15
75	800	0.14	0.20
76	150	0.35	0.23
76	2000	0.23	0.23
76	3600	0.23	0.23
77	1600	0.15	0.16
77	3400	0.15	0.16
78	1200	0.17	0.20
80	1200	0.11	0.13
81	1200	0.09	0.14
82	1400	0.22	0.21
83	1800	0.13	0.13
83	5800	0.13	0.13
84	1200	0.10	0.14
85	5000	0.17	0.18
86	1800	0.15	0.17
87	1200	0.18	0.20
88	1200	0.10	0.13
88	7600	0.13	0.13
90	7200	0.22	0.22
91	700	0.16	0.20
92	1200	0.11	0.14
92	9200	0.12	0.14
93	600	0.20	0.23
93	1200	0.21	0.23
93	3200	0.22	0.23
94	1200	0.11	0.11
94	4800	0.11	0.11
95	2800	0.12	0.13
96	1400	0.09	0.14
97	1200	0.13	0.17

110
Information Only

98	1200	0.10	0.12
98	9200	0.12	0.12
99	1200	0.20	0.21
100	600	0.15	0.19
Max	9400	0.35	0.25
Min	150	0.07	0.08

Note: columns 5, 6, and 7 - 1 is yes, and 0 is no

APPENDIX C: ANALYSIS FILES ON CD'S

Information Only